The Institute of Paper Chemistry

Appleton, Wisconsin

Doctor's Dissertation

An Investigation of the Relation Between Carboxyl Content and Zeta Potential

Richard Thomas Clapp

June, 1972

AN INVESTIGATION OF THE RELATION BETWEEN CARBOXYL CONTENT AND ZETA POTENTIAL

A thesis submitted by

Richard Thomas Clapp

B.S. 1966, Western Michigan University
M.S. 1968, Lawrence University

in partial fulfillment of the requirements
of The Institute of Paper Chemistry
for the degree of Doctor of Philosophy
Appleton, Wisconsin

June, 1972

TABLE OF CONTENTS

SUMMARY

The purpose of this study was to determine the relationship between the zeta potential and the carboxyl content of a fibrous system in order to provide a better understanding of the origin of the negative charge of carboxyl containing fibers. This involved investigation of the dissociation of carboxyl groups and the influence of dissociated carboxyl groups on the resulting zeta potential.

Dacron fibers and dacron with adsorbed polyacrylic acid (PAA) were used. Adsorption experiments were carried out in order to characterize the nature of the adsorbed PAA. Potentiometric titrations of slurries, of both the dacron and dacron-PAA fibers, gave the carboxyl content of the fibers and their dissociation behavior. Turbidity titrations were used to determine PAA concentrations before and after adsorption and the difference was used to calculate the amount of PAA adsorbed. It was found that more carboxyl groups were present on the dacron-PAA fibers than could be accounted for by PAA adsorption. This information along with the adsorption characterization indicated that the PAA was adsorbed as a monolayer and existed as a porous, partial-draining, hydrophilic network.

Streaming current measurements were made on pads of these fibers formed from dilute suspension between Ag-AgCl electrodes at various fluid velocities, pH values, and electrolyte concentrations. An equation based on the Happel flow model (describing fluid flow perpendicular to cylinders) was used to calculate zeta potentials from the streaming current data. Results were obtained for fibers with varying carboxyl content and degrees of dissociation.

The results of this study could be interpreted in terms of ion binding and solvent orientation effects. Ion binding (counterions held within the volume occupied by the PAA) acts to reduce the negative charge of the dissociated carboxyl groups. Solvent orientation involves the orientation of water molecules

into high density layers at the surface, which increases the thickness of immobilized solvent forcing the slip plane to move further into the medium, resulting in a lower zeta potential.

For both dacron itself and the dacron-PAA fiber with the highest amount of adsorbed PAA, the zeta potentials increased only slightly with increased degree of dissociation. In addition, for the latter fiber the zeta potentials were slightly more negative than the dacron itself. These results could be explained in terms of the dominance of solvent orientation associated with the ionized carboxyl groups over the ion binding effect.

For the two dacron-PAA samples with low amounts of adsorbed PAA, the zeta potentials first increased, then leveled off with increasing degree of dissociation, and the zeta potentials were more negative than either the dacron itself or the dacron with the high amount of adsorbed PAA. These results were interpreted as indicating that solvent orientation was a minor effect at low degrees of dissociation but was more important at high degrees of dissociation.

An analysis of literature data on the variation of zeta potential for cellulose fibers containing various substituents, suggests that solvent orientation is the major factor in determining the zeta potential of these fibers. Increasing the carboxyl content of cellulose by oxidation results in less negative zeta potentials. Because of the scattered arrangement of carboxyl groups along the cellulose molecules, the ion binding effect would be small. Solvent orientation would, however, increase with increasing carboxyl content. For cellulose fibers containing hydrophobic substituents, literature data show that more negative zeta potentials result from increased degrees of substitution. Since hydrophobic groups would be expected to decrease the amount of solvent orientation, these results are also consistent with the interpretation that solvent orientation is the major factor in determining the zeta potential of cellulose fibers.

INTRODUCTION

Colloidal phenomena are important in several areas in the paper industry. These include such areas as formation, fiber flocculation, retention of fillers and fines, dispersion of additives, and treatment of water and effluents. In order to understand these phenomena, much use has been made of the concepts of zeta potential and electric double layer theory.

The study of colloidal phenomena includes investigation of electrokinetic effects. Models of an electric double layer, composed of a charged surface and a layer of oppositely charged counterions, have been proposed to account for these electrokinetic effects. A fundamental measure of electrokinetic effects is the zeta potential, which is the potential drop across the movable part of the double layer. At the present time, different methods for measuring the zeta potential seldom give the same result. However, it has been demonstrated that relative values of zeta potential can be measured and these can give an indication of when coagulation conditions are being approached.

Most solid materials which come in contact with a liquid develop a charge through such mechanisms as ionization or ion adsorption. With hydrophilic substances, the exact source of this charge may be obscured due to complicating factors such as polarity, swelling, hydration, or morphology.

Because of such complicating factors, the exact source of the charge on cellulose has not been determined. The research program described here was designed to determine whether carboxyl groups can give rise to a negative zeta potential and, if so, to find out some of the factors which affect the magnitude of this zeta potential. With this knowledge, it may be possible to clarify the origin of the cellulose charge.

LITERATURE REVIEW

The study of electrokinetic phenomena has been greatly influenced by several classical references (1, 2). Several reviews of current ideas and studies in this field are also available (3-5). Several textbooks in the field of surface chemistry also give good general discussions of electrokinetic phenomena (6-8).

Since this literature is available, the discussion of general concepts will be brief. A more complete discussion of the study of electrokinetic effects of fibrous plugs (mats) will be given. Emphasis will be placed on the effects of certain variables on the calculated zeta potential (ζ) and on ideas concerning the origin of the charge on cellulose fibers.

ELECTRICAL DOUBLE LAYER

DOUBLE LAYER MODEL

Electrokinetic effects are associated with the movement of one of two phases (solid or liquid phase) and the associated electrical current. Four groups of electrokinetic effects have been described in which an applied current causes movement of one phase relative to the other or in which the movement of one phase relative to the other generates an electrical potential. Sennett and Olivier (5) discuss these effects in some detail.

To account for these observed electrokinetic effects, an electrical double layer model was proposed. In 1879, Helmholtz (9) described a capacitor model, consisting of a charged surface with a parallel layer of counterions in the liquid phase near the interface. A model which described a diffuse layer of immobile counterions was later proposed independently by Gouy (10) and Chapman (11). In 1924 Stern (12) modified the Gouy-Chapman model to include an immobile,

inner region of adsorbed ions with finite ionic sizes. Stern's model, with an immobile, inner layer of adsorbed ions (Stern Layer) and a mobile, diffuse outer layer of counterions (Gouy-Chapman or diffuse layer), is the basis for the present-day electrical double layer concept.

Recent modification of double layer theory includes the model described by Levine, Mingins, and Bell (13). It is based on proposals by Grahame (14) and Devanthan (15) and includes a thin layer of chemisorbed ions, which lie in the inner Helmholtz plane (I.H.P.). This is followed by a layer of hydrated counterions which lie in the outer Helmholtz plane (O.H.P.). The diffuse layer thus extends from the O.H.P. out to the bulk solution. Devanthan and Tilak (16) give an excellent description of this model.

Figure 1 illustrates the essential features of the electric double layer including the concept of the O.H.P. The terms used in Fig. 1 are listed below.

ψ = the electrostatic potential at some distance x from the surface

ψ_o = the potential at the surface

ψ_δ = the potential at the O.H.P. or the potential drop across the diffuse layer

δ = thickness of the immobile Stern layer

ζ = experimentally determined estimate of the potential at the hydrodynamic shear plane

κ = Debye-Huckel constant ($1/\kappa$ is an approximation of the double layer thickness)

The discussion of double layer models provides a basis for evaluating the meaning of the zeta potential. Assuming that the double layer model is valid and the hydrodynamic shear plane coincides with the O.H.P., then ζ should equal ψ_δ. However, considerable discrepancy has been found between values calculated for ζ and ψ_δ. These discrepancies become large when the surface potential is

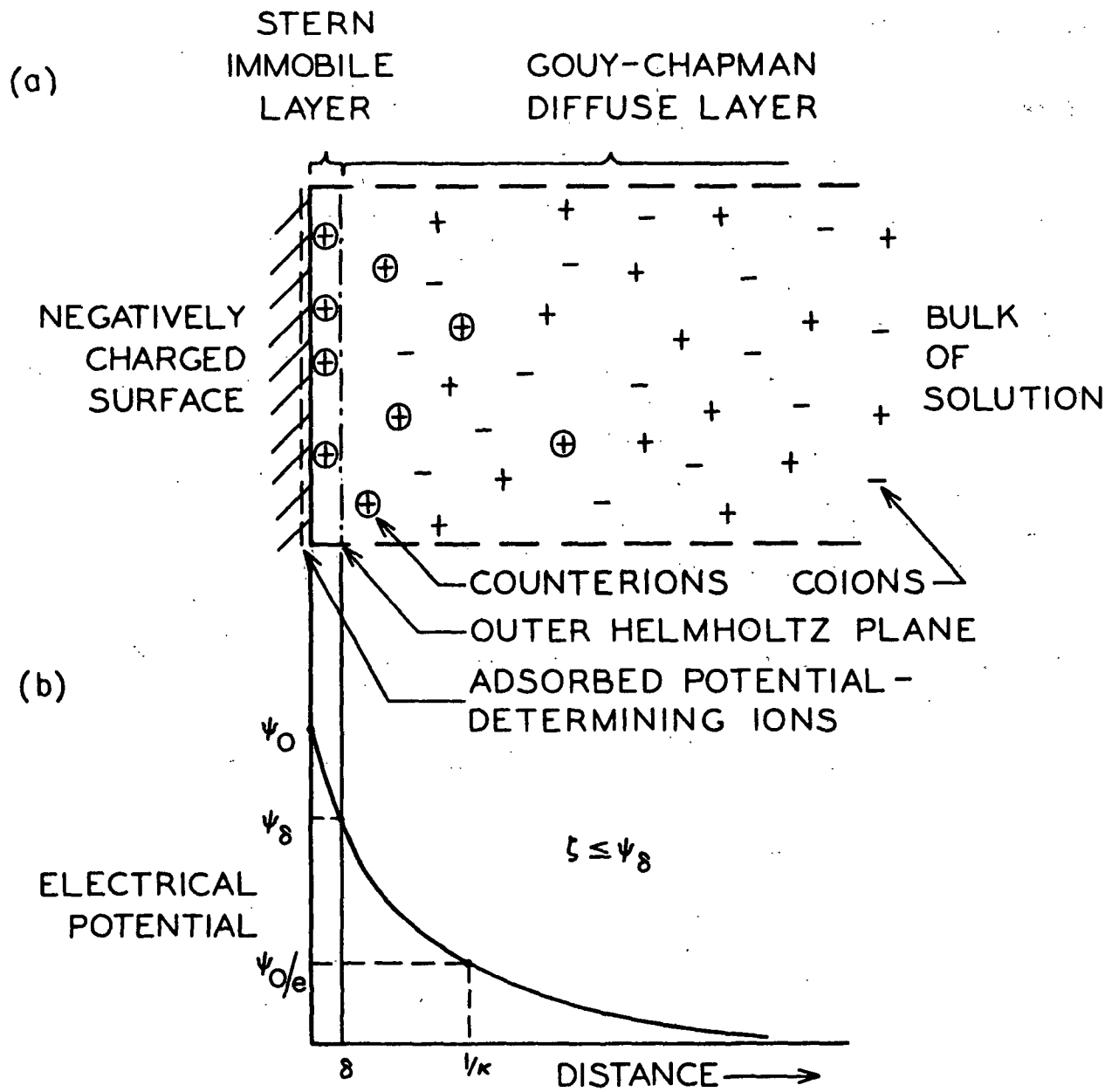

Figure 1a. Model of the Electric Double Layer

The Marked Counterions Represent Ions in Excess Compared to the Bulk Phase. The Number of Counterions Equals the Number of Negative Charges on the Surface.

Figure 1b. Potential Distribution in the Double Layer

high and when the electrolyte concentration is also high ($c > 10^{-3}M$). Reasons for these discrepancies are discussed later.

CALCULATION OF DOUBLE LAYER POTENTIAL

Zeta Potential

In electrokinetic phenomena, there is relative motion between a charged surface and the bulk solution. This relative motion originates at a slip plane. The zeta potential, however, is not strictly a phase boundary potential since it is developed within the fluid region. It can be regarded as the potential difference between a point some distance from the surface and a point on the shear plane.

The phenomenon called streaming current or streaming potential involves the flow of a liquid past a stationary charged surface. The flow of bulk solution carries with it the excess charge of the diffuse layer. This charge can be measured as either a current or as a potential, depending on experimental conditions.

The derivation of the streaming potential (or current) equation given here is due to Smoluchowski (8, 17). This equation is based on laminar flow through a tube with circular cross section. A more general derivation of Equation (1) shows that an equation of similar form is also obtained for a porous plug (2). The Smoluchowski equation is

$$E = \zeta PD/4\pi\eta k \qquad (1)$$

where

E = potential developed across a tube due to liquid flow

P = pressure applied to liquid to cause flow

η = viscosity

k = specific conductance

Potential at the O.H.P.

The Stern model provides a method for determining the potential at the O.H.P. This method involves equations more complex than that for ζ and experimentally, it is also more complex. Basically, ψ_δ is calculated from the total surface charge density, σ (5), where

$$\sigma = \sigma_S + \sigma_G \ . \qquad (2)$$

Here, σ_S represents the surface charge density of the Stern layer and σ_G represents the surface charge density of the Gouy-Chapman layer.

Stern proposed that counterions could be considered as divided between a diffuse layer of point charges and an immobile layer of thickness δ able to contain a certain maximum number of counterions per unit area. A Langmuir-type adsorption isotherm equilibrium is assumed to determine the relation between the number of ions in solution and the number adsorbed. The adsorbed charge per unit area is given by

$$\sigma_S = n\sigma_m \Big/ \left[n + A \exp\left(- \frac{ze\psi_\delta + \phi}{k_1 T} \right) \right] \qquad (3)$$

where

n = concentration of counterions

σ_m = charge corresponding to a monolayer of counterions

A = frequency factor

z = counterion valence

ϕ = adsorption potential of the counterions adsorbed to the surface

k_1 = Boltzmann constant

The evaluation of σ_G is done by integrating the space charge density from $x = \delta$ to $x = \infty$. Equation (4) is the result of this calculation (1, 5).

$$\sigma_G = - \frac{D}{4\pi} \left(\frac{d\psi}{dx} \right)_{x=\delta} \qquad (4)$$

The term $(d\psi/dx)$ is then evaluated using the combined Poisson-Boltzmann relation [see Equation (21), Appendix I]. ψ_δ can then be determined from an experimental value for σ and a trial-and-error solution of Equations (3) and (4) so that values calculated for σ_s and σ_m satisfy Equation (2).

LIMITATIONS OF THE DOUBLE LAYER MODEL

The theories used to develop the concept of a double layer are based on several assumptions. An understanding of these assumptions is necessary in order to choose experimental conditions that will allow meaningful zeta potentials to be calculated.

Validity of the Poisson-Boltzmann Equation

The Poisson-Boltzmann equation is used to relate the distribution of ions to the potential. This equation has been found to be a reasonable approximation for 1-1 electrolytes when the concentration, c, is less than 0.01M and ψ_δ is less than 100 mv., or when $c < 0.1M$ and $\psi_\delta < 50$ mv. (13, 18).

The assumptions made in deriving this equation are: (1) The ions are unpolarized, point charges, (2) the dielectric properties of the fluid are uniform throughout the diffuse layer, and (3) ionic interactions are negligible. Several references (5, 19-21) discuss methods to correct the Poisson-Boltzmann distribution by accounting for deviations from these assumptions.

Viscosity Variations Within the Diffuse Layer

Lyklema and Overbeek (22) discuss corrections which can be made to ζ calculated from electrophoresis data to account for variations in the viscosity of water in the diffuse layer due to an electric field. It was found that the corrections became important only at high electrolyte concentrations ($c > 10^{-3}M$ and $\psi_\delta > 100$ mv. for 1-1 electrolyte).

At present, little has been done to determine the viscosity in the presence of an electric field. The usual assumption is that the diffuse layer viscosity is the same as that of the bulk solution at low electrolyte concentrations and low potentials.

Dielectric Constant Variations

The dielectric constant (permittivity) is also assumed to have the same value in the diffuse layer as it has in the bulk solution. Lyklema and Overbeek (22) studied the effect of the dielectric constant and concluded that viscosity variations were more significant than the variations in the dielectric constant. It was later shown that their analysis of viscosity effects were overestimated (23). Hunter (24) reanalyzed the effect of varying viscosity and dielectric constant on ζ. His results show the effect of dielectric constant to be comparable to that of viscosity.

Liquid Immobilization at the Interface

It has been hypothesized that several layers of water could be immobilized at the solid-liquid interface (22, 25). Assuming this to be the case, then the hydrodynamic shear plane would be farther from the interface than the O.H.P.

Calculations based on this assumption (22) show that for a 10 A. distance between the O.H.P. and the shear plane, $\psi_\delta \cong \zeta$ for a 1-1 electrolyte only when $\underline{c} < 10^{-3}\underline{M}$ and $\psi_\delta < 50$ mv.

Nonequilibrium Double Layer

The approaches used in developing a model to describe the double layer assume that the double layer is at equilibrium. The flow of current, which occurs in streaming current measurements, may alter the double layer structure. Delehay (7) concluded from the literature of nonequilibrium double layer effects that this was

probably the case only at high current flows. Sparnaay (26) made a similar conclusion from calculations for liquid flow perpendicular to a porous electrode and current flowing through a double layer.

STREAMING CURRENT MEASUREMENTS ON FIBROUS SYSTEMS

In analyzing electrokinetic phenomena, it is necessary to apply a valid hydrodynamic flow model. The description of flow in simple systems like capillary tubes has been well established. However, for complicated systems such as fiber mats, completely rigorous hydrodynamic theory has not yet developed to the point where flow can be accurately described. Models have been developed which describe macroscopic flow satisfactorily.

A brief review of streaming current studies of fibrous systems will be given to show the development of this technique.

COMPARISON OF STREAMING CURRENT AND STREAMING POTENTIAL METHODS

The streaming current method uses a low resistance galvanometer to measure the current flowing externally between the two electrodes. With the streaming potential method, however, a high resistance potentiometer is placed across the electrodes and the potential difference between the two electrodes is measured (here, the current flows internally, between the electrodes). The advantage of the latter is that very little current flows through the electrodes, thus lessening problems due to electrode deterioration. This advantage is offset by several disadvantages. These are: (1) It is necessary to accurately determine the electrical resistance of the mat, and (2) it is necessary to theoretically calculate a correction for surface conductance (this is difficult if not impossible for fibrous systems).

The main drawback of the streaming current method is that experimental conditions used must be such that the current flowing between the electrodes is not so high as to provide polarization of the electrodes, and the resistance of the mat must be much higher than that of the galvanometer.

DEVELOPMENT OF STREAMING CURRENT THEORY FOR FIBROUS MATS

Neale and Peters (27) first reported the use of streaming current techniques to measure the zeta potential of fibrous mats. They had used a streaming potential method but abandoned this in favor of the streaming current technique in order to simplify experimental techniques.

Goring and Mason (28) used the streaming current method in their study of fibrous materials. They found that this method was more sensitive than streaming potential measurements at low plug resistances. In comparing results from the same fiber mat, Goring and Mason found that the current calculated from streaming potential measurements was the same as that obtained from streaming current measurements if a d.c. (direct current) method was used to obtain the mat resistance.

Use of a capillary model to predict flow through fibrous mats gives rise to the following equation (29):

$$I\eta L/\Delta PD = -\{A\zeta/[4\pi/(Le/L)^2]\}(1 - \alpha c_1) \qquad (5)$$

where

I = streaming current

L = mat thickness

ΔP = overall frictional pressure drop across pad

A = cross-sectional area of mat

(Le/L) = tortuosity factor (Le is the equivalent path length)

α = specific volume of fibers

$\underline{c}_1$ = mat concentration

$(1-\alpha\underline{c}_1)$ = porosity, ε, of the mat

As discussed by Biefer and Mason (30), several discrepancies arise with the use of this equation. These are a continually decreasing zeta potential with decreasing porosity, excessively large specific volume values (about 1.5 times that calculated from permeability data with the same fiber mats), and nonlinear $[\underline{I}\eta\underline{L}/\Delta\underline{P}\underline{D}]$ vs. $\underline{c}$ curves.

Biefer and Mason (30) also found a specific volume discrepancy for smooth, nonfibrillated fibers such as nylon and dacron. They then proposed an explanation based on tortuosity variations to account for this. Using an empirical fit of the experimental data, they found that the specific volume discrepancies disappeared if the tortuosity factor in Equation (5) was assumed to vary with porosity. While this treatment removed the specific volume discrepancy, no explanation was offered for a tortuosity variation with porosity.

Chang and Robertson (31) suggested that interactions between neighboring fibers during compression could affect specific volumes and permeability. Such interactions would also be expected to affect electrokinetic properties. In order to account for particle interactions, they introduced an exponential term into the zeta potential equation. The equation thus had the form

$$I\eta L/\Delta PD = (A\zeta/4\pi)e^{-Bc} \qquad (6)$$

where $\underline{B}$ is a constant.

The use of Equation (6) represents some improvement in the analysis of streaming current data in that it gives linear plots of $\underline{c}$ vs. $\ln[\underline{I}\eta\underline{L}/\Delta\underline{P}\underline{D}]$. However, because of the empirical nature of the exponential term, there is no reason why its use should be favored over other equations based on the capillary model [Equation (5)].

Happel and Brenner (32) have analyzed the flow relative to particle assemblages of complex geometry. From this they concluded that the Kozeny-Carman concept of a porous bed as a system of capillaries can only be applied to isotropic porous media where orientation effects are absent. Fiber mats are definitely anisotropic and thus the capillary model is probably inadequate for describing streaming current phenomena.

Ciriacks (29) has studied the application of an alternative flow model for streaming current data. This flow model was proposed by Happel (33) to predict flow perpendicular to an array of cylinders. Ciriacks has concluded that the Happel flow model represents a marked improvement over the capillary model approach to streaming current phenomena in fiber mats.

While Ciriacks' treatment of the streaming current phenomenon does not give an absolute value for the zeta potential, it does give satisfactory results when porosity changes are made since the resulting ζ is independent of porosity. Figure 2 shows results obtained by Ciriacks using both the Happel flow model and the capillary flow model on streaming current data from the same fiber mat. Appendix I gives the derivation of the streaming current equation using the Happel flow model.

VARIABLES AFFECTING THE CALCULATED ZETA POTENTIAL

The study of electrokinetic phenomena has been based on theoretical predictions which use the Poisson-Boltzmann equation. Much work has been reported in the literature which is concerned with the effect of variables such as ion type and concentration, and surface properties of the material in question, in order to provide experimental support for the use of double layer models. Some of these results will be discussed here, particularly those results concerned with fibrous systems.

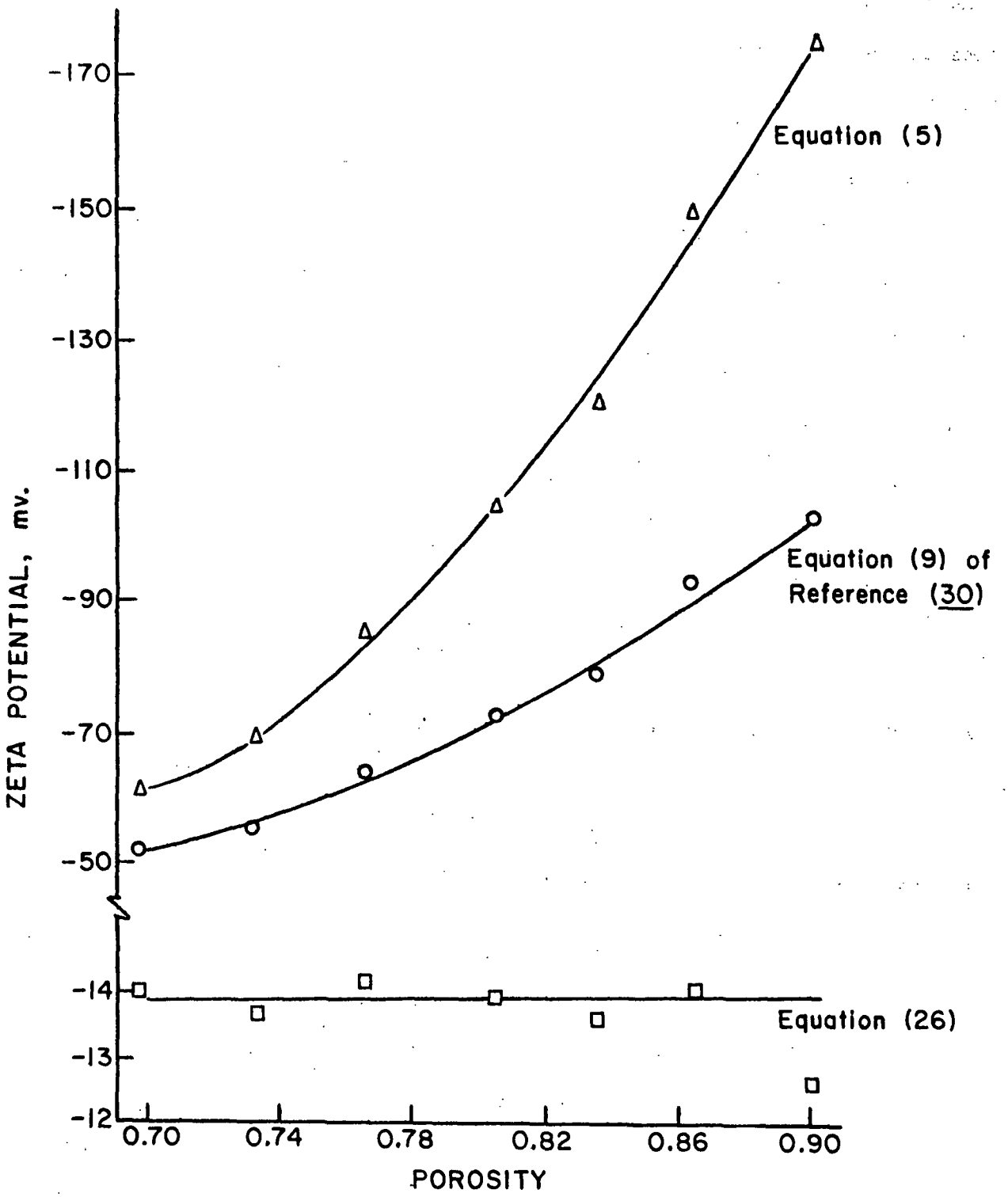

Figure 2. Zeta Potential vs. Porosity for a Dacron Mat at 10^{-4} M KCl (29)

ION TYPE AND CONCENTRATION

Numerous studies have been reported concerning the effect of various salt solutions on the zeta potential of fibers. A few of these studies will be reviewed and summarized.

Neale and Peters (27) used the streaming current method to measure the zeta potential of cotton fibers and found that ζ decreased in magnitude with increasing concentrations for solutions of LiCl, NaCl, and KCl. Hastbacka and Nordman (34) measured ζ for a sulfite pulp as a function of the concentration of $AlCl_3$ and $ThCl_4$. They reported an initial increase in the magnitude of ζ followed by a decrease when the solution concentration was increased. With $ThCl_4$ at high concentrations, a reversal in sign of ζ was reported (ζ became positive).

Yurev and Pozin (35) studied pulps which had been saturated with Ca, Cu, and Al ions from 0.1N solutions at various pH levels. They reported that the zeta potential decreased in magnitude with increasing amounts of adsorbed ion.

Ciriacks (29) studied the effect of the concentration of KCl and $CaCl_2$ on zeta potential of dacron fibers. He found that as the electrolyte concentration was increased, ζ decreased in magnitude for both salts. Also, the observed ζ in the $CaCl_2$ solutions was lower in magnitude than in KCl solutions.

These results have generally been explained in terms of "collapse" of the double layer. According to the Gouy-Chapman equations, the higher the electrolyte concentration, the more rapid the decrease in the potential vs. distance from the O.H.P. Also, for a given concentration, the double layer thickness decreases with increasing valence in approximate proportion to the inverse sixth power as predicted by the Schulze-Hardy rule. Reversals of sign, while not common, may occur due to adsorption of multivalent cations.

In general, studies of the effect of ion type and concentration give results which are explainable in terms of the double layer models which have been proposed. Because of this they provide some evidence that these models are correct.

SURFACE CHARACTERISTICS

Many studies have also been reported which are concerned with surface properties. Factors such as surface roughness and chemical composition of the surface have been shown to have great effects on the zeta potential.

As discussed by Davies and Rideal (6, page 140), a solid surface may ordinarily have "valleys" which are of the order of 10^{-6} or 10^{-7} cm. below the surface. During shear, the moving liquid will not penetrate these irregularities but will slide across them. Surface roughness could, therefore, increase the charge-bearing surface relative to the hydrodynamic plane of shear and thereby increase the magnitude of ζ. Studies on materials with smooth and rough surfaces tend to confirm this hypothesis (6, page 140).

A few studies have been made concerning the effect of substituent groups on the zeta potential of fibers.

Balodis (36) found that for acetylated and propionated cellulose fibers, ζ first decreased then increased in magnitude as the degree of substitution (D.S.) was increased. Bukhteev and Yur'ev (37) studied the effect of p-nitrobenzoyl and aminonitrobenzoyl substitution on the zeta potential of cellulose. It was found that as the D.S. was increased, the magnitude of the zeta potential increased. A similar behavior was reported by Bukhteev and Yur'ev (38) for benzyl-, methyl-, cyanoethyl-, and diethyl-amino-cellulose.

Several studies have been made to determine the effect of carboxyl groups on the zeta potential. Neale and Peters (27) found that the magnitude of ζ for an

oxidized cotton fiber was less than that of the unoxidized fiber. Ninck Blok (39) found that the magnitude of the zeta potential decreased in a regular manner as the carboxyl content of cellulose was increased from about 0.01 to 0.05 meq./g. of cellulose. Yur'ev and Pozin (40) reported similar results for samples of cotton and bleached sulfite pulp which had been oxidized. Lafaye and Jacquelin (41) have reported that oxidation of rayon fibers decreased the magnitude of the zeta potential.

ORIGIN OF THE CHARGE AT A SOLID-LIQUID INTERFACE

Studies of the zeta potential of materials lead to questions concerning the origin of the charge on these materials. The charge on a dispersed solid in a lyophobic sol is usually caused by adsorption of ions. The source of the charge on lyophilic sols is obscured by factors such as polarity, hydration, swelling, and macromolecular structure.

MECHANISMS BY WHICH CHARGES ORIGINATE

In general, there are three mechanisms by which a solid surface can become charged (5):

(1) The crystal lattice of a solid may contain a net positive or negative charge due to interior defects or lattice substitutions by ions of different valency. In contact with water, the compensating ions dissociate to form the counterions of the double layer. Solids containing ionizable groups may be considered as belonging to this class.

(2) Sparingly soluble ionic solids dispersed in water dissolve to an extent determined by their solubility product. An equilibrium will exist between ions making up the surface of the solid

and these same ions in solution. Solids of this class are characterized by having potential-determining ions.

(3) Some solids are capable of specific adsorption of particular ions. These ions may be strongly adsorbed or chemisorbed by formation of a surface complex. This mechanism is usually not responsible for the entire charge or potential of a solid surface. It is, however, frequently a complicating factor in other mechanisms.

POSSIBLE ORIGINS FOR THE CHARGE ON CELLULOSE

Several theories have been proposed to account for the negative surface charge on cellulose fibers. These theories generally suggest that ionization, adsorption of suitable ions, or the structure of water immediately surrounding the carbohydrate surface are responsible for the surface potentials.

Neale and Peters (27) considered three possible means for fibers to acquire a negative charge. These were dissociation of a proton, adsorption of suitable ions, and acquisition of electrons of water. Measurements of ζ for cotton, oxidized cotton, and vinyon (copolymer of vinyl chloride and vinyl acetate) showed a decrease in the magnitude of ζ with an increase in the dissociation of structural groups. The magnitude of ζ also decreased with increasing salt concentrations. They concluded that the negative potential was somehow a result of water and may arise from orientation of these molecules at the fiber surface, although no explanation was given.

Jacquelin and Bourlas (42) studied the effects of several preliminary treatments on ζ for a kraft pulp. Demineralization was found to increase the magnitude of ζ and their conclusion was that these results are consistent with the hypothesis that carboxyl groups may be responsible for the negative charge of pulp fibers.

Stamm (43) has suggested that the zeta potential of pulp fibers may be the result of ionized hydroxyl groups. Balodis (36) used this hypothesis to explain his results of ζ measurements on esterified pulp fibers.

Neale and Standring (44) measured the Donnan potentials of cellophane samples which had been oxidized to various degrees. They found that the Donnan potential increased in magnitude in a linear manner with increasing carboxyl content. It was also determined that the Donnan potential was zero at zero carboxyl content. From these data, they concluded that the charge on cellulose was due to carboxyl groups.

PRESENTATION OF THE PROBLEM

In general, the literature review has shown that in the development of electric double layer theory, the models proposed to account for double layer effects give reasonable results for 1-1 electrolytes when $\underline{c} < 0.01\underline{M}$ and $\psi_\delta < 100$ mv. The application of present theories to nonequilibrium conditions (current flowing through the diffuse layer) appears valid. Possible effects of viscosity and dielectric constant variations within the diffuse layer as well as liquid immobilization near the O.H.P. may require that $\underline{c}$ be less than $0.01\underline{M}$ and $\psi_\delta < 50$ mv. in order that ζ, as calculated from the classical electrokinetic equations, be approximately equal to ψ_δ.

The application of the electric double layer models to the study of electrokinetic effects requires the incorporation of a flow model. For fibrous systems, streaming current techniques have been used fairly successfully. However, the use of the capillary model to describe the flow through fibrous mats has resulted in several discrepancies. The anisotropic nature of fibers seems to be the cause of these discrepancies. The work of Ciriacks (29), in which the Happel flow model was used, has resulted in an improved method for calculating ζ for fibrous systems.

The results of streaming current studies of fibrous systems show that cellulose fibers have a negative charge. However, there has been no conclusive proof concerning the origin of this charge.

The hypothesis has been made that the negative charge on cellulose fibers originates from carboxyl groups. However, it has been reported that increasing the carboxyl content of the fibers by oxidation results in a less negative zeta potential. Since carboxyl groups are highly electronegative, it would seem that if they were the source of the negative charge, increasing the number of carboxyl groups would result in a more negative charge on the fiber.

Several questions arise from the literature data on carboxyl content vs. zeta potential. The studies which have been reported all used oxidation procedures to increase the carboxyl content of cellulose fibers. These oxidation procedures undoubtedly affected the physical structure of the fiber as well as the chemical composition. The effect of structural changes on the calculated zeta potentials is not understood and this could drastically affect the zeta potential, as calculated from streaming current measurements.

The use of the capillary model also casts some doubt on the reported carboxyl content vs. zeta potential relationships since the use of this flow model has been shown to give rise to discrepancies in the calculated zeta potentials.

In order to clarify these questions, the present study was undertaken. The objective of this study was to investigate the relationship between carboxyl content and zeta potential for a well-defined fibrous system, and to determine the reasons for the behavior found.

This investigation required a cylindrical, nonswelling fiber with a varying carboxyl content. This would allow the application of the Happel flow model to streaming current data in order to calculate the zeta potential of the fiber.

The primary objectives of this study were, thus:

1. Determine the zeta potential vs. carboxyl content behavior for a well-defined fiber system through the application of streaming current techniques using the Happel flow model.
2. Investigate the nature of the dissociation of the carboxyl groups and the influence of this on the resulting zeta potentials.
3. Ultimately provide a better understanding of the origin of the negative charge on cellulose fibers and the behavior of this charge under varying pH and ionic strength conditions.

EXPERIMENTAL

The approach used in this study required a material whose carboxyl content could be changed without appreciably changing other chemical or physical characteristics. In order to determine the zeta potential of the material, it was decided to use the streaming current method used by Ciriacks (29). This required cylindrical, nonswelling fibers.

In order to fulfill these requirements as closely as possible, a dacron fiber with adsorbed polyacrylic acid (PAA) was used. The dacron-PAA system was essentially nonswelling and the amount of adsorbed PAA could be varied so that the carboxyl content of the fiber could be changed.

FIBER-POLYMER SYSTEM

The dacron fibers used in this study were obtained from the same batch as those used by Ciriacks (29). They were Du Pont Type 54, semidull polyester staple. The fibers had a length of 6.0 mm. and a diameter of 17.4 μm., with a specific volume of 0.67 cc./g. Prior to use, the fibers were extracted with ethanol and warm (50°C.) distilled water.

Nylon and glass fibers were considered for use in this study. Ciriacks (29) was unable to obtain reproducible ζ values with nylon fibers. Preliminary adsorption experiments with glass fibers were of questionable value due to high exchange capacities as measured by the NaCl-$NaHCO_3$ method. Thus, neither nylon nor glass fibers were used in this study.

Two samples of PAA were used in this study. Preliminary adsorption experiments were performed with a sample of PAA which was synthesized from acrylonitrile. The PAA used for the final adsorption experiments was a commercially available sample.

The synthesized PAA was prepared according to methods described by Sorenson and Campbell (45) and Sonnerskog (46). Essentially, this involves a free radical polymerization of acrylonitrile to give polyacrylonitrile. This polymer was hydrolyzed with NaOH to give PAA.

DACRON-PAA ADSORPTION EXPERIMENTS

Preliminary adsorption experiments were done so that the amount of PAA adsorbed could be approximated and the adsorption process could be characterized. This was accomplished by determining the effects of concentration, pH, time, and amount of washing on the amount of PAA adsorbed.

The adsorption experiments were run according to the following basic procedure.

A sample of dacron (usually 2.5 g.) was placed in a polyethylene bottle with 150 ml. of PAA solution at the desired concentration and pH. The bottles were placed on a rotator, at room temperature, for 100 hours. A sample of the PAA solution was then removed for analysis and the fibers were removed and filtered. Washing was done by placing the fibers in a 500-ml. flask with 250 ml. of distilled water. The flask was shaken for one minute and the slurry was filtered. This operation was repeated four times.

To determine the effect of concentration, a solution of PAA at pH 4 with a carboxyl content of 0.5 meq./100 ml. was prepared. Aliquots of this solution were diluted with water at pH 4, and the basic adsorption procedure was followed from this point.

The effect of pH was determined by running adsorption experiments at pH 2, 4, 7, and 10. The pH of the PAA solution (0.5 meq./100 ml. carboxyl content) was adjusted with HCl or KOH.

Experiments were conducted for various time intervals to determine the effect of this variable. Samples were removed from the rotator after the desired time interval and analyzed.

The effect of washing was determined in an experiment where 7.5 g. of dacron was placed in 450 ml. of PAA solution. After the adsorption process, the fibers were filtered and divided by weight into three equal samples. The samples were then washed 5, 10, and 25 times using the procedure described previously.

Three methods were used to determine the amount of PAA adsorbed onto the fibers. These methods were potentiometric titrations, turbidity titrations, and the $NaCl$-$NaHCO_3$ method as described in TAPPI Standards (47).

POTENTIOMETRIC TITRATIONS OF FIBER SLURRIES

Potentiometric titrations were used to determine the carboxyl content of the fibers (before and after PAA adsorption). The method used here was based on techniques described by Kenchington (48) for the titration of polymers and by Ant-Wuorinen and Visapaa (49) for the titration of cellulose fibers containing carboxyl groups.

Basically, one experimental titration consisted of the following: A 2-g. sample of the fiber was weighed accurately and placed in 200 ml. of 0.1M KCl. This slurry was placed in a titration cell and stirred. Purified nitrogen was bubbled through the slurry to remove CO_2. Aliquots of 0.2N HCl or KOH were added with a microburet and the pH was monitored.

Appendix II gives the details of the experimental apparatus used in these titrations.

TURBIDITY TITRATIONS OF PAA SOLUTIONS

An independent measurement of the amount of PAA adsorbed was provided by turbidity titrations of the PAA adsorption solutions. The difference in the amount of PAA in the adsorption solutions before and after adsorption gave the amount of PAA adsorbed.

This technique was described by Lopatin (50) and Lauria (51) and has been used to measure the adsorption of PAA on various substrates.

The method involves the titration of a polyanion (ionized PAA) with a polycation, poly (N-n-butyl 4-vinyl pyridinium bromide) (PVPB). The turbidity which develops on adding small quantities of the titrant under continuous stirring is measured by light scattering. Titrations of solutions of known polyanion concentration enables a calibration curve to be constructed. From this, the concentration of unknown polyanion solutions can be determined. The accuracy of the method has been reported as 0.2 p.p.m. (50, 51).

PVPB was synthesized by a procedure described in Appendix II. The turbidity which developed after adding aliquots of a PVPB solution to the PAA solutions was measured at 90° with a Brice-Phoenix light-scattering instrument.

NaCl-$NaHCO_3$ METHOD

This method depends on the ion exchange capacity of the carboxyl groups to determine the carboxyl content of the fiber.

Briefly, the procedure for this method is as follows: The moisture content of the fiber sample is determined, and it is dispersed to about 1% consistency in a 0.1N HCl solution for two hours. The sample is then filtered and washed with distilled water, that has been saturated with carbon dioxide, until all the acid has

been removed. The wet sample is then weighed and allowed to equilibrate with a sodium chloride-sodium bicarbonate solution for one hour. The solution is then filtered through a clean, dry, fritted-glass filter and an aliquot of the filtrate is titrated with 0.1N HCl. The difference between the $NaHCO_3$ concentration of the filtrate and the original $NaCl$-$NaHCO_3$ solution is a measure of the ion exchange capacity of the fibers.

ZETA POTENTIAL MEASUREMENTS

The method used to measure the zeta potential of the fibers required several criteria from the experimental assembly. The fibers had to be formed into mats with the axes of the fibers perpendicular to the fluid flow and the flow system had to be capable of constant-rate permeation with deaerated fluids. Also, electrodes which did not polarize easily were required. The experimental assembly used to meet these requirements will be discussed in general terms here, and details will be given in Appendix II.

ELECTRODES

It is not possible to have completely nonpolarizable electrodes, but silver-silver chloride electrodes approach this ideal state (52). Electrodes were constructed from silver sheets according to the procedure given in Appendix II. The mat was formed directly on the downstream electrode. The other electrode was placed on top of the mat after it had been formed.

MAT FORMATION

The fibers were slurried at 0.01% consistency to minimize flocculation. The slurry was gravity fed to the forming tube with the downstream electrode in place. The electrolyte solution was pumped out of the bottom of the forming tube and part of this electrolyte was saved for subsequent permeation.

The low consistency used in forming the mat resulted in mats which consisted mainly of fibers whose axes were perpendicular to the fluid flow. As discussed by Ciriacks (29), edge effects will cause fibers next to the edge of the tube to have some orientation in the direction of flow.

Figure 3 is a schematic diagram of the apparatus used to form the mats and Fig. 4 is a photograph of the forming tube.

PROCEDURE FOR MEASURING STREAMING CURRENT

When the pad was formed on the downstream electrode, a second electrode was placed on the pad. This electrode was connected to a hydraulic ram so that the pad could be compressed.

Electrolyte solution was then fed to the top of the forming tube and pumped through the pad at various velocities. The streaming current, I_s, was measured by means of a low-resistance galvanometer at each fluid velocity at several porosities.

Measurements were made of each of the following parameters during the streaming current runs: pad thickness, load applied to the pad, pressure drop across the pad, electrical resistance of the pad, pad weight, flow rate, current, electrolyte concentration, and electrolyte pH. Appendix II gives the details of these measurements.

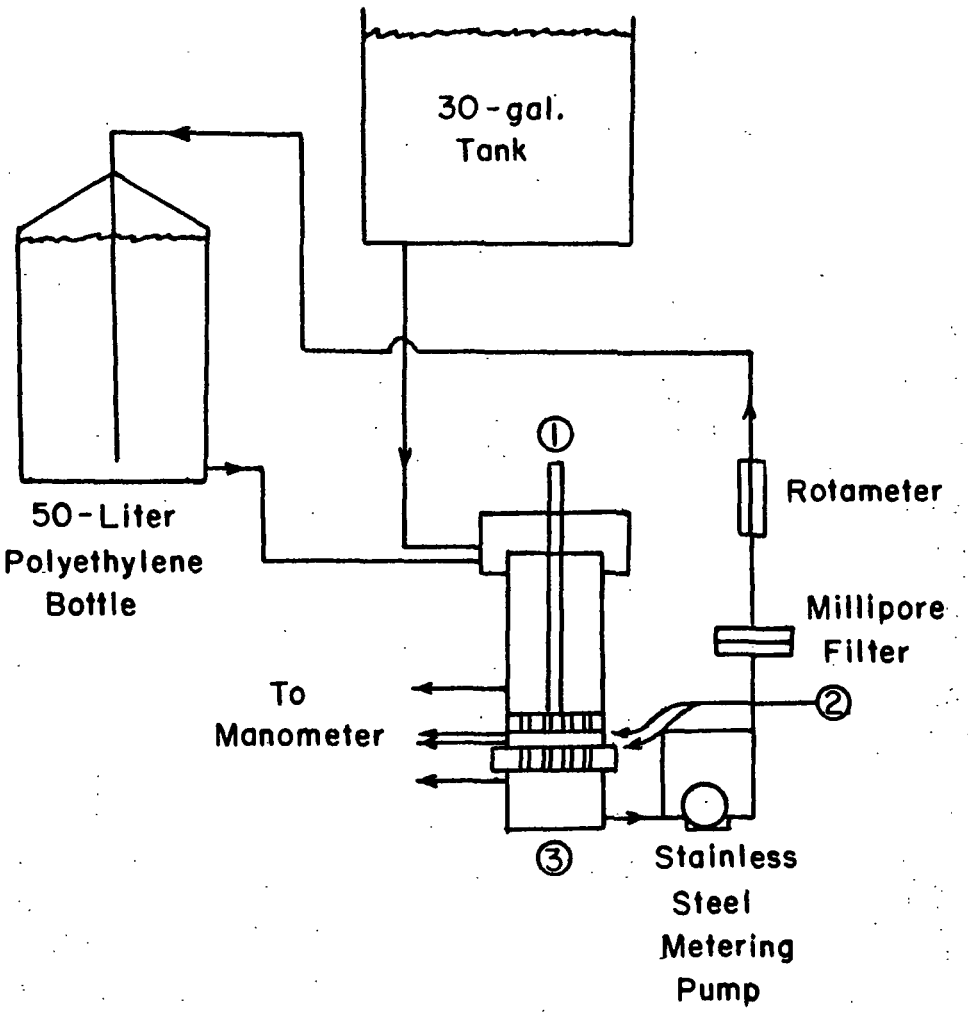

Figure 3. Flow System for Streaming Current Measurements

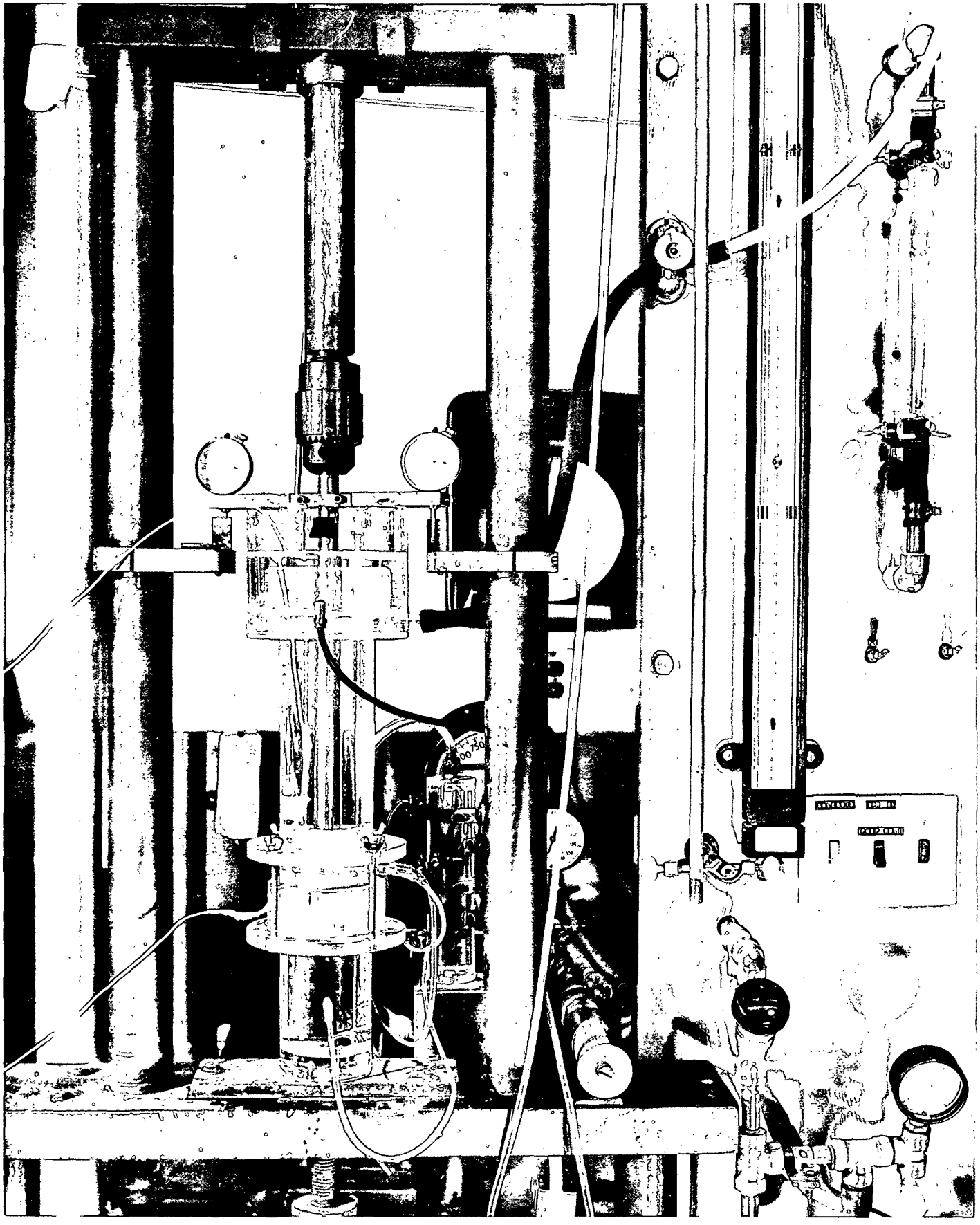

Figure 4. Streaming Current Apparatus — Forming Tube

RESULTS AND DISCUSSION

DACRON PAA ADSORPTION

Polymer adsorption is a complex field and it is difficult to make generalizations about the subject. In attempting to describe polymer adsorption, various sophisticated models have been developed, which are based on a mass action approach, and have included various assumptions concerning adsorption statistics (e.g., a Gaussian distribution of end-to-end distances). It has been found, however, that most polymer adsorption data fit the simple Langmuir equation within experimental error (8, p. 409). In addition, adsorption has been found to level off after several days or months and this adsorption is partially reversible only at high surface coverage (8). In systems involving polyelectrolytes, adsorption is highly dependent on pH. The nature of this dependence is, of course, contingent upon the adsorbate and adsorbent being used.

Several studies involving the adsorption of polymethacrylic acid (PMAA) and PAA have been reported in the literature. Michaels and Morelos (53) investigated the adsorption of PAA on kaolinite in the pH range of 5 to 8. They found that PAA was adsorbed up to about 0.4 meq. carboxyl/100 g. of kaolinite. Also, the adsorption decreased as pH was increased. Lopatin (50) and Lauria (51) found similar behavior with PMAA and PAA on anatase.

Nestler (54) studied the adsorption of PAA on calcium sulfate crystals in saturated $CaSO_4$ solutions and found that adsorption increased with increasing pH. In this study, it was also reported that equilibrium was reached quite rapidly, in about 10 minutes, and that adsorption was essentially irreversible.

Lauria (51) studied the adsorption of PAA on polymethacrylate beads, polystyrene beads, and anatase. He found no changes in adsorption after 30 hours.

It was also reported that partial desorption occurred in water at the same pH as the absorbent after 70 hours.

With these studies in mind, initial adsorption experiments were designed to characterize the adsorption of PAA on dacron fibers. The results of these experiments were then used to determine conditions to be used to obtain dacron-PAA fibers for use in later experiments.

The dacron fibers used in this study have been described previously. The PAA used for these experiments was synthesized from acrylonitrile. The viscosity of the polyacrylonitrile was measured in DMF using a number 75 Ubbelohde viscometer. The molecular weight was calculated from the equation

$$[\eta] = 1.75 \times 10^{-3}(M)^{0.66} \qquad (7)$$

where $[\eta]$ is the intrinsic viscosity and ($\underline{M}$) is the viscosity average molecular weight (55, 56). The molecular weight was found to be 48,000. Assuming no change in the D.P. of the polymer upon hydrolysis, the resulting PAA would have a molecular weight of about 58,000 (D.P. of 800).

Figures 5 and 6 and Table VII in Appendix III give the results of these adsorption experiments. Here the values plotted on the ordinate are the difference in carboxyl content of the fibers before and after adsorption. The carboxyl contents were determined by the NaCl-$NaHCO_3$ method as described in TAPPI Standards (47) and are expressed as meq. of carboxyl/100 g. of dacron fiber.

The measured carboxyl contents have an estimated average error of ± 0.05 meq./100 g. Repeat measurements have given error ranges of 0.02 to 0.2 meq./100 g. Wilson and Mandel (57) have made a statistical study of the use of the NaCl-$NaHCO_3$ method and found that the coefficient of variation was 20% for fibers containing 0.5 meq./100 g. carboxyl content and 5% for fibers containing 5 meq./100 g.

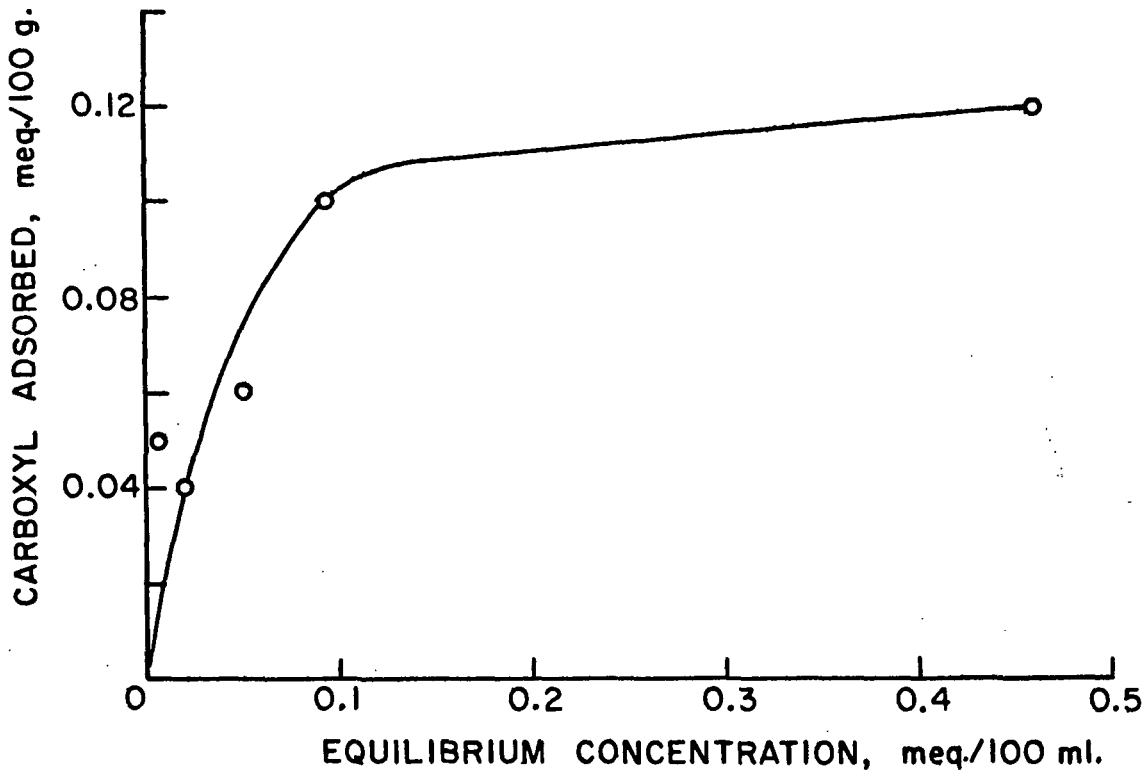

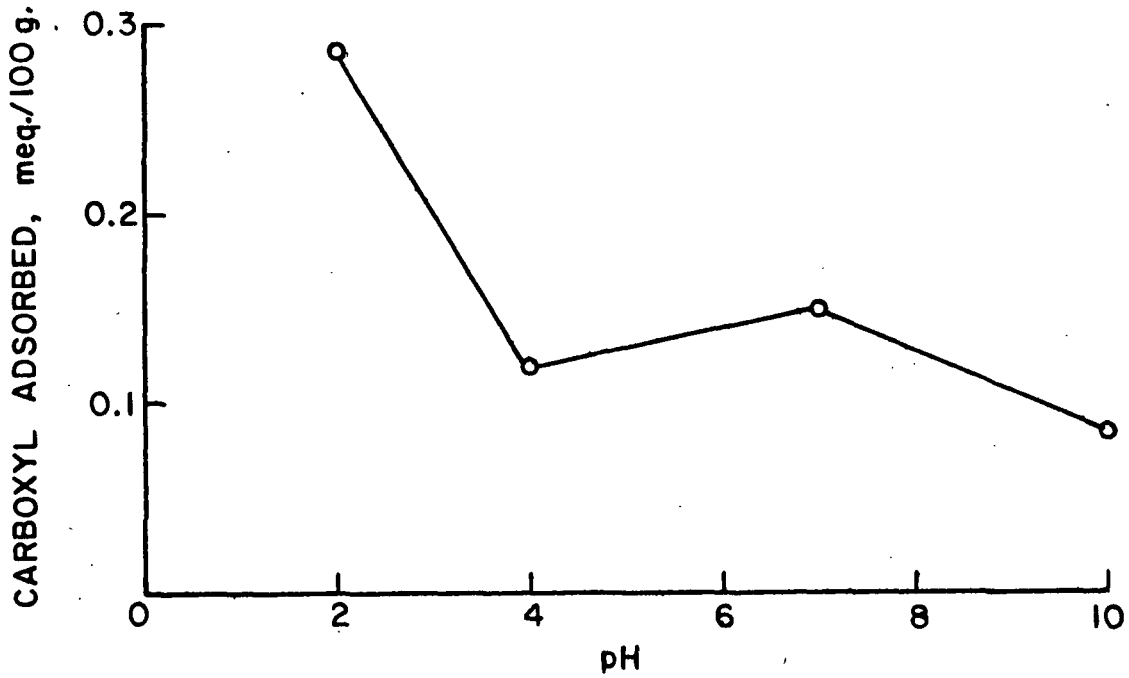

Figure 5. Dacron-PAA Isotherms

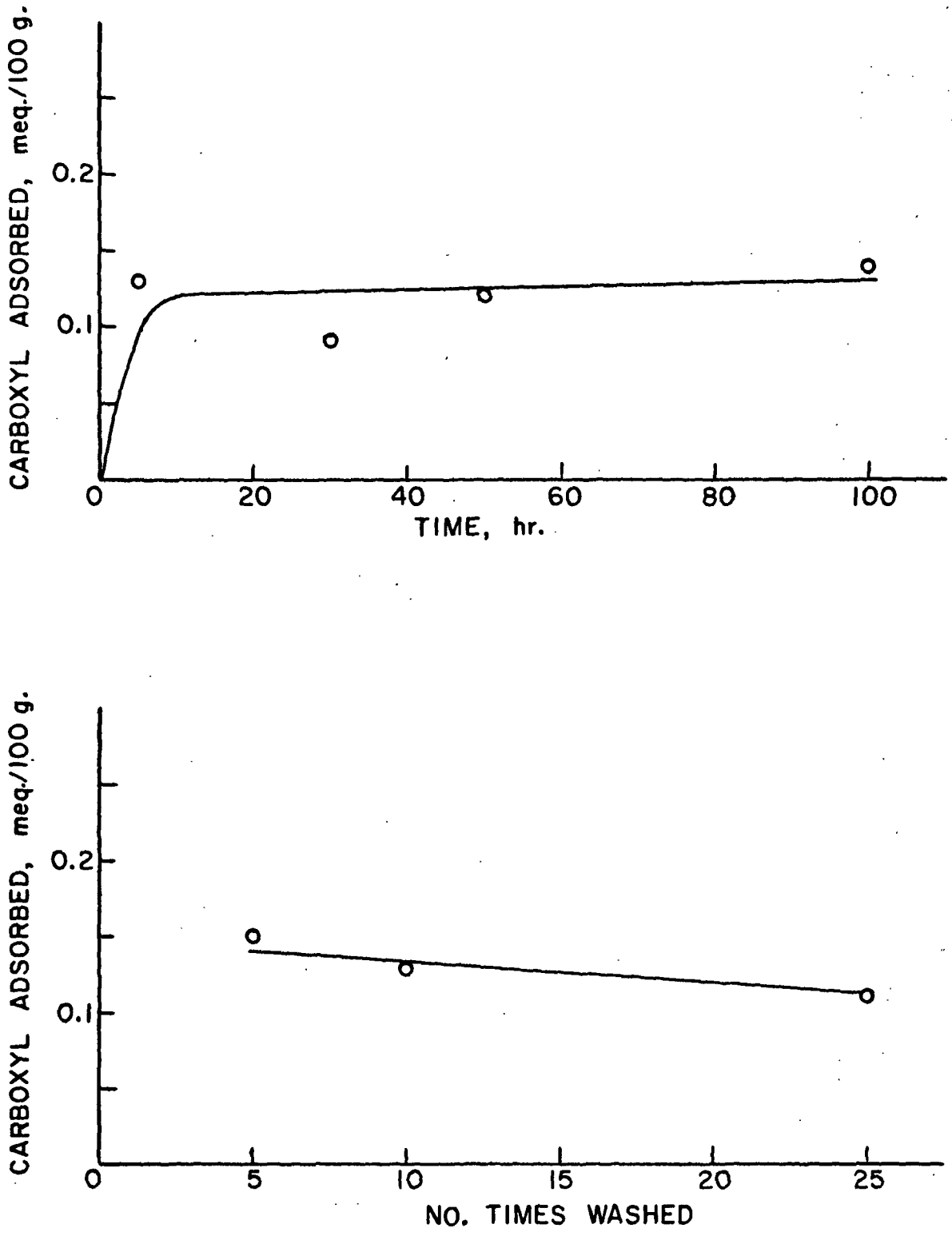

Figure 6. Dacron-PAA Isotherms

The equilibrium concentrations of PAA for these initial experiments were determined by means of conductivity titrations. This technique involved adding aliquots of HCl or KOH to the polymer solution and measuring the conductivity. A plot of conductivity vs. amount of HCl or KOH added results in a curve with a sharp discontinuity indicating the end point of the titration. The accuracy of these determinations was about ± 2%.

From the data, it can be concluded that the dacron-PAA system is fairly typical of polymer adsorption in so far as equilibrium concentration, time, and degree of washing are concerned. The pH isotherm is consistent with results found by previous workers in that adsorption falls off with increasing pH.

The time isotherm indicates that equilibrium is probably reached in less than ten hours. The washing experiment shows only a slight decrease in carboxyl content as the fibers are repeatedly washed. This indicates that the PAA is essentially irreversibly adsorbed. Potentiometric titrations were used to measure PAA removal during the zeta potential runs. This will be discussed later.

The measurement of the carboxyl content requires an acid wash (1% HCl) as an initial treatment to displace metal cations from the carboxyl groups. Measurements with and without this acid wash were made to determine the effect of this treatment. No difference was found and it was concluded that this treatment did not cause desorption of the PAA.

In summary, these initial adsorption data indicate that for the dacron-PAA system, typical polymer adsorption behavior was found. Maximum adsorption, for the conditions used here, was about 0.3 meq. carboxyl/100 g. of dacron. Maximum adsorption occurred in less than 10 hours and the PAA was essentially irreversibly adsorbed. Adsorption was greatest at low pH.

POTENTIOMETRIC TITRATIONS OF DACRON-PAA

Potentiometric titrations of the dacron-PAA fiber system were performed for two reasons. First, a more accurate and reproducible method was needed for determination of the carboxyl content of the fibers, and, second, it was necessary to determine the ionization behavior of the carboxyl groups.

The initial titrations involved samples from adsorption experiments which had been carried out at three conditions in order to provide different carboxyl contents. These conditions were chosen from the adsorption studies described previously. Table I describes the conditions and the measured carboxyl contents. The fibers titrated here were prepared in adsorption runs consisting of 15 g. of dacron slurried in 1 liter of PAA solution for 120 hours. The fibers were washed 10 times after adsorption. The PAA used in these experiments was a commercially obtained sample with a molecular weight of about 120,000, as determined by viscosity measurements.

TABLE I

CARBOXYL CONTENTS OF DACRON AND DACRON-PAA FIBERS FROM POTENTIOMETRIC TITRATIONS

Fiber	Initial PAA Concentration, meq./100 g.	pH	Carboxyl Content, meq./100 g.
A	0.25	2.0	0.962 0.985 0.997
C	0.25	10.0	0.697 0.713
B	0.025	2.0	0.626 0.619
Blank		6.8	0.585 0.593 0.601 0.587

The results found for these titrations indicated that the carboxyl content could be measured quite accurately. Duplicate experiments showed a scatter of ± 0.01 meq./100 g. which corresponds to 1-2%. As seen in Table I, low pH and high initial concentration of PAA resulted in high carboxyl contents. This was consistent with the previous adsorption studies.

A new set of adsorption runs was then made to determine the effect of washing and drying. The adsorption experiments were carried out in a similar manner except that, after washing, part of the fibers were stored under distilled water prior to the titrations. The remainder of the fibers were used in the streaming current studies and, after drying, they were then titrated.

The results of these titrations are shown in Table II. These data show that the agitation and drying steps of the streaming current runs do not affect the carboxyl content values as determined by the potentiometric titration method.

TABLE II

CARBOXYL CONTENT OF FIBERS BEFORE AND AFTER DRYING

Fiber	pH	Initial PAA Concentration, meq./100 g.	Carboxyl Content, meq./100 g.	
			Water Slurry	After Drying
Blank	6.8	--	0.595	0.586
Dacron + PAA (A)	1.75	0.25	0.996	0.991
			1.05	0.987
Dacron + PAA (B)	2.0	0.025	0.641	0.649
			0.635	0.629
Dacron + PAA (C)	10.0	0.25	0.702	0.701
			0.698	0.711

The titration data from the later titrations were used to calculate degree of ionization curves for the fibers used. These curves are shown in Fig. 7. From these data, it is seen that the carboxyl groups of the blank fiber are

easiest to dissociate. Next comes Fiber C (as labeled in Table II), followed by B and A. Thus, as a sequence for ease of dissociation, it was found that: blank < C < B < A. It should be noted that for all fibers there was little difference in the dissociation behavior.

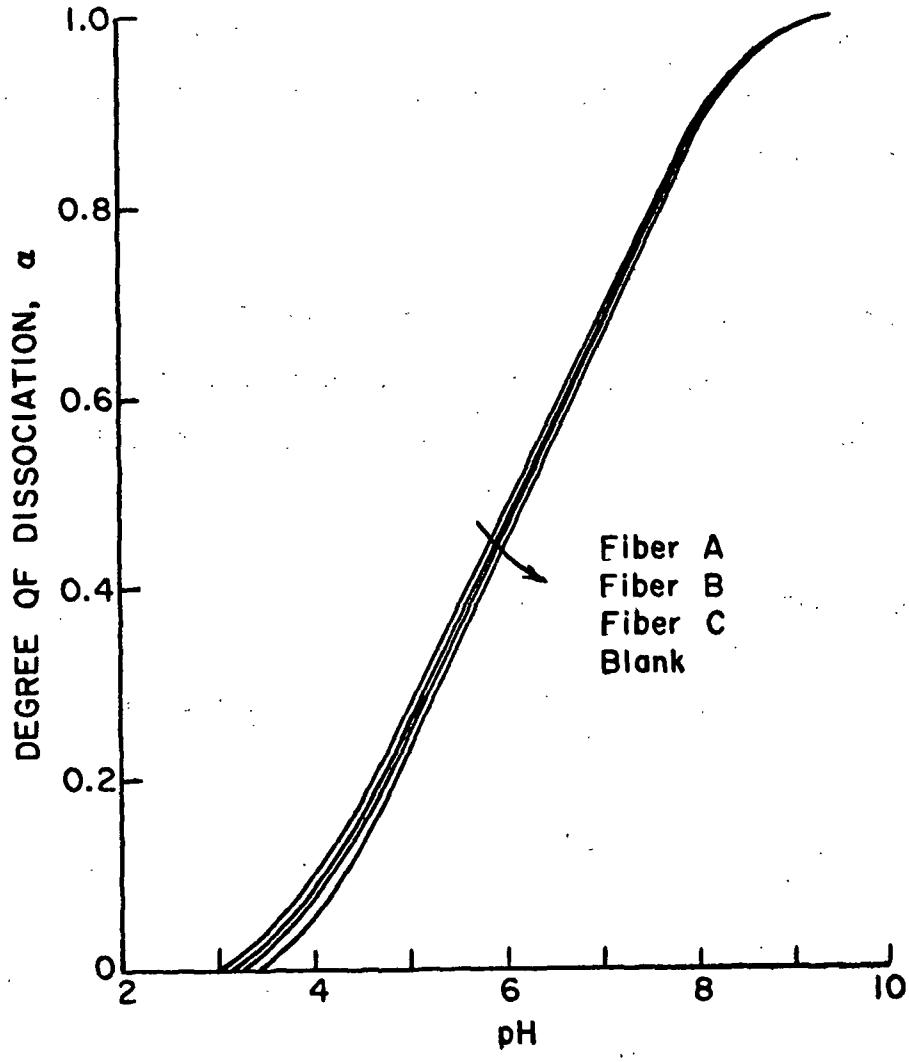

Figure 7. Degree of Dissociation

In general, the potentiometric titrations of the dacron-PAA fibers gave an accurate measurement of the carboxyl content of the fibers; they showed that there was no change in carboxyl content after streaming current runs were made, and they provided a description of the degree of dissociation as a function of pH. In addition, they confirmed that adsorption was greatest at low pH and high initial PAA concentration.

Appendix IV gives the calculations and the data for the potentiometric titrations.

TURBIDITY TITRATIONS

In order to obtain a measurement of the actual amount of PAA adsorbed, turbidity titrations were performed on the adsorption solutions. This technique measures the concentration of PAA in solution. The difference in concentration of the solution before and after contact with the dacron fibers was attributed to adsorption. The method has been used previously in PAA adsorption studies and the accuracy of the PAA concentrations as measured by this method has been reported at 0.2 p.p.m.

Table III gives the results of these titrations in terms of PAA adsorbed by the fibers. For comparison, the carboxyl content of the fibers as measured by the potentiometric titrations is also given. Appendix V gives the data and the details of the calculations used in determining the amount of PAA adsorbed.

In explaining these results, the assumption was made that the turbidity titration method gave the actual amount of PAA adsorbed on the surface of the fiber. The potentiometric titrations, however, give the carboxyl content of the fiber (both dacron carboxyl groups and PAA carboxyl groups) exposed to the solution. For all the dacron-PAA fibers, the potentiometric titrations showed a higher carboxyl

content than could be accounted for by the amount of PAA adsorbed. This indicates that the dacron carboxyl groups are influencing the potentiometric titrations.

TABLE III

AMOUNT OF PAA ADSORBED BY DACRON

Fiber	Adsorption Conditions	Carboxyl Content Pot. Titrations, meq./100 g.	PAA Adsorbed Turb. Titrations, meq./100 g.
Blank	--	0.59	--
Dacron + PAA (A)	pH 1.75 0.25 meq./100 ml.	1.03	0.9
Dacron + PAA (B)	pH 2.0 0.025 meq./100 ml.	0.64	0.2
Dacron + PAA (C)	pH 10.0 0.25 meq./100 ml.	0.70	0.1

The dacron-PAA fiber with the highest carboxyl content, Fiber A in Table III, has a carboxyl content only slightly higher than that which can be attributed to PAA adsorption. This dacron-PAA fiber could, therefore, be almost completely covered with PAA. The other two dacron-PAA fibers, B and C in Table III, are probably incompletely covered or the PAA layer may be quite "porous" in nature, thereby allowing the dacron carboxyls to be titratable by the potentiometric titration method.

ZETA POTENTIAL MEASUREMENTS

One of the main objectives of this study was to measure the zeta potential of fibers with varying carboxyl contents and to explain the behavior found. The dacron-PAA fibers described in Tables II and III were used in streaming current experiments and the resulting data were used to calculate the zeta potentials for the fibers. These calculations were done using the streaming current equation

based on the Happel flow model as described by Ciriacks (29). Appendix I gives a summary of the derivation of this equation. Appendix VI gives the streaming current data and a description of the calculations and corrections performed to obtain the calculated zeta potentials.

It should be pointed out that while the calculated values for ζ are not absolute values, the relative values calculated for fibers at differing conditions should be comparable. Also, it has been demonstrated that use of the Happel flow model rather than the usual capillary model results in improved values for ζ (29).

Streaming current runs were made at three different ionic strength levels and at five different pH conditions for the dacron and dacron-PAA fibers. The results of these experiments are summarized in Table IV and Fig. 8-10. The neutral electrolyte for all runs was KCl and the pH was adjusted with HCl or KOH.

In general, the zeta potential data show the following trends:

1. The zeta potential becomes less negative as the carboxyl content is increased (for dacron-PAA fibers).
2. The zeta potential becomes more negative as the pH is increased from 4 to about 7.
3. The zeta potential does not change as the pH is increased from about 7 to 10.
4. As the electrolyte concentration is increased, the zeta potential becomes less negative.
5. For all conditions, the zeta potential of the dacron itself was less negative than for the dacron with adsorbed PAA.

TABLE IV

ZETA POTENTIAL VALUES
(-mv.)

Electrolyte pH and Fiber	5×10^{-4} M [Cl^-]	1×10^{-4} M [Cl^-]	2×10^{-5} M [Cl^-]
pH 6.8			
Blank	8.0	13.4	13.2
A	9.6	14.3	14.6
B	14.5	19.9	20.5
C	13.7	19.0	19.6
pH 4.0			
Blank	7.5	10.9	--
A	8.9	11.3	--
B	10.7	16.5	--
C	10.0	15.3	--
pH 10.0			
Blank	7.9	13.2	--
A	9.6	14.6	--
B	14.2	19.7	--
C	13.2	19.0	--
pH 5.0			
Blank	--	--	12.9
A	--	--	14.0
B	--	--	18.9
C	--	--	17.7
pH 9.0			
Blank	--	--	13.6
A	--	--	14.8
B	--	--	20.1
C	--	--	19.0

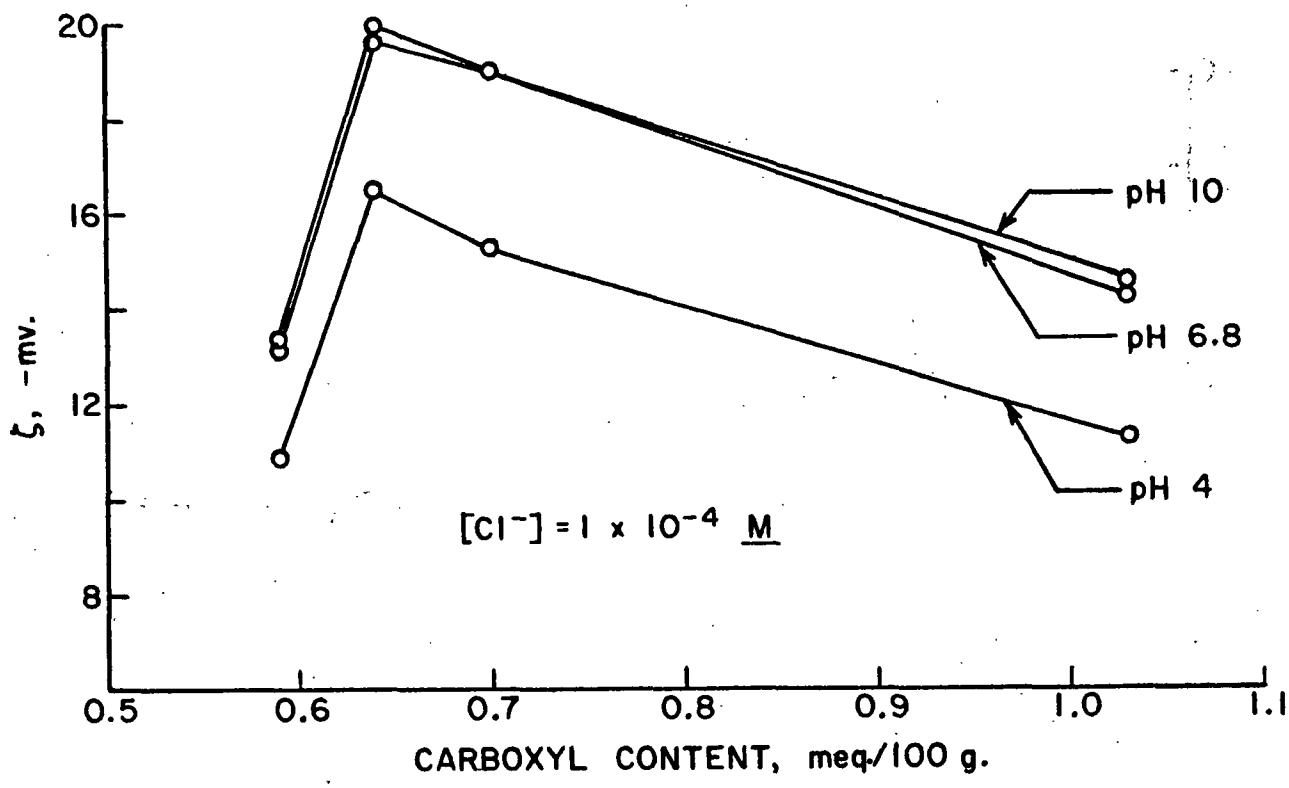

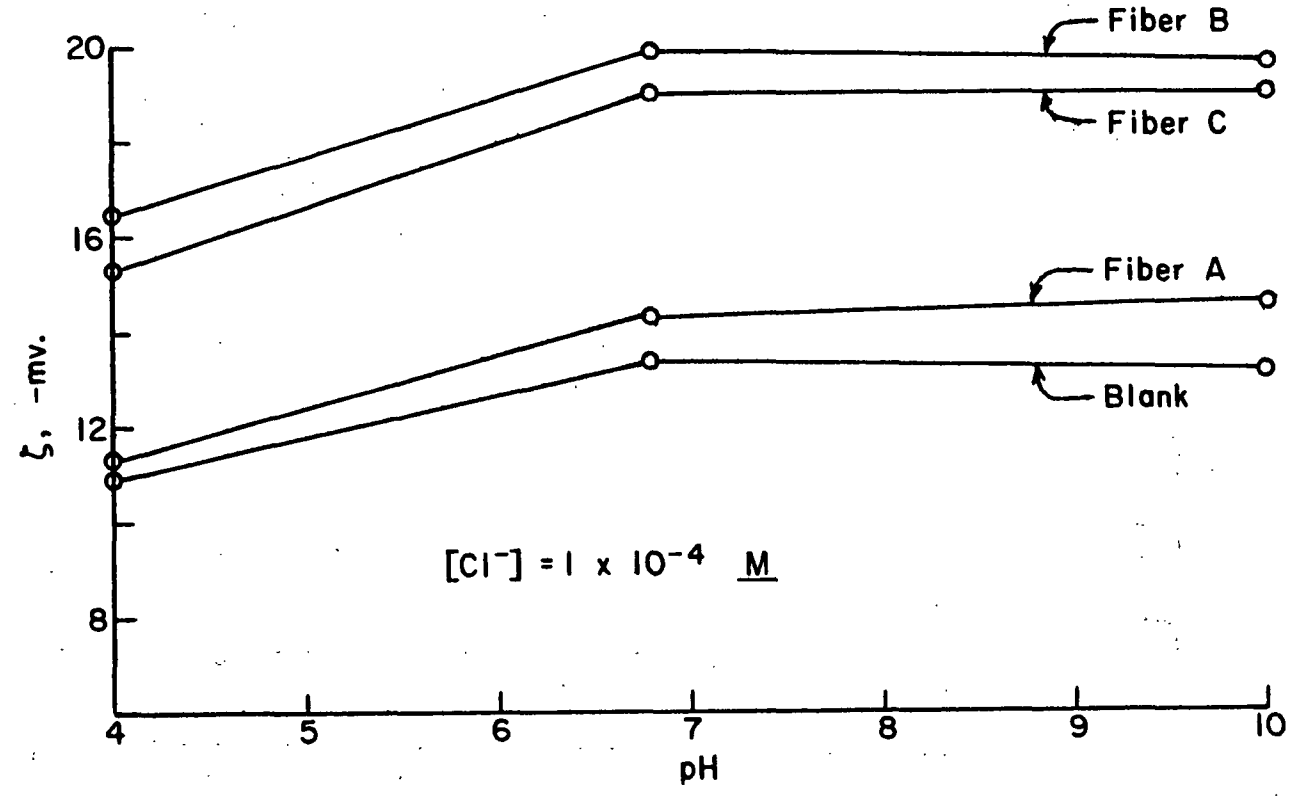

Figure 8. Zeta Potentials

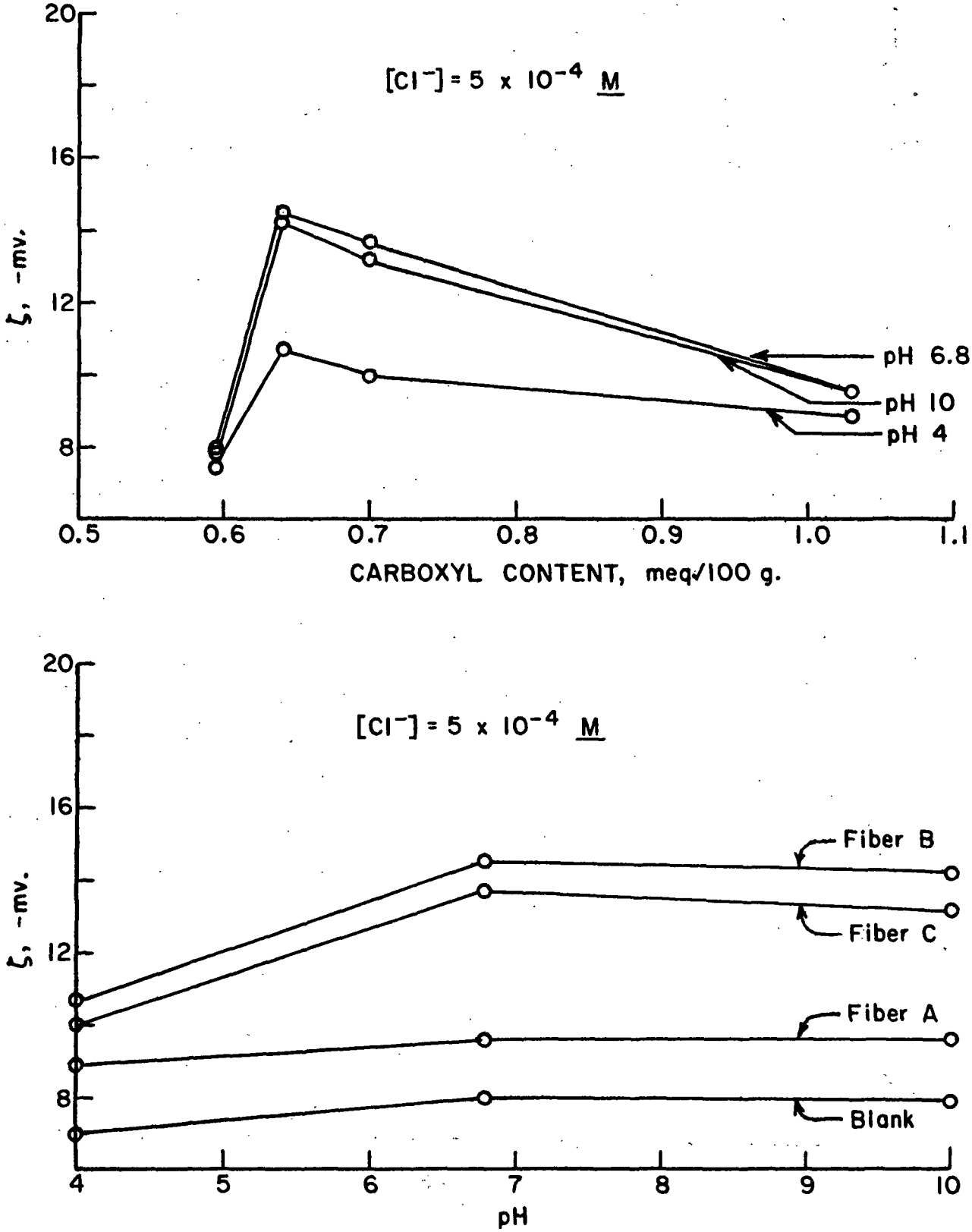

Figure 9. Zeta Potentials

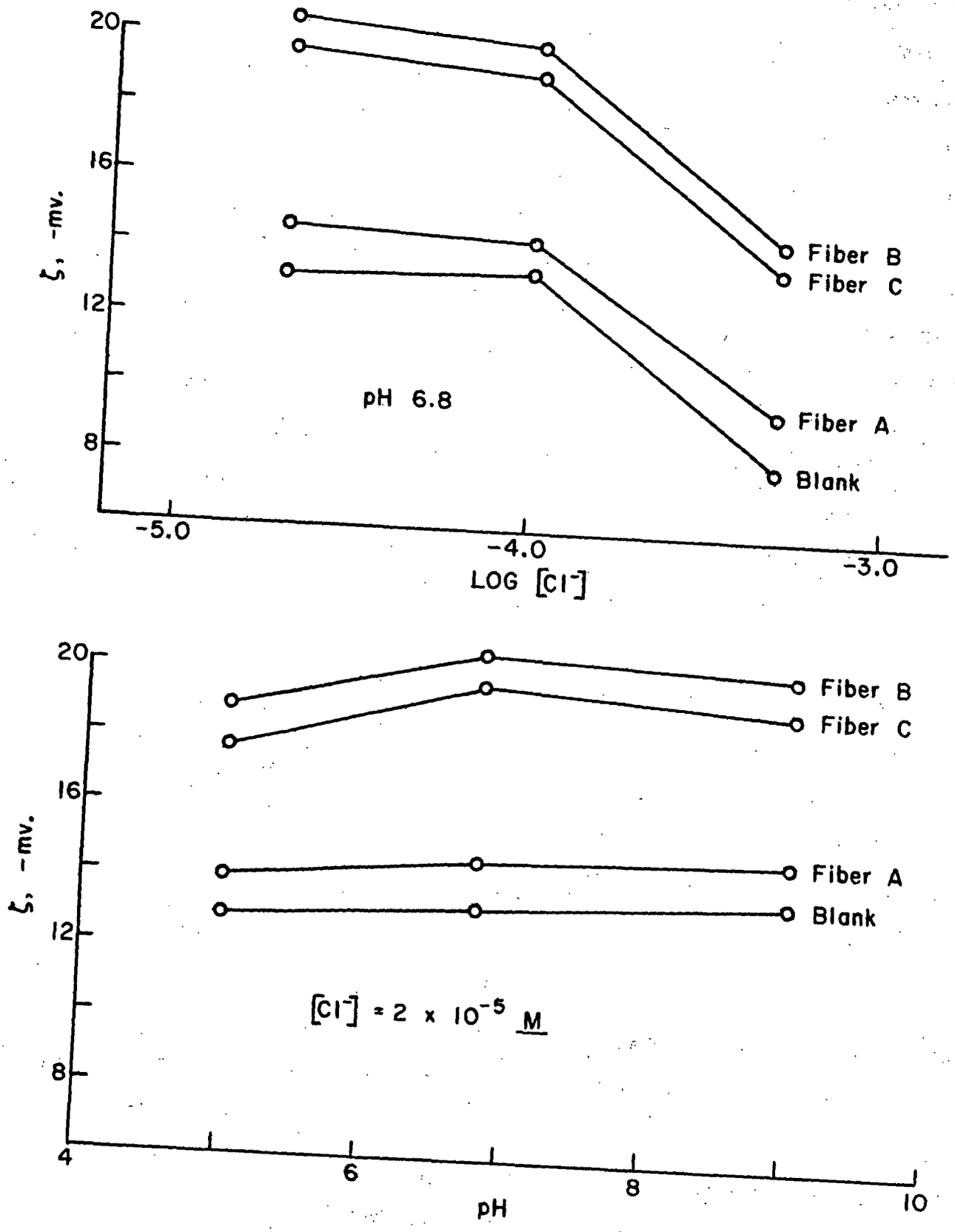

Figure 10. Zeta Potentials

The measured zeta potential variation with carboxyl content found in this study agrees with that reported in the literature for oxidized cellulose fibers. It was thought that the oxidation procedures used to increase the carboxyl content of cellulose fibers could change the morphology of these fibers in addition to their chemical structure. The resulting zeta potentials might not then be comparable because of changes in morphology. In addition, use of the capillary model could cause additional complications in determining the zeta potential variation with carboxyl content. In this study, however, zeta potential measurements have been made on a well-defined fiber system using the Happel model to predict fluid flow through the fiber mats. The resulting zeta potential data thus represent an improved measure of the variation of zeta potential with carboxyl content. In addition, zeta potential data are available for a range of electrolyte concentrations and pH values.

STRUCTURE OF ADSORBED PAA

Theories concerning the size and configuration of adsorbed polymers are in the beginning stages of their development. At the present time a lack of suitable methods prevents the exact size and shape of adsorbed polymers from being determined. Even though precise data are unobtainable, several approximations can be made which allow a reasonable estimate of the size and configuration of the adsorbed PAA used in the present study to be made.

Studies of adsorbed polymers have shown that these molecules retain approximately the same size and shape after adsorption that they had in solution (58, 59). The size of adsorbed polymers has been approximated for a few systems by means of viscosity measurements on small spheres and by means of flow measurements through capillaries, before and after adsorption (58, 59). Studies of polyelectrolyte adsorption have shown that results obtained are consistent with the assumption that

these polymers are also similar in size and shape before and after adsorption (51, 54). Also, it is generally believed that polymers are adsorbed in the form of loops (8, 60) and that these loops compete with solvent molecules for the available attachment sites. This is also consistent with the assumption that there is little change in the configuration and size of the polymer when adsorption occurs.

With the above discussion in mind, the assumption will be made that the PAA of the present study does not change its size or configuration appreciably upon adsorption. Several approximations concerning the PAA in solution can be made and these provide support for this assumption. The results obtained from the adsorption studies and the potentiometric and turbidity titrations also support this assumption.

The commercially obtained PAA sample used in the present study (except for the initial adsorption experiments) had a viscosity average molecular weight of 120,000. This was determined by measuring viscosities in dioxane at 30°C. and using the viscosity-molecular weight relation of Newmann, et al. (61):

$$[\eta] = 0.85 \times 10^{-3} M^{\frac{1}{2}} . \qquad (7)$$

The PAA thus has a D.P. of about 1700.

From statistical theories of polymer solutions it can be shown that the radius of gyration, $\underline{R}_g$, is given by:

$$\langle R_g^2 \rangle = (1/6)nb^2 \left(\frac{1+\cos\theta}{1-\cos\theta}\right)\left(\frac{1+\overline{\cos\phi}}{1-\overline{\cos\phi}}\right) \qquad (8)$$

where $\langle \underline{R}_g^2 \rangle$ is the average value of $\underline{R}_g^2$, $\underline{n}$ is the number of bonds, $\underline{b}$ is the bond length, and $\left(\frac{1+\cos\theta}{1-\cos\theta}\right)$ and $\left(\frac{1+\overline{\cos\phi}}{1-\overline{\cos\phi}}\right)$ are terms to correct for carbon-carbon bond angles and steric hindrances. The value of $\left(\frac{1+\cos\theta}{1-\cos\theta}\right)$ is 2 for C-C chains and the

value of $\left(\frac{1+\overline{\cos\phi}}{1-\overline{\cos\phi}}\right)$ is about 3.3 for PAA (61, 62). Even though this equation is based on a simplified model of a flexible, linear polymer, the calculated $\underline{R}_g$ should approximate the true value.

The value of $\underline{R}_g$ obtained from Equation (8) can be used to calculate a projected area (area of a plane covered by the projection of the molecule) for the adsorbed PAA. Comparison of this area with the available surface area of the dacron fibers would then give an indication of whether the adsorbed PAA is indeed similar in size to the PAA in solution. Equation (9) was used to calculate the projected area covered by the adsorbed PAA:

$$A = (C)(N_o(1/DP)(\pi R_g^2)) \qquad (9)$$

where $\underline{A}$ is the area covered by the PAA per 100 g. of fiber, $\underline{C}$ is the carboxyl content of adsorbed PAA in equivalents per 100 g., and $\underline{N}_o$ is Avogadro's number. The results of calculations using the carboxyl content of the adsorbed PAA, as determined by the turbidity titrations, are given in Table V. It should be noted that the use of $\underline{R}_g$ in this calculation does not consider excluded volume or electrostatic effects. PAA has a tightly coiled spherical configuration at low pH and an extended, rodlike configuration at high pH. Thus, the actual area covered by the PAA is probably lower than the calculated value at low pH and higher than the calculated value at high pH.

TABLE V

AREA COVERED BY ADSORBED PAA

Fiber	PAA Adsorbed, meq./100 g. fiber	Calculated Area Covered by PAA, A.^{2}/100 g.	
		$\underline{R}_g$ = 92 A. [Equation (9)]	$\underline{A}_m$ = 20 A.^{2} [Equation (10)]
A	0.9	8.5×10^{21}	11.0×10^{21}
B	0.2	1.9×10^{21}	2.4×10^{21}
C	0.1	1.0×10^{21}	1.2×10^{21}

Geometric surface area of dacron = 1.5×10^{21} A.^{2}/100 g. fiber.

Also included in Table V are the results of calculations based on an area per monomer of 20 A^2. This value was obtained by means of a surface balance from a force-area curve of PAA spread on an 0.1N HCl solution which was also 0.1M in calcium ions (54). It is thought that this value represents the surface area covered if the PAA segments were lying flat on the surface (54). Nestler (54) and Lauria (51) have used this value to calculate approximate surface area coverage for adsorbed PAA. Equation (10) was used to calculate the area that the adsorbed PAA would cover if it were lying flat.

$$A = (C)(N_o)(A_M) \qquad (10)$$

where A, C, and N_o have the same meaning as in Equation (9), and A_M is the area per monomer unit (20 $A.^2$).

The initial adsorption studies showed that the adsorbed PAA followed a Langmuir-type isotherm. This type of isotherm is generally found when monolayer adsorption occurs (8, 50). Previous studies of PAA adsorption (51, 54) on various substrates have shown adsorption to follow a Langmuir isotherm and monolayer adsorption was postulated for these studies. Thus, monolayer adsorption is likely for the present study and this is an assumption used in the above calculations.

The calculated values in Table V show that the use of R_g results in areas covered by the PAA that are about equivalent to or higher than the geometric surface area of the fiber. Fiber A was obtained with adsorption conditions of high PAA concentration and low pH and, therefore, represents a "saturated" condition: Since Fiber A corresponds to a position on the equilibrium isotherm at high concentration, practically no more PAA can be adsorbed onto this fiber. Fibers B and C, however, have less than the maximum amount of adsorbed PAA since these fibers were obtained at low PAA concentration or high pH conditions. Table V also shows that

the PAA is not lying flat on the surface, since the area covered by the PAA, if this were the case, is larger than the surface area of the dacron (except for Fiber C). Thus, the adsorbed PAA has a looped configuration and the assumption that the PAA does not change its size or configuration when adsorption occurs is reasonable.

As discussed previously, the turbidity and potentiometric titrations have shown that more carboxyl groups are present on the fibers than can be accounted for by PAA adsorption. It was concluded from this information that the adsorbed PAA had a somewhat porous configuration since the dacron carboxyl groups were accessible to the solution.

In summary, the adsorbed PAA has a similar size and shape as it had in solution. Thus, the dacron-PAA surface can be considered as a hydrophilic, partial-draining network of carboxyl groups. The adsorbed PAA will thus have many of the properties it has in solution.

It should be noted that since the adsorbed polymers compete with solvent molecules for attachment sites, there is probably a dynamic attachment-removal-reattachment process occurring. If this is the case, then the adsorbed PAA might be expected to change its configuration somewhat if the pH of the surrounding solvent was changed. PAA in solution changes from a tightly coiled sphere to a rodlike configuration when the degree of dissociation is increased. Similar changes may occur with the adsorbed PAA, although configuration changes would be restricted somewhat due to the attachment to the rigid surface.

CHARGE BEHAVIOR OF POLYELECTROLYTES

Since the adsorbed PAA is expected to have properties similar to PAA in solution, some of the properties of polyelectrolytes in solution will be examined in order to determine the effect of these properties on the charge behavior. Of particular

interest is the effect of the degree of dissociation on ion binding and on hydration, and the way these properties affect the charge behavior.

ION BINDING

Counterions in polyelectrolyte solutions are generally classified into three categories: (1) counterions moving freely outside the region or volume occupied by the polyelectrolyte, (2) those bound but mobile within the polyelectrolyte region, and (3) those bound to individual charged groups of the polyelectrolyte. The latter two types of counterions, (2) and (3), are indicated by the term ion binding or bound counterions. In the remainder of this paper, the terminology ion binding and bound counterions refer to those counterions which are contained within the volume occupied by the polyelectrolyte. The equilibrium between free counterions and bound counterions is obviously very important in determining the thermodynamic properties of polyelectrolytes.

Ion binding theory is just beginning to be developed and even though quantitative agreement with theory has been obtained for only a few types of experiments, qualitatively the agreement between theory and observation is good.

Three generalizations are considered valid in ion binding theory, and these are important in the present study: (1) For rodlike and spherical polyelectrolytes, the charge distribution is such that at the center of the volume occupied by the polyelectrolyte there is little free charge, but near the surface of this volume there is a concentration of free charge; (2) as the degree of dissociation is increased, the fraction of bound counterions increases; (3) when the concentration of polyelectrolyte is increased (with a fixed number of ionized groups per molecule), the apparent number of charges per molecule decreases (63, p. 449, 457; 64, p. 15-16, 40). These generalizations are illustrated in Fig. 11 to 13.

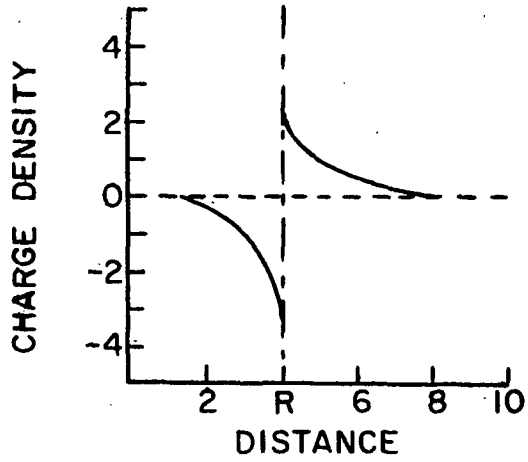

Figure 11. Charge Distribution at Surface of Polymer Sphere (63)

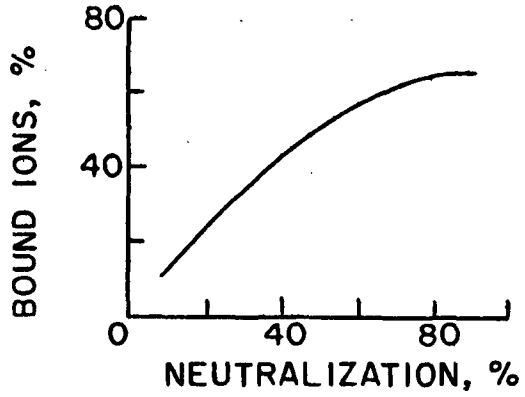

Figure 12. Ion Binding for Polyacrylic Acid (63)

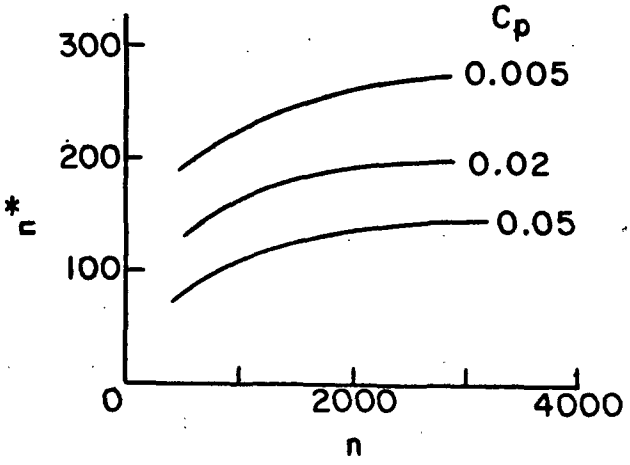

Figure 13. Number of Effective Charges per Molecule (n^*) vs. Total Number of Charged Groups per Molecule (n) at Various Concentrations (C_p) (64). C_p is in Equivalents/Liter

Figure 11 shows the free charge distribution as a function of distance from the center of a spherical polymer. This charge distribution was calculated from an approximation developed from assumptions concerning the ionic distribution and the electric potential inside and outside the volume occupied by the polyelectrolyte (63, 65).

The fraction of bound counterions, plotted as a function of the degree of dissociation, α, is shown in Fig. 12 for PAA and sodium ions (63, 66). The fraction of bound counterions increases somewhat linearly up to a point where about 60 to 70% of the carboxyl groups are neutralized, and then levels off with further increases in α. A similar behavior would be expected for potassium ions.

Oosawa (64) has developed an expression to relate the apparent degree of dissociation to the charge density for solutions of spherical polyelectrolytes based on the electric potential energy in the volume occupied by the polyelectrolyte. Figure 13 shows the relationship between the number of effective charges per molecule, n^*, and the total number of ionized groups per molecule, n, as a function of the concentration of ionizable groups. In Fig. 13, it is seen that at a fixed number of ionized groups per molecule, the effective charge per molecule (number of ionized carboxyl groups minus the number of bound counterions) decreases as the concentration of polyelectrolyte is increased. Also, at a fixed concentration of polyelectrolyte, the effective charge per molecule increases only slightly as the total number of charges per molecule is increased. This has been attributed to a "condensation" phenomenon whereby increasing the number of ionized groups on a polyelectrolyte molecule increases the number of bound counterions, while the concentration of free counterions remains nearly unchanged (64).

HYDRATION OF POLYELECTROLYTES

In recent years it has been found that the degree of orientation of the solvent (water) in the immediate vicinity of a charged group plays an important role in the behavior of polyelectrolytes (64, 67, 68). The technique used to investigate solvent orientation are based on changes in the volume or density of solutions either by direct measurement or through the use of refractivity measurements.

Normally, water contains clusters of hydrogen bonded molecules which continuously form and disappear. These clusters are similar to the crystal structure of ice and are called icelike structures. In the immediate vicinity of charged groups, these icelike structures are not formed; instead, the water molecules are oriented in a region of high density (67). The high density results from the absence of icelike structures and presumably from dipole-dipole orientation of the water molecules. It would also seem likely that this high density water has a higher viscosity than normal water.

Measurements of the volume and density changes of PAA solutions as a function of the degree of dissociation have been made with several cations (67, 68) and in order to explain the results of these experiments, the following model has been proposed (64, 67):

At low values of α, each charged group (dissociated carboxyl group) orients the water molecules around itself forming a region of high density. If a spherical region is assumed and the average density is 1.1, then the radius of this region is about 3 A., as calculated from solution volume changes.

As the average distance between charged groups becomes smaller (α increases), the volume of high density water accompanying the dissociation of one carboxyl group will begin to be influenced by neighboring groups. With 3-A. spheres

around the carboxyl groups, this interference or overlap will begin to occur when α is about 0.3. When α becomes greater than about 0.3, the region of oriented water molecules gradually becomes cylindrical around the polymer molecule rather than spherical around individual groups. Accompanying this change is a change in the configuration of the polymer molecule from a coiled sphere to a rodlike configuration. From solution volume measurements, the radius of this cylinder of oriented water molecules is about 6 A. when α is 1.0. Figure 14 illustrates the changes predicted by this model.

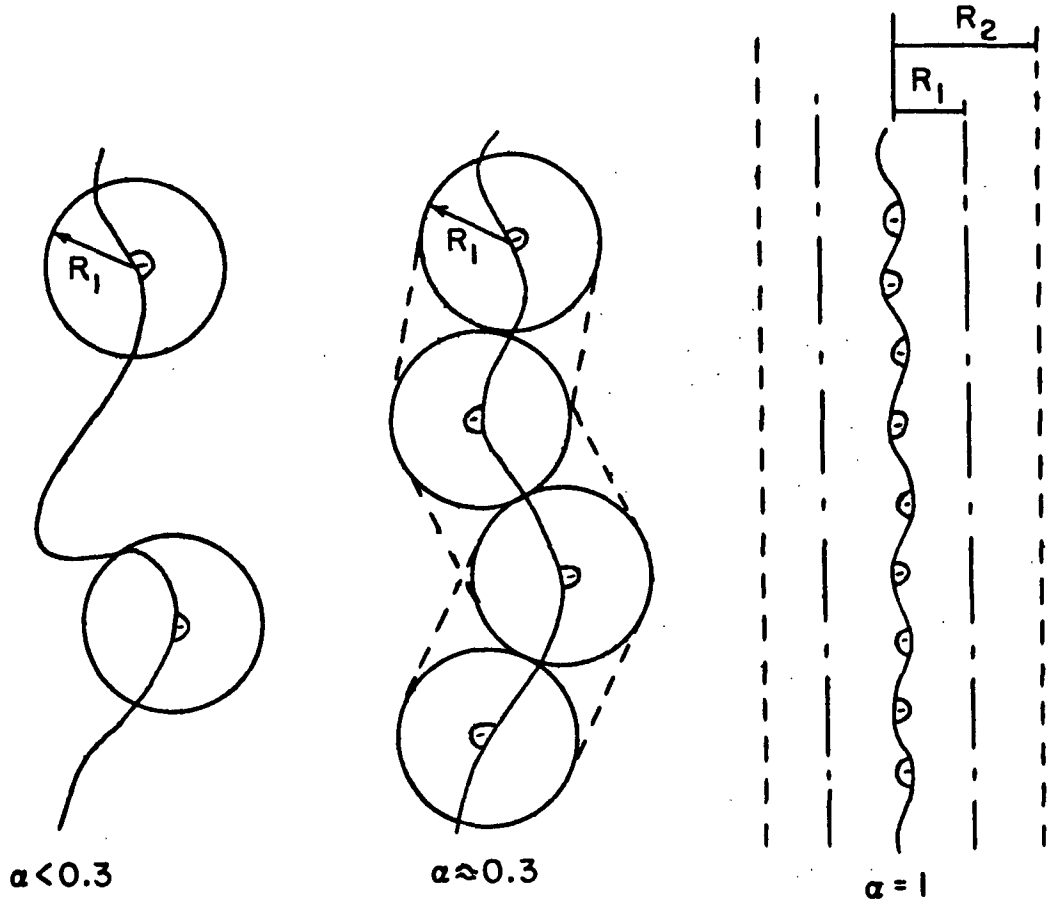

Figure 14. Illustration of Spherical and Cylindrical Hydration Regions Around Polyelectrolyte Molecule at Various Degrees of Neutralization (65). ($R_1 \cong 3$ A.; $R_2 \cong 6$ A.; ⊖ Indicates Position of Ionized Group)

This model is consistent with estimates of the electric field around polyelectrolytes and it is consistent with measured viscosity differences of solutions of polyelectrolytes in which various cations are used to neutralize the charges (67).

Begala and Strauss (68) have also measured volume and density changes of PAA associated with the neutralization of this polyelectrolyte by various cations. In order to interpret their results, they estimated that the thickness of oriented water associated with the PAA consisted of four layers of water molecules when α equalled 0.0, and eleven layers of water molecules when α was 1.0.

It thus appears that PAA has a layer of high-density, oriented solvent associated with it, and the thickness of this layer of oriented solvent increases with increasing degree of dissociation. At the present time, the exact amount of solvent orientation is not known, but the estimates given above represent reasonable values.

CHARGE BEHAVIOR OF THE ADSORBED PAA

From the previous discussion of the charge behavior of polyelectrolytes in solution, it is apparent that this behavior is dependent on ion binding and solvent orientation. These effects, in turn, are related to the degree of dissociation and polyelectrolyte concentration. Since the adsorbed PAA is similar in size and shape to PAA in solution, the charge behavior of the adsorbed PAA should also be similar. Therefore, it should be possible to qualitatively predict the charge behavior of the adsorbed PAA as a function of the degree of dissociation and the carboxyl content, and this charge behavior should be related to the measured zeta potentials.

For hydrophobic materials, the potential at the O.H.P., ψ_δ, is related to the surface charge density of the Stern layer and the Gouy-Chapman layer. For

the dacron-PAA system, there is no discrete, well-defined surface, and hence it is difficult to distinguish a Stern layer or a Gouy-Chapman layer. It would seem, however, that an immobilized layer, comparable to the Stern layer, would exist around the PAA molecules. A mobile layer would also be present and it would penetrate, to some extent, the volume occupied by the adsorbed PAA because of its partial-draining characteristic. Changes in the charge behavior of the adsorbed PAA can be likened to changes in the surface charge density of the Stern layer of hydrophobic materials (i.e., the immobile layer) resulting in changes in ψ_δ. Likewise, a change in the charge behavior of the adsorbed PAA would result in a change in the counterion concentration in the solvent around the adsorbed PAA (similar to the mobile layer of hydrophobic systems) resulting in a change in the measured zeta potential. Figure 15, based on Webb's work (25), illustrates how the zeta potential can change with increasing amounts of oriented solvent.

If the charge of the fibers (as measured by the zeta potential) is a result of the presence of ionized carboxyl groups, then the behavior of the zeta potential, when changes are made in the carboxyl content, pH, and ionic strength, should be explainable in terms of the expected charge behavior of the carboxyl groups.

Of the mechanisms which have been previously used to account for the development of a charge on a solid substance in contact with water, that mechanism involving the dissociation of ionizable groups is the most applicable in the present study. Thus, it will be hypothesized that the charge of the dacron-PAA fibers is due to the dissociation of carboxyl groups. The remainder of this section will be a discussion of the results obtained, showing that these results can be explained in terms of ion binding and solvent orientation effects, thus providing support for this hypothesis.

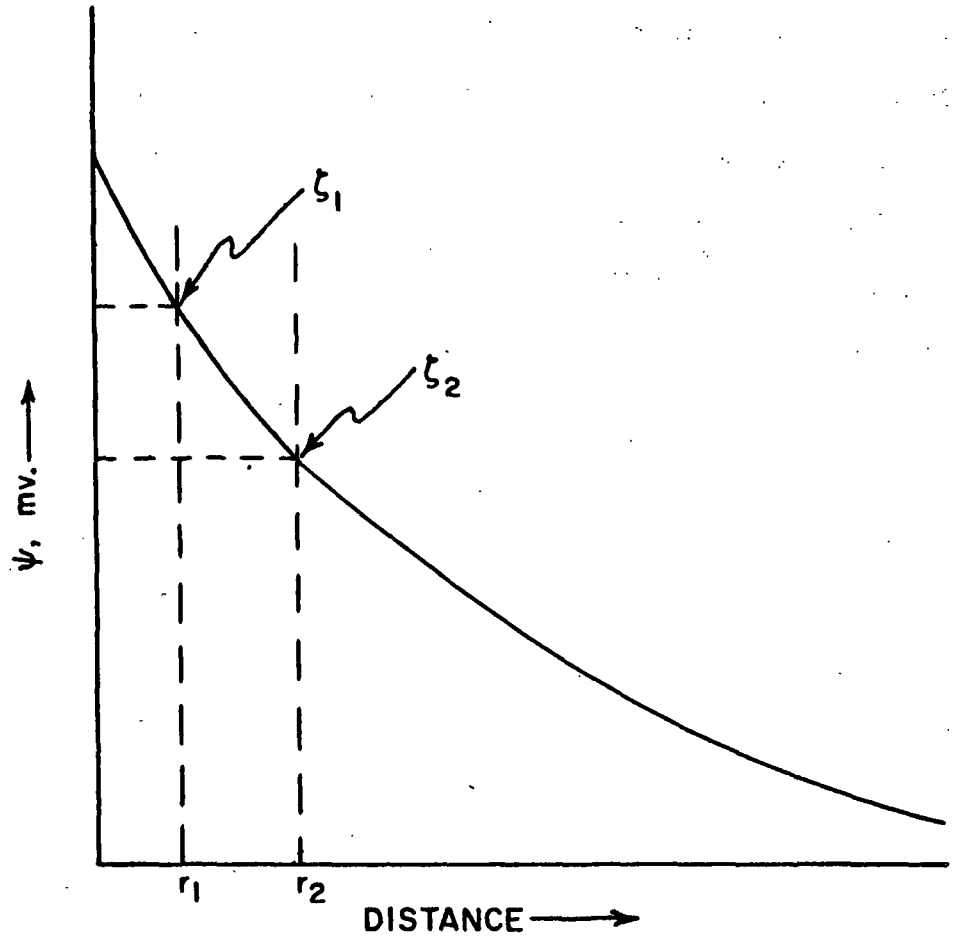

Figure 15. Illustration of Change in ζ with Increasing Thickness of Immobile Region

EFFECT OF DEGREE OF DISSOCIATION

The dissociation of a carboxyl group obviously gives rise to a negative charge. This charge will be neutralized somewhat, or made less negative by the effects of ion binding. In addition, orientation of solvent molecules around the dissociated carboxyl groups will increase the distance from the source of the charge to the slip plane (the defined location of the zeta potential). Since the counterion charge density decreases exponentially with distance from the source of the charge (Poisson-Boltzmann equation), the zeta potential will decrease with increased solvent orientation. Figure 15 illustrates the relationship between distance and potential.

The zeta potential data were found to become more negative as the pH was increased from 4 to 7 and then level off as the pH was increased further, to a value of 10 (see Fig. 8-10). The explanation of this is as follows:

During the change in pH from 4 to 10, the percentage of carboxyl groups which ionize increases from about 10% to almost 100%. The fraction of counterions bound to the PAA also increases over this range, increasing somewhat regularly up to a degree of dissociation of about 0.7 (which occurs at about pH 7) and then leveling off as α increases further to about 1.0 (see Fig. 12). Since the number of bound counterions is less than the number of ionized carboxyl groups, the effective charge (number of ionized carboxyl groups minus the number of bound counterions) of the PAA will increase, i.e., become more negative as the pH is increased from 4 to 10.

An additional factor during the pH change from 4 to 10 is the increase in solvent orientation around individual carboxyl groups or the PAA molecules. When α is less than about 0.3 (less than pH 5), a small amount of solvent orientation is present in the PAA and this is confined to spherical regions around the ionized carboxyl groups. These spherical regions molecules begin to overlap when α is approximately 0.3, becoming cylindrical around the PAA molecule and increasing in thickness. Thus, while the effective charge of the PAA is becoming more negative, the number of layers of oriented water molecules is also increasing.

For the dacron-PAA fibers, the zeta potential becomes more negative as the pH is increased from 4 to 7, indicating a dominating effect of the increased number of ionized carboxyl groups, with their associated ion binding, over increasing solvent orientation. Above pH 7, the zeta potential levels off, indicating a balancing effect of solvent orientation against the increased number of ionized carboxyl groups.

EFFECT OF CARBOXYL CONTENT

When the carboxyl content is increased, the charge behavior of the adsorbed PAA becomes more complex. With an increased carboxyl content, the fraction of ionized carboxyl groups, at any given pH, changes only slightly (Fig. 7), but the number of ionized carboxyl groups per unit area of fiber does increase. It might, therefore, be expected that since the number of ionized carboxyl groups per unit area increases (with increasing amount of adsorbed PAA), the zeta potential should become more negative at a given pH. It was found, however, that Fibers B and C, with the lowest amount of adsorbed PAA, had the most negative zeta potentials, while Fiber A and the dacron itself had the least negative zeta potentials. This behavior can be interpreted in the following manner:

The dacron fiber itself is made from polyethylene terephthalate which contains terminal carboxyl groups. The chemical structure of this compound is given below:

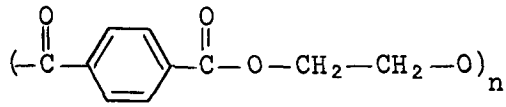

(11)

where n is the degree of polymerization and has a value of several hundred (69). When the PAA is adsorbed, the carboxyl groups of the PAA are also present on the fiber surface, and while they tend to cover the dacron carboxyl groups, they do not shield them completely from the solution.

Van Gils (70) measured the specific gravity of dacron fibers in heptane and water and found that the specific gravity in water was always higher. This result was attributed to a layer of oriented water molecules near the surface of the dacron. Increasing the number of ionized carboxyl groups on the dacron (by increasing the pH of the water) was found to increase the amount of this high-density water. Thus, in the present study, it is likely that a layer of high-density, oriented water molecules exists at the dacron surface.

As shown in Fig. 9 and 10, the zeta potential of the blank dacron was found to become only slightly more negative as the pH was increased from 4 to 10. This indicates that the layer of oriented solvent is the main factor in determining the zeta potential of the blank dacron. Increasing the number of ionized carboxyl groups on these fibers, by increasing the pH, does increase the number of negative charges on the fibers, but it also increases the amount of oriented solvent. With an increased amount of oriented solvent, even though the negative charge of the fibers is greater, the zeta potential may become only slightly more negative since the slip plane will be located farther from the source of the charge (farther from the surface).

Also in Fig. 9 and 10, it is seen that Fiber A (highest amount of adsorbed PAA) exhibits the same behavior as the blank dacron, except that Fiber A is slightly more negative than the blank dacron. Fiber A has approximately 0.9 meq./100 g. of adsorbed PAA, and from Table V, using an $\underline{R}_g$ value of 92 A., it is seen that this amount of PAA should cover the dacron completely, and it probably exists as a network of interpenetrating PAA molecules. Calculations based on the number of molecules adsorbed show that the PAA must have a radius of slightly less than 40 A. if the PAA molecules are just touching each other. This indicates that the PAA of Fiber A is densely packed on the surface of the dacron, which is consistent with the monolayer coverage indicated by the Langmuir isotherm. Because of this close packing, it is possible that an integrative effect of solvent orientation results, extending the high-density water layer from the PAA. If this were the case, then it would be expected that this layer of oriented solvent would also be the major factor in determining the zeta potential of Fiber A. Fiber A does have a higher carboxyl content than the blank dacron and this is probably the reason that the zeta potential of Fiber A is more negative than that of the blank dacron at any

given pH. However, it appears that for both Fiber A and the blank dacron the zeta potential is dominated by a layer of oriented solvent.

Referring back to Fig. 15, it can be seen that increasing the thickness of the slip plane from r_1 to r_2 will result in a less negative zeta potential. For the dacron and dacron-PAA fibers, it is difficult to determine the effect of adsorbed PAA on the value of ψ_o or the shape of the ψ vs. distance curve. Since only carboxyl groups are involved, the shape of the ψ vs. distance curve, from the outer surface of the volume occupied by the adsorbed PAA, would not be expected to change upon addition of PAA. Within the region occupied by the PAA, the shape of the curve would be affected, however.

The value of ψ_o would become somewhat more negative, with increasing carboxyl content, but the effects of ion binding would result in a less than proportional increase in ψ_o as compared with the increase in carboxyl content. It seems likely that for the hydrophilic surface of the dacron-PAA fibers, increased amounts of oriented solvent would increase the distance between the slip plane and the source of the charge, along similar ψ vs. distance curves, thereby resulting in a less negative zeta potential.

It should be noted that since the adsorbed PAA is only partially draining, its presence (charged or uncharged) would shift the slip plane further from the surface and thereby result in a less negative zeta potential.

In Fig. 8-10 it was also shown that the zeta potentials of Fibers B and C were more negative than those of either Fiber A or the blank dacron at all pH levels studied. The less negative ζ at low pH values and more negative ζ at high pH values indicates that the charge of the ionized carboxyl groups is more important for Fibers B and C than for Fiber A or the blank dacron. (The behavior of ζ with increasing pH was discussed previously.)

From the data presented in Table V, it was shown that the adsorbed PAA of Fibers B and C probably also completely covers the surface of the dacron. The density of PAA on Fibers B and C is, however, much less than that of A. It is, therefore, unlikely that a layer of high-density water would completely envelop the adsorbed PAA of these two fibers since the adsorbed PAA is less dense. The zeta potential of Fibers B and C is thus likely to be determined mainly by the amount of adsorbed PAA and the charge behavior of this PAA. That is, the dacron surface will have a layer of high-density water, but the adsorbed PAA probably extends beyond the oriented solvent. The charge behavior of these fibers, then, was probably affected a great deal by the adsorbed PAA: At low pH values, there is only a small amount of oriented solvent associated with the PAA even though the dacron itself probably has a layer of oriented water molecules, and hence ζ is more negative than for the blank dacron; at high pH values, the amount of oriented solvent associated with the PAA molecules increases and ζ levels off but is still more negative than the dacron itself.

Fiber C is less negative than Fiber B, and two reasons could account for this behavior. First, Fiber C has less PAA than Fiber B and it could therefore have a lower charge per unit area. Second, the PAA of Fiber C was adsorbed from a solution at high pH. This PAA would be in an extended, rodlike configuration and, therefore, may lie flatter on the surface than the PAA of either Fibers A or B. If this were the case, then the oriented solvent associated with the dacron itself may affect the PAA of Fiber C more than that of Fiber B.

It should be noted that in Fig. 8 the blank dacron and Fiber A have a greater slope, in the pH vs. ζ curve, below pH 7 than in either Fig. 9 or 10. This behavior cannot be explained by the arguments given above, and at present no explanation can be given for this behavior.

In addition to the solvent orientation effects discussed above, two other factors must be considered when the carboxyl content of the fiber is increased. These are changes in counterion binding and changes in degree of dissociation.

With regard to counterion binding, it was shown in Fig. 13 that for polyelectrolytes the effective charge (number of ionized groups minus the number of bound counterions) decreases with increasing concentration. Using the equations of Oosawa (64), for polyelectrolytes in solution, it can be shown that even though the amount of adsorbed PAA increases ninefold (from 0.1 to 0.9 meq./100 g.), the change in the effective charge, per 100 g. of fiber, is less than twofold. These calculations are summarized in Appendix VII. It should be noted that these calculations are not strictly valid since the concentrations encountered in the present study are quite high and the adsorbed PAA is not exactly like PAA in solution in that the adsorbed PAA is not surrounded on all sides by other PAA molecules (the adsorbed PAA is "two-dimensional"). However, a similar phenomenon would be expected to occur, that is, the number of effective charges per 100 g. of fiber would not increase as rapidly as the total carboxyl content of the fibers.

With regard to degree of dissociation changes, Fig. 7 shows that when the carboxyl content of the fibers is increased, a slightly lower fraction of the carboxyl groups are dissociated at any given pH. This behavior is due to increased electrostatic interactions associated with the increased carboxyl content. The effect of this factor would not be as important as the effect of solvent orientation.

To summarize these arguments, the dacron and dacron with adsorbed PAA all contain ionizable carboxyl groups. The ionized carboxyl groups give rise to a negative charge which is reduced somewhat by the effects of ion binding. Solvent orientation appears to play a major role in the resulting zeta potential of these

fibers. The dacron fiber itself has a layer of high-density water at its surface and increasing the number of ionized carboxyl groups of the blank dacron increases the thickness of the oriented water. The slip plane would then move farther from the surface and the zeta potential would change only slightly. It appears that Fiber A has a layer of oriented solvent that envelops the adsorbed PAA and thus the zeta potential of Fiber A is determined mainly by the oriented solvent (through the location of the slip plane) and thus its behavior as the pH is changed is similar to that of the blank dacron. Fibers B and C, however, have much less adsorbed PAA than Fiber A, and the adsorbed PAA of these fibers is probably not enveloped by a layer of oriented solvent. Fibers B and C thus have a more negative zeta potential than either blank dacron or Fiber A. In addition, ion binding acts to reduce the increase in the number of effective charges per fiber when the carboxyl content of the fibers is increased.

It is not possible at the present time to quantitatively show that ionized carboxyl groups are responsible for the negative zeta potential of these fibers. However, the change in ζ resulting from changes in degree of dissociation or changes in carboxyl content can be interpreted qualitatively in terms of solvent orientation and ion binding.

EFFECT OF ELECTROLYTE CONCENTRATION

In this study, the electrolyte concentration of the permeant used for the zeta potential measurements was varied from 2×10^{-5}M to 5×10^{-4}M. Over this range of concentrations, the charge behavior of the carboxyl groups will not change too much. The zeta potential measurements show that the zeta potential falls off at electrolyte concentrations greater than 10^{-4}M. The decrease in zeta potential with an increase in ionic strength is a common characteristic of zeta potential measurements, for

example, as observed by Ciriacks (29) with these dacron fibers, and has been attributed to collapse of the electric double layer.

CHARGE BEHAVIOR OF CELLULOSE FIBERS

In a previous section, the results of several studies concerning the zeta potential of cellulose fibers were described. In general, these results showed that when cellulose fibers were oxidized to various degrees, the carboxyl content increased and the zeta potential became less negative. Also, when various substituent groups were added to the cellulose (e.g., acetyl, propionyl, p-nitrobenzoyl, methyl groups), the zeta potential became more negative with increased degree of substitution (25, 34-38). The same reasoning used to interpret the results of the present study may be applied to these studies of cellulose fibers.

It should be noted that while it is generally not possible to compare the zeta potential values obtained in one study with those of another study, the trends found within a particular study should be valid. The reason for this is that zeta potential values are particularly sensitive to such factors as the electrokinetic effect measured (i.e., streaming current, electrophoretic mobility, etc.), the shape of the particle, the flow model used to calculate ζ, and impurities which may be present (71).

For cellulose fibers containing carboxyl groups, ion binding and solvent orientation would affect the zeta potential in a manner similar to that described for the dacron-PAA fibers. With cellulose fibers, the carboxyl groups would be much farther apart, and thus ion binding effects may not be too important. Thus, solvent orientation is indicated as being the more important effect in determining the zeta potential.

Goring (72) has suggested that the water near the surface of carbohydrates does not contain the typical low-density, icelike structures that are found in normal water. Ionized carboxyl groups could increase the orientation of this water to a greater extent, thus accounting for less negative zeta potentials with increased carboxyl contents.

Goring (72) has also suggested that hydrophobic groups on carbohydrates enables the water near the surface of the carbohydrate to assume the normal, low-density, icelike structures. Thus, the effects of oriented solvent molecules at the surface would be removed. The fact that addition of nonpolar groups to cellulose fibers results in increasingly negative zeta potentials thus provides additional support to the hypothesis that the zeta potential measured for these fibers is mainly a function of the degree of solvent orientation at the surface.

Again, these arguments do not show that ionized carboxyl groups are entirely responsible for the negative zeta potential of cellulose fibers, but the carboxyl groups are responsible for the changes in the zeta potential when changes are made in the carboxyl content of cellulose fibers.

CONCLUSIONS

In this study, zeta potential measurements were made on dacron fibers and dacron with adsorbed PAA, under conditions of varying carboxyl content, pH, and electrolyte concentration.

Since ion binding and solvent orientation are known to affect the charge behavior of polyelectrolytes in solution, these effects were examined for the adsorbed PAA of the present study. When the carboxyl content and/or the degree of dissociation increases at the fiber surface, (1) the amount of ion binding increases resulting in a less than proportional increase in the effective charge of the fiber surface, and (2) the amount of water oriented into high-density layers next to the surface increases, causing the slip plane to move further from the surface which results in a less negative zeta potential.

For both the dacron itself and the dacron-PAA fiber with the high amount of adsorbed PAA, the slight increase in zeta potential with increased degree of dissociation could best be explained in terms of the dominance of solvent orientation associated with the ionized carboxyl groups, over ion binding effects. The observation that the zeta potential of the dacron-PAA sample with the high amount of adsorbed PAA was only slightly more negative than the dacron itself, in spite of the higher carboxyl content, was also interpreted in terms of a dominating effect of solvent orientation.

For the two dacron-PAA samples with the low amounts of adsorbed PAA, the zeta potentials first increased, then leveled off with increasing degree of dissociation. Also, the zeta potentials of these fibers were more negative than either the dacron itself or the dacron-PAA sample with the high amount of adsorbed PAA. These results were taken as being indicative of solvent orientation being a minor effect at low

degrees of dissociation but being a dominating effect at high degrees of dissociation. It was also concluded that the segment density of the adsorbed PAA for the fibers with the low amounts of adsorbed PAA was less than that of the dacron-PAA sample with the high amount of adsorbed PAA. Thus, the amount of oriented solvent associated with the former was less than the latter, which accounts for the more negative zeta potential of the former.

Data reported in the literature on the zeta potentials of cellulose fibers containing various substituents show that the zeta potential becomes less negative upon addition of carboxyl groups through oxidation, but becomes more negative upon substitution with hydrophobic groups. Therefore, the results of the present study are consistent with the data on oxidized cellulose fibers. It would be expected that the dominating effect in the zeta potential of cellulose fibers is also solvent orientation, as the ion-binding effect would be minimized due to the random distribution of the carboxyl groups along the oxidized cellulose molecules. With hydrophobic groups on cellulose fibers, the amount of oriented solvent is decreased; thus these results are also consistent with the explanation that the dominating factor in determining the zeta potential is the amount of oriented solvent.

The adsorption of PAA onto the dacron was found to be typical of polymer adsorption as far as the effects of equilibrium concentration, time, and degree of washing were concerned. The greatest amount of adsorption occurred at low pH. The adsorbed PAA could not be removed by washing and it was therefore concluded that the adsorption process was essentially irreversible.

The equilibrium concentration isotherm was found to be a Langmuir-type isotherm and this was taken as being indicative of monolayer adsorption. Potentiometric titrations and turbidity titrations were performed and from these results it was

concluded that the adsorbed PAA was porous or partial draining in character. Calculations of the size of PAA in solution and on the dacron surface supported this characterization. This indicated that the adsorbed PAA was similar in size and shape to PAA in solution and, therefore, factors which affect PAA in solution would also affect the adsorbed PAA in a similar manner.

FUTURE WORK

One area of research that needs much more work is the area of solvent structuring. The orientation of water molecules at a surface has been used to interpret results in a number of systems. However, this phenomenon is not understood very well. The problems involved in the study of solvent orientation are difficult, but an understanding of this phenomenon is necessary in order to fully characterize the nature of the solid-liquid interface — particularly hydrophilic surfaces.

Ion binding has been indicated as being important in the present study, but quantitative results of this phenomenon were not obtained. One method for obtaining data on ion binding would be through the use of radioactive isotopes. The activity of bound cations could be measured and used to calculate the amount of ion binding under various conditions.

Since the zeta potential values reported in this study are relative values, it is difficult to use them in further calculations (e.g., calculations of charge density). It should be possible to put these values on a more absolute basis by following Ciriacks' (29) suggestion: Obtain a more accurate value for the total number of fibers contributing to the streaming current.

It should be possible to adsorb PAA or PMAA onto TiO_2 or Fe_2O_3 particles and then measure the electrophoretic mobility of these particles. Zeta potentials calculated from these measurements could be compared with those calculated for this study. An advantage of using these particles is that they have a higher surface area per weight of particles. The amount of polymer adsorption could thus be measured more accurately. Corrections are available for spherical particles and use of these corrections would permit electrolyte concentrations and pH ranges to be extended. Comparison of the zeta potentials obtained could put the streaming current measurements on a more absolute basis.

Use of small spherical particles may permit the thickness of adsorbed polymers to be measured through the use of viscosity techniques. Volume and density measurements on suspension of these particles could also yield information on solvent structuring effects.

SYMBOLS AND ABBREVIATIONS

A = cross-sectional area of bed, cm.^{2}; frequency factor; fiber surface area

A. = Angstrom unit, 10^{-8} cm.

A_m = area per monomer unit for PAA

a = radius of cylindrical fiber, μm.; ampere

B = constant

b = radius of Happel's fluid envelope; length of monomer, A.

C = carboxyl content, equivalents per 100 g. of fiber

C, D_1, E, F = constants in Happel's equation which vary with porosity

C_1, C_2 = hydrogen ion concentration, moles/liter

°C. = Centigrade degree

C_4 = 9×10^8, a constant to convert units in streaming current equation

c = electrolyte concentration, moles/liter

c_1 = uniform bed density, g./cc.

D = permittivity (dielectric constant) of the bulk liquid (stat-coulomb)^2/(dynes cm.^{2})

D.P. = degree of polymerization

E = potential developed across a tube due to liquid flow, mv.

e = electronic charge; base of Naperian logarithm, 2.7128....

f_1, f_2 = activity coefficient

ΔH = overall frictional pressure drop across mat, cm. in CCl_4-H_2O manometer

I = streaming current from a porous bed, μa.

I_f = flow current between electrodes with no bed present, μa.

I_r = residual current (at zero liquid flow), μa.

I.H.P. = inner Helmholtz plane

K_o = symbol for zero-order modified Bessel function of the second kind

k = specific conductance, $cm.^{-1}ohm^{-1}$

k_1 = Boltzmann constant

L = overall mat thickness, cm.

L/L = tortuosity factor

l = fiber length, cm.

M = moles/liter; molecular weight

meq. = 10^{-3} equivalents

N = number of fibers contributing to streaming current

N_o = Avogadro's number

n = concentration of counterions, moles/liter; number of statistical elements or monomers; number of ionized groups per polyelectrolyte molecule

$n_i(r)$ = number of ions per cc. of type i at distance r from fiber surface

$n_i(\infty)$ = number of ions per cc. in bulk solution

n' = the number of counterions per polyelectrolyte molecule

n^* = $n - n'$, the effective charge of a polyelectrolyte molecule

O.H.P. = outer Helmholtz plane

P = pressure applied to a cylindrical tube to cause flow

ΔP = overall frictional pressure drop across pad, $dynes/cm.^2$

PAA = polyacrylic acid

PMAA = polymethacrylic acid

PVPB = poly(N-n-butyl 4-vinyl pyridinium bromide)

p.p.m. = parts per million

R = radius of polymer molecule in solution, cm.; resistance, ohms

$\langle R_g^2 \rangle$ = average value of radius of gyration, squared, $A.^2$

r = radial distance from axis of cylinder

S_o = specific surface area per unit volume of porous bed, $cm.^2/cc.$

S_v = specific surface area per unit volume of particle, $cm.^2/cc.$

$\underline{T}$ = absolute temperature, °K

$\underline{T}_1$, $\underline{T}_2$, $\underline{T}_3$, $\underline{T}_4$ = terms in streaming current equation

$\underline{U}$ = superficial approach velocity above porous bed, cm./sec.

$\underline{U}_\theta$ = angular velocity for case of a fluid moving perpendicular to a stationary cylinder

$\vec{\underline{u}}$ = velocity vector

$\underline{v}_\theta$ = angular velocity in Happel equation

$\underline{x}$ = distance from surface

$\underline{x}$, $\underline{y}$, $\underline{z}$ = coordinates

$\underline{z}$ = ion valence

α = fiber specific volume, cc./g.

Δ = difference or change in

δ = thickness of immobile layer, A.

ε = porosity or void fraction

ζ = zeta or electrokinetic potential, mv.

$\zeta_{\underline{c}}$ = calculated zeta potential, mv.

η = viscosity of the bulk liquid, centipoises

$[\eta]$ = intrinsic viscosity

θ = angular component in cylindrical coordinates

κ = Debye-Huckel constant $(\mu m.)^{-1}$

μ = micro (10^{-6})

ρ = excess charge per unit volume, ions/cc.

σ = total surface charge density, esu/cm.^{2}

$\sigma_{\underline{G}}$ = surface charge of Gouy-Chapman layer

$\sigma_{\underline{M}}$ = surface charge corresponding to a monolayer of counterions

$\sigma_{\underline{S}}$ = surface charge density of Stern layer

τ = thickness of diffuse layer, μm.

ϕ = adsorption potential of the counterions adsorbed to the surface

ψ = average electrical potential at a distance r (of x) from solid surface, mv.

ψ_o = electrical potential at the surface, mv.

ψ_δ = average electrical potential at plane of closest approach of ion centers (O.H.P.), mv.

∇ = Laplace operator

ACKNOWLEDGMENTS

The author would especially like to acknowledge the guidance, assistance, and encouragement of his Faculty Advisory Committee: Dr. Dale G. Williams, Dr. Thomas M. Grace, and Mr. John W. Swanson.

Many other faculty members, staff personnel, and fellow students also provided valuable assistance during the course of this study. Although space does not allow acknowledgment of all these individuals, the author does wish to express his appreciation for their help. Among these people, several provided particularly helpful assistance and the author would like to extend special thanks to them: Mr. Bruce Andrews, Dr. Gary Baum, Mr. Marvin Filz, Mr. Harold Grady, Mr. Orlin Kuehl, Mr. Jerome Popp, Mr. Bruce Schubring, and Mr. Paul Van Rossum.

Finally, sincere thanks are extended to my wife, Marti, for her understanding and encouragement during the time spent on this study.

LITERATURE CITED

1. Verwey, E. J. W., and Overbeek, J. Th. G. Theory of the stability of lyophobic colloids. New York, Elsevier, 1948. 205 p.

2. Kruyt, H. R. Colloid science. Vol. 1. New York, Elsevier, 1952. 389 p.

3. Grahame, D. C., Chem. Revs. 41:441-501(1947).

4. Colloidal stability in aqueous and non-aqueous suspension. Disc. Faraday Soc. 42:7-322(1966).

5. Sennett, P., and Olivier, J. P., Ind. Eng. Chem. 57:32-50(1965).

6. Davies, J. T., and Rideal, E. K. Interfacial phenomena. New York, Academic Press, 1961. 468 p.

7. Delehay, P. Double layer and electrode kinetics. New York, Interscience, 1965. 321 p.

8. Adamson, A. W. Physical chemistry of surfaces. 2d ed. New York, Interscience, 1967. 747 p.

9. Helmholtz, H., Wied. Ann. 7:337(1879).

10. Gouy, G., J. Phys. Rad. 9:457(1910).

11. Chapman, D. L., Phil. Mag. 25:475(1913).

12. Stern, O., Z. Elektrochem. 30:508(1924).

13. Levine, S., Mingins, J., and Bell, G. M., Can. J. Chem. 43:2834-66(1965).

14. Grahame, D. C., Chem. Revs. 41:441-501(1947).

15. Devanthan, M. A. V., Trans. Faraday Soc. 50:373(1954).

16. Devanthan, M. A. V., and Tilak, B. V. K., Chem. Revs. 65:635-84(1965).

17. Smoluchowski, N. V., Bull. Acad. Sci., Classe Sci. Math. Nat. 1903:184.

18. Haydon, D. A. In Danielli, Pankhurst, and Riddiford's Recent progress in surface science. Vol. 1. p. 94-158. New York, Interscience, 1965.

19. Devillez, C., Sanford, A., and Steinchen, A., J. Colloid Interface Sci. 25: 295-310(1967).

20. Sparnaay, M. J., Rec. Trav. Chim. 81:395-416(1962).

21. Bolt, G. H., J. Colloid Sci. 10:206-18(1955).

22. Lyklema, J., and Overbeek, J. Th. G., J. Colloid Sci. 16:501-12(1961).

23. Stitger, D., J. Phys. Chem. 68:3600-2(1964).

24. Hunter, R. J., J. Colloid Interface Sci. 22:231-9(1966).

25. Webb, J. T. An investigation of electric double layer concepts and colloidal stability of TiO_2 dispersions. Doctor's Dissertation. Appleton, Wis., The Institute of Paper Chemistry, 1971.

26. Sparnaay, M. J., Trans. Faraday Soc. 53:306-14(1957).

27. Neale, S. M., and Peters, R. H., Trans. Faraday Soc. 42:478-87(1946).

28. Goring, D. A. I., and Mason, S. G., Can. J. Research 28B, no. 6:307-38(1950).

29. Ciriacks, J. A. An investigation of the streaming current method for determining the zeta potential of fibers. Doctor's Dissertation. Appleton, Wis., The Institute of Paper Chemistry, 1967.

30. Biefer, G. J., and Mason, S. G., Trans. Faraday Soc. 55:1239-45(1959).

31. Chang, M. Y., and Robertson, A. A., Can. J. Chem. Eng. 45:66-71(1967).

32. Happel, J., and Brenner, H. Low Reynolds number hydrodynamics. Englewood Cliffs, N. J., Prentice-Hall, 1965. 553 p.

33. Happel, J., A.I.Ch.E. Journal 5, no. 2:174-7(1959).

34. Hastbacka, K., and Nordman, L., Paperi Puu 45, no. 6/7:353-8(1963).

35. Yurev, V. L., and Pozin, S. S., Izvest. Vysshikh Ucheb. Zaved., Lesnoi Zh. 3, no. 4:149-52(1960); Russ.; ABIPC 32:1652.

36. Balodis, V., Appita 21, no. 3:96-103(1967).

37. Bukhteev, B. M., and Yur'ev, V. I., Mater. Nauch.-Tekh. Konf. Leningr. Lesotekh. Akad. no. 4:25-30(1966); Russ.; ABIPC 38:3361.

38. Bukhteev, B. M., and Yur'ev, V. I., Mater. Nauch.-Tekh. Konf. Khim-Tekhnol. Fak. Leningr. Lesotekh. Akad. 1967:73-81; Russ.; ABIPC 39:885.

39. Ninck Blok, C. J. J. The sizing of paper as a colloid chemical phenomenon. Doctor's Dissertation. The Netherlands, The University of Utrecht, 1952.

40. Yur'ev, V. I., and Pozin, S. S., Kolloid Zh. 23, no. 4:499-503(1961); Russ., Engl. sum.; ABIPC 31:5907.

41. Lafaye, J. F., and Jacquelin, G., Paper and Timber 4a:1-7(1968).

42. Jacquelin, G., and Bourlas, H., Tech. Rech. Papet. no. 3:49-58(1964).

43. Stamm, A. F. Wood and cellulose science. New York, Ronald, 1964. 549 p.

44. Neale, S. M., and Standring, P. T., Proc. Royal Soc. A 213:530-45(1952).

45. Sorenson, W. R., and Campbell, T. W. Preparative methods of polymer chemistry. p. 149-234. New York, Interscience, 1961.

46. Sonnerskog, S., Acta Chem. Scand. 9:1649-55(1955).

47. TAPPI Standard T 237 su-63.

48. Kenchington, A. W. Analytical information from titration curves. In Alexander and Block's Analytical methods of protein chemistry. p. 353. New York, Pergamon Press, 1960.

49. Ant-Wuorinen, O., and Visapaa, A., Paperi Puu 49:737-46, 801-10(1967).

50. Lopatin, G. The adsorption of polymethacrylic acid from solution. Doctor's Dissertation. Brooklyn, N. Y., Polytechnic Institute of Brooklyn, 1961.

51. Lauria, R. J. The adsorption of polymeric acids onto solid surfaces. Doctor's Dissertation. Brooklyn, N. Y., Polytechnic Institute of Brooklyn, 1962.

52. Ives, D. J. G., and Janz, G. J. Reference electrodes. New York, Academic Press, 1961. 633 p.

53. Michaels, A. S., and Morelos, O., Ind. Eng. Chem. 47:1801-9(1955).

54. Nestler, C. H., J. Colloid Interface Sci. 26:10-18(1968).

55. Krigbaum, W. R., and Kotiliar, A. M., J. Polymer Sci. 32:323-41(1958).

56. Onyon, P. F., J. Polymer Sci. 22:13-18(1956).

57. Wilson, W. K., and Mandel, J., Tappi 44:131-5(1961).

58. Rowland, F. W., and Eirich, F. R., J. Polymer Sci. Pt. A-1:2401-21(1966).

59. Rowland, F. W., Bulas, R., Rothstein, E., and Eirich, F. R., Ind. Eng. Chem. 57, no. 9:46-52(1965).

60. Healy, T. W., and LaMer, J. K., J. Colloid Sci. 19:323-32(1964).

61. Newmann, S., Krigbaum, W. R., Laugier, C., and Flory, P. J., J. Polymer Sci. 14:451-62(1954).

62. Tanford, C. Physical chemistry of macromolecules. New York, John Wiley and Sons, Inc., 1961. 710 p.

63. Rice, S. A., and Nagasawa, M. Polyelectrolyte solutions. New York, Academic Press, 1961. 568 p.

64. Oosawa, F. Polyelectrolytes. New York, Marcel Dekker, Inc., 1971. 160 p.

65. Nagasawa, M., and Kagawa, I., Bull. Chem. Soc. Japan 30:961(1957).

66. Huizenga, J. R., Grieger, P. F., and Wall, F. T., J. Am. Chem. Soc. 72:4228 (1950).

67. Ikegami, A., J. Polymer Sci. Part A-2:907-21(1964).

68. Begala, A. J., and Strauss, U. P., J. Phys. Chem. 76:254-60(1972).

69. Noller, C. R. Chemistry of organic compounds. Philadelphia, W. R. Saunders Co., 1957. 978 p.

70. Van Gils, G. E., J. Colloid Interface Sci. 30:272-3(1969).

71. Swanson, J. W. Unpublished material, 1967.

72. Goring, D. A. I., Pulp Paper Mag. Can. 67:T519-24(1966).

73. Fuoss, R. M., and Strauss, U. P., J. Polymer Sci. 3:246-63(1948).

74. Jones, G., and Bradshaw, B. C., J. Am. Chem. Soc. 55:1780-7(1933).

75. Morgan, R. J. A study of the phenomenon of rheological dilatancy in aqueous pigment suspension. Doctor's Dissertation. Appleton, Wis., The Institute of Paper Chemistry, 1967.

76. Fuoss, R. M., and Sadek, H., Science 110:552-5(1949).

77. Jones, R. L. The effect of fiber structural properties on the compression response of a fibrous mat. Doctor's Dissertation. Appleton, Wis., The Institute of Paper Chemistry, 1962.

78. Han, S. T. The status of the sheet-forming process — a critical review. Appleton, Wis., The Institute of Paper Chemistry, Dec. 31, 1965. 342 p.

APPENDIX I

DERIVATION OF THE STREAMING CURRENT EQUATION

FLOW MODEL

It is important to use a valid hydrodynamic flow model when analyzing electrokinetic phenomena. Flow equations have been well established for simple systems such as uniform-diameter capillaries. However, flow through a porous mat cannot be described by means of such systems.

Happel (33) proposed a model for flow perpendicular to an assembly of cylinders. The creeping motion equations for two-dimensional flow around cylinders were derived from the equation of motion.

In this approximation of flow, it is assumed that two concentric cylinders, as shown in Fig. 16, represent a model for flow through an array of cylinders. The outer cylinder (radius b) is assumed to be a frictionless surface. The liquid fraction of the cell model is equated to the overall void fraction of the array of cylinders. The equation of motion was solved for the case of a solid cylinder moving perpendicular to its axis in a fluid. The particular Happel velocity equation used here is given in cylindrical coordinate below:

$$u_\theta = U(\sin\theta) - v_\theta$$

$$= -\sin\theta\{U - [3Cr^2/8 + D_1 \ln(r)/2 + D_1/4 + E - F/r^2]\} \qquad (12)$$

where

u_θ = theta component of velocity for the case of fluid moving perpendicular to a stationary cylinder

U = fluid velocity approaching the cylinder (superficial approach velocity)

v_θ = fluid angular velocity for the case of a solid cylinder moving perpendicular to its axis in a fluid cell of radius b

r = radial distance from axis of cylinder

C, D, E, F = constants which vary with the porosity of the unity cell (or mat).

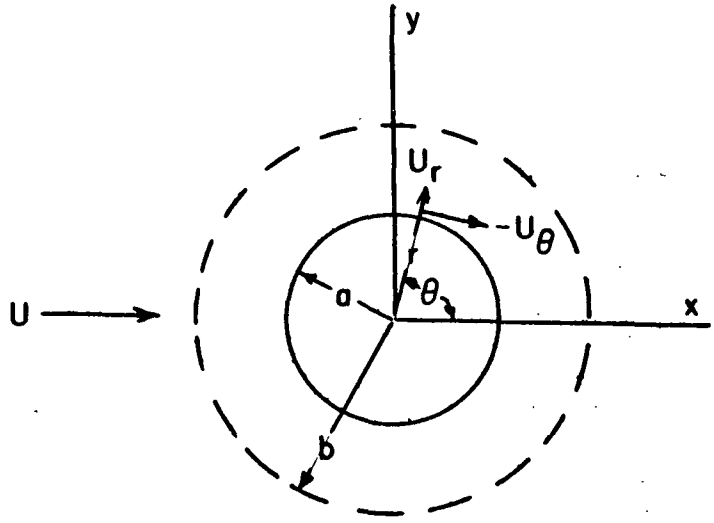

U = Fluid velocity
a = Radius of cylinder
b = Radius of fluid envelope

Figure 16. Free Surface Model for Flow Perpendicular to One Cylinder

This free surface model does not consider effects caused by cylinders in physical contact, or by cylinders bending which could occur at low void fractions. The only orientation necessary is for all of the fibers to be in a y-z plane which is perpendicular to the flow (x-direction).

DERIVATION OF THE STREAMING CURRENT EQUATION

The following is a brief derivation of the streaming current equation. This is based on the derivation given by Ciriacks (29).

Equation (13), shown below, gives the total streaming current, I, passing through a plane, S, perpendicular to flow (Fig. 17).

$$I = \iint_s \rho \vec{u} \cdot d\vec{S} \qquad (13)$$

where

ρ = excess charge per unit volume, or charge density

$\vec{u}$ = velocity vector

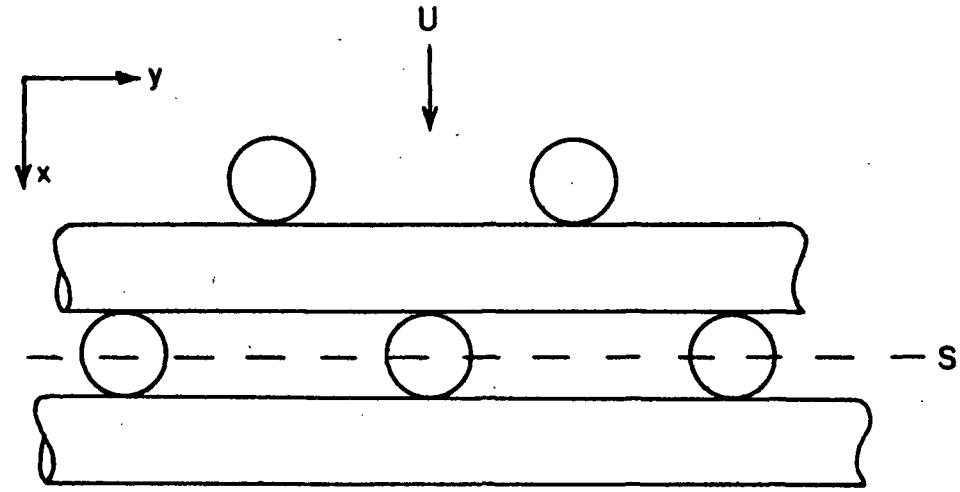

Figure 17. Idealized View of Mat of Cylindrical Fibers

For the case of an assembly of cylinders, $\vec{u}$ can be approximated by Happel's equation. The number of fibers contributing to the total streaming current across plane S can be approximated from geometrical considerations. An expression for the charge density, ρ, as a function of the potential, ψ, is developed for a cylindrical surface. The combination of these relationships into Equation (13) then gives the streaming current equation.

NUMBER OF FIBERS CONTRIBUTING TO TOTAL CURRENT

It is necessary to estimate the number of fibers contributing to the total streaming current, I, passing through the plane S. Both the number of fibers which are intersected by S and those which do not intersect this plane but still contribute to I must be considered.

Three processes by which counterions can be transported to the electric double layer are liquid flow, ion migration in an electric field caused by a charged fiber surface, and diffusion caused by a concentration gradient. Ciriacks (29) has discussed these processes and concluded that liquid flow was the dominant means of ion transport.

In order to approximate N, the number of fibers contributing to the total current, it is assumed that all fiber segments which are "visible" in the upstream projection of S (i.e., all the fiber required to cover on projection the cross-sectional area of the mat) contribute to I.

Thus,

$$N = A/2al \tag{14}$$

where

A = cross-sectional area of fiber mat

a = radius of cylindrical fiber

l = length of fiber

It should be noted that since the value of N is only an approximation, the values calculated for ζ are only relative values.

The substitution of Equation (14) into Equation (13) gives

$$I = -\frac{A}{al}\int_0^1 \int_a^{a+\tau} \rho u_\theta dr dz \ . \tag{15}$$

ION DISTRIBUTION WITHIN DIFFUSE LAYER

An expression for the excess charge density, ρ, as a function of the potential, ψ_o, must be developed for a cylindrical surface.

Equation (16) is the well-known Poisson equation and gives the relation between the average electrical potential, ψ, and ρ at any point.

$$\nabla^2\psi = -4\pi\rho/D \tag{16}$$

where

∇^2 = Laplace operator

D = dielectric constant

Assuming that the counterion distribution is uniform at all surfaces equidistant from the fiber surfaces, ψ is a function only of r, the radial distance. Thus, Equation (16) becomes

$$\frac{1}{r}\frac{\partial}{\partial r}\left[r\frac{\partial\psi}{\partial r}\right] = -4\pi\rho(r)/D \ . \tag{17}$$

The Boltzmann equation is used to give the relation between the concentration, $n_i(r)$, of ions of type i at a radial distance, r, the potential, and the ion concentration, $n_i(\infty)$, in the bulk solution:

$$n_i(r) = n_i(\infty)\ \exp\ [-z_i e\psi(r)/(k_i T)] \tag{18}$$

where

z_i = ion valency

e = electronic charge

k_i = Boltzmann constant

T = absolute temperature

The value for excess charge density, ρ, is given by

$$\rho(r) = \sum_i z_i e n_i(r) \ . \tag{19}$$

For a 1-1 electrolyte with $\psi < 10$ mv. and $T = 298°K$, Equation (19) reduces to:

$$\rho(r) = -2n_i(\infty)e\psi/k_1 T \ . \tag{20}$$

Substituting this equation into Equation (17) gives the Poisson-Boltzmann equation for a cylindrical surface:

$$\frac{1}{r}\frac{d}{dr}\left[r\frac{d\psi(r)}{dr}\right] = \kappa^2\psi \qquad (21)$$

where κ is the Debye-Huckel constant and

$$\kappa^2 = 8\pi n_i(\infty)e^2/(Dk_iT) \ . \qquad (22)$$

Equation (21) can be solved with the use of Bessel functions, using the boundary condition $\psi = \psi_\delta$ at $\underline{r} \cong \underline{a}$. The resulting solution is combined with Equations (17) and (21) to give:

$$\rho(r) = -[D\kappa^2\psi_\delta/4\pi][K_o(\kappa r)/K_o(\kappa a)] \qquad (23)$$

where $\underline{K}_o$ is the symbol for zero-order modified Bessel function of the second kind.

STREAMING CURRENT EQUATION

Substitution of Equations (12) and (23) into (15) then gives the streaming current caused by flow perpendicular to the axis of cylindrical fibers. The resulting equation, after integrating with respect to $\underline{z}$, is the following:

$$I = -\frac{AD\kappa^2\zeta_c}{4a\pi K_o(\kappa a)}\int_a^{a+\tau} K_o(\kappa r)[U - (3Cr^2/8 + D_1\ln(r)/2 + D_1/4 + E - F/r^2)]dr \qquad (24)$$

where $\underline{\zeta_c}$ is the experimental value of ψ_δ.

Equation (24) cannot be integrated exactly; thus, numerical integrations using Newton-Cotes quadrative were performed. Also, for large values of $\kappa\underline{r}$ (>10), the Bessel function, $\underline{K}_o$, can be approximated by the asymptotic expansion and

$$K_o(\kappa r)/K_o(\kappa a) = (a/r)^{\frac{1}{2}}\exp(\kappa a - \kappa r) \ . \qquad (25)$$

Combining Equations (24) and (25) and solving for ζ_c gives the following:

$$\zeta_c = -4C_4\pi a\kappa^{-2}(I/U)/[AD(T_3 - 0.375CT_1 - 0.5D_1T_2 - T_3(E + 0.25D_1) + FT_4] \quad (26)$$

where

$$D_1 = -2/\ln[1/(1 - \varepsilon)^{0.5}] + 4[(1 - \varepsilon)^2 - 1]/[(1 - \varepsilon)^3 + 1] \quad (27)$$

$$F = D_1a^2/[4(1 - \varepsilon)^2 + 4] \quad (28)$$

$$C = -8F(1 - \varepsilon)^2/a^4 \quad (29)$$

$$E = 1 + F/a^2 - 0.5D_1(\ln a + 0.5) - 0.375Ca^2 \quad (30)$$

$$T_1 = a^{0.5}\int_a^{a+\tau} \exp(\kappa a - \kappa r)r^{1.5}dr \quad (31)$$

$$T_2 = a^{0.5}\int_a^{a+\tau}[\exp(\kappa a - \kappa r)\ \ln r/r^{0.5}]dr \quad (32)$$

$$T_3 = a^{0.5}\int_a^{a+\tau}[\exp(\kappa a - \kappa r)/r^{0.5}]dr \quad (33)$$

$$T_4 = a^{0.5}\int_a^{a+\tau}[\exp(\kappa a - \kappa r)/r^{2.5}]dr \quad (34)$$

$C_4 = 9.0$, constant to convert units to the same system

Appendix VI gives the computer program used to solve for ζ_c at each porosity level from the experimental data.

The reader is referred to Ciriacks (29) for a more detailed development of this derivation.

APPENDIX II

DETAILS OF EXPERIMENTAL APPARATUS

POTENTIOMETRIC TITRATIONS

The potentiometric titrations described here were based on a method suggested by Kenchington (48). Basically, one experimental titration consisted of placing 2 g. of the fiber along with 200 ml. of 0.1M KCl in a Lucite cell. This slurry was then stirred with a motor-driven, propeller-type stirrer to disperse the fibers. The cell was then placed in a water bath at 25.0°C. and a paddle-type stirrer was used to keep the fibers dispersed. Nitrogen was bubbled through the slurry to exclude carbon dioxide. The pH of the slurry was monitored with a Corning pH meter.

All solutions used were made up with deaerated distilled water. The nitrogen, which was bubbled through the fiber slurry, was first bubbled through three carbon dioxide traps consisting of 50% KOH solution. This was followed by a 1% sulfuric acid trap and a water trap. This procedure for introducing nitrogen into the titration cell kept carbon dioxide out without causing changes in the slurry volume.

The pH meter used here was a Corning Model 12 Research pH meter. The electrodes were a Corning calomel reference electrode and a Corning Triple Purpose Reference electrode.

Figure 18 is a schematic diagram of the experimental assembly.

TURBIDITY TITRATIONS

Polyvinyl pyridine (PvPy) was synthesized by emulsion polymerization according to the method of Fuoss and Strauss (73). In this method, 360 cc. of toluene were boiled to expel air and cooled with a stream of nitrogen. A 40-cc. volume of freshly distilled 4-vinyl pyridine and 1.2 g. of benzoyl peroxide were added. The mixture

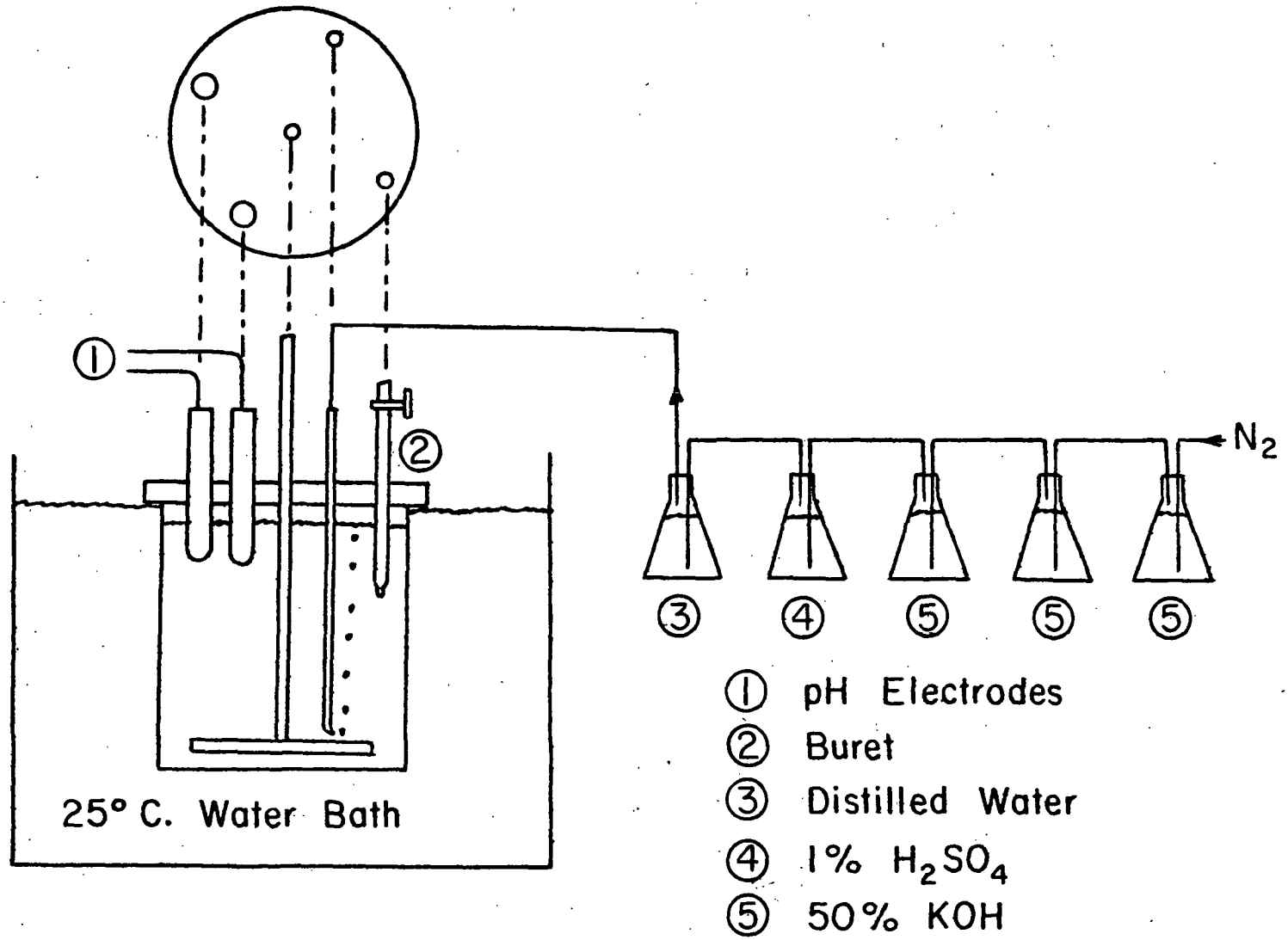

Figure 18. Schematic Diagram of Potentiometric Titration Assembly

was stirred in a water bath at 50°C. for 48 hours. The insoluble polymer was filtered, washed twice with benzene, and dried in a vacuum at 40°C.

PVPB was prepared by dissolving 3 g. of the purified PvPy in 57 g. of nitromethane. A 24.2-g. mass of n-butyl bromide was then added slowly with stirring. The mixture was stirred slowly at 55°C. in a water bath for 4 days. Next, the solvent and excess butyl bromide were removed by distillation at reduced pressure. The product was dissolved in ethanol, filtered, and precipitated in dioxane. This purification process was repeated and finally the PVPB was dried under vacuum.

Light scattering was measured with a Brice-Phoenix Universal Light Scattering Photometer (Phoenix Precision Instrument Co., Philadelphia, Pa.) at an angle of 90°.

ZETA POTENTIAL MEASUREMENTS

ELECTRODES

The electrodes used in the streaming current apparatus were fabricated from 0.016-in. blank silver stock obtained from Engelhard Industries, Newark, N. J., and had a purity of 99.99%. The silver blank was drilled with 1/16-in. holes to give approximately a 30% cross-sectional area open to flow. The blank was then cut to give a 3-in. diameter electrode with a 1/4 × 3-in. pigtail left on the disk. Electrical connections were made by soldering a 20-gage stranded, insulated wire to the pigtail.

The backs of the silver disks and the pigtails were coated with G.E. Silicone Rubber (General Electric Co., Providence, R. I.). This material was removed from the perforations by suction prior to curing.

Prior to anodization, a careful cleaning procedure was followed. This consisted of polishing the surface with 320-C silicone carbide paper, followed by

polishing with crocus cloth. The surface was then polished with silver polish, washed with 95% ethanol, and rinsed with distilled water. The silver disks were then fastened to the Lucite supports with three 8-lb. monofilament lines threaded through the perforations.

Anodization was carried out in the apparatus shown in Fig. 19 and 20. The electrode supports were placed in the apparatus and deaerated 0.1N HCl was pumped into the anodizing tube. Gas bubbles were removed by tapping the anodizing tube and moving the top electrode up and down in the solution.

Current was supplied to the electrodes at a current density of 1.0 milliamp./cm.^{2} from a high-voltage d.c. power supply. The current direction was changed every 15 minutes for 1.5 hours. Anodizing was then carried out for 0.5 to 1.0 hour. This procedure produced a uniform brown coating of AgCl. The current reversal technique was necessary to achieve stable electrodes in which the residual current was close to 0.0 μa. After several days' storage in 10^{-4}M KCl with the electrodes shorted together, the residual current ranged from 0.0 to 1.0 μa.

The electrodes were stored, shorted together, in the forming tube under deaerated 10^{-4}M KCl. Direct contact with light was avoided by wrapping the forming tube with a black cloth.

WATER

Careful attention was paid to the water supply. Distilled water was produced by a Precision water still (Precision Scientific Co., Chicago, Ill.), rated at 3-5 gal./hr. The feed water was deionized prior to distillation.

The distilled water was deaerated by boiling and then filtered (Millipore filter, Millipore Filter Co., Bedford, Mass. with 0.45-μm. average pore size) before use.

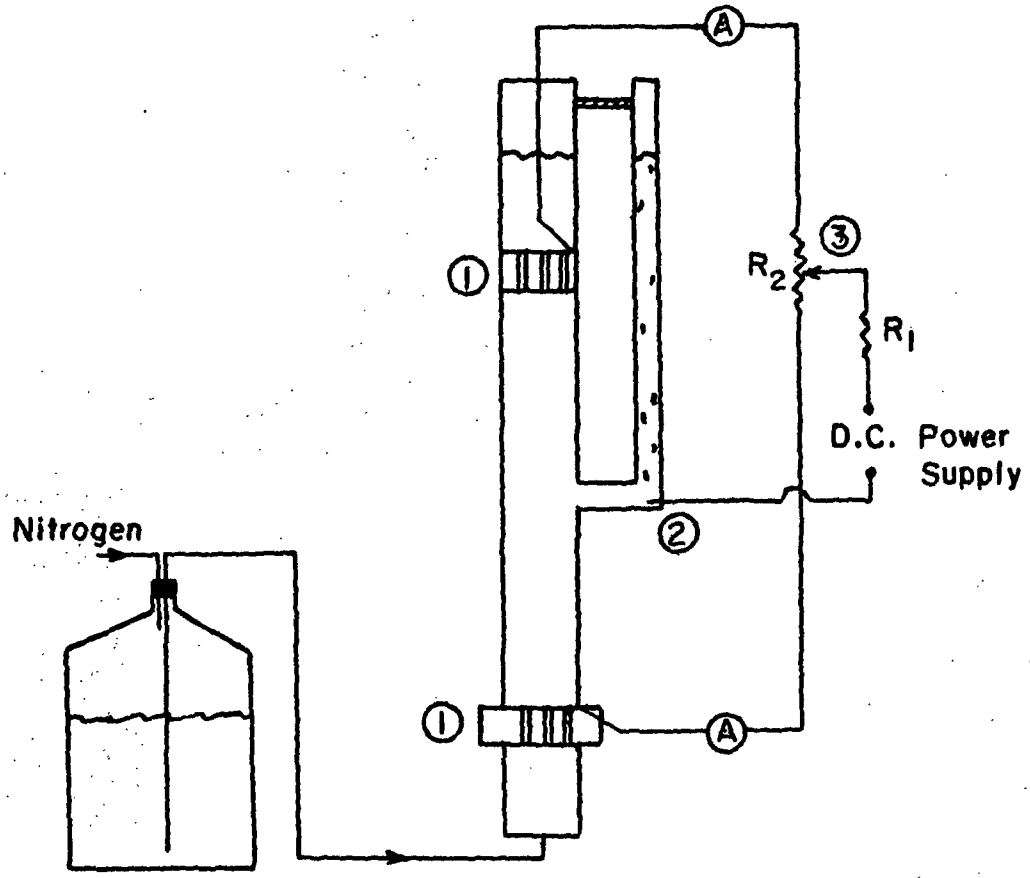

① Electrode and Plastic Support

② Platinum Wire

③ Slide Wire Resistor Adjusted to Keep Same Current Through Each Ammeter (R_1 = 1000 and R_2 = 690 Ohms)

Figure 19. Apparatus for Forming Silver-Silver Chloride Electrodes

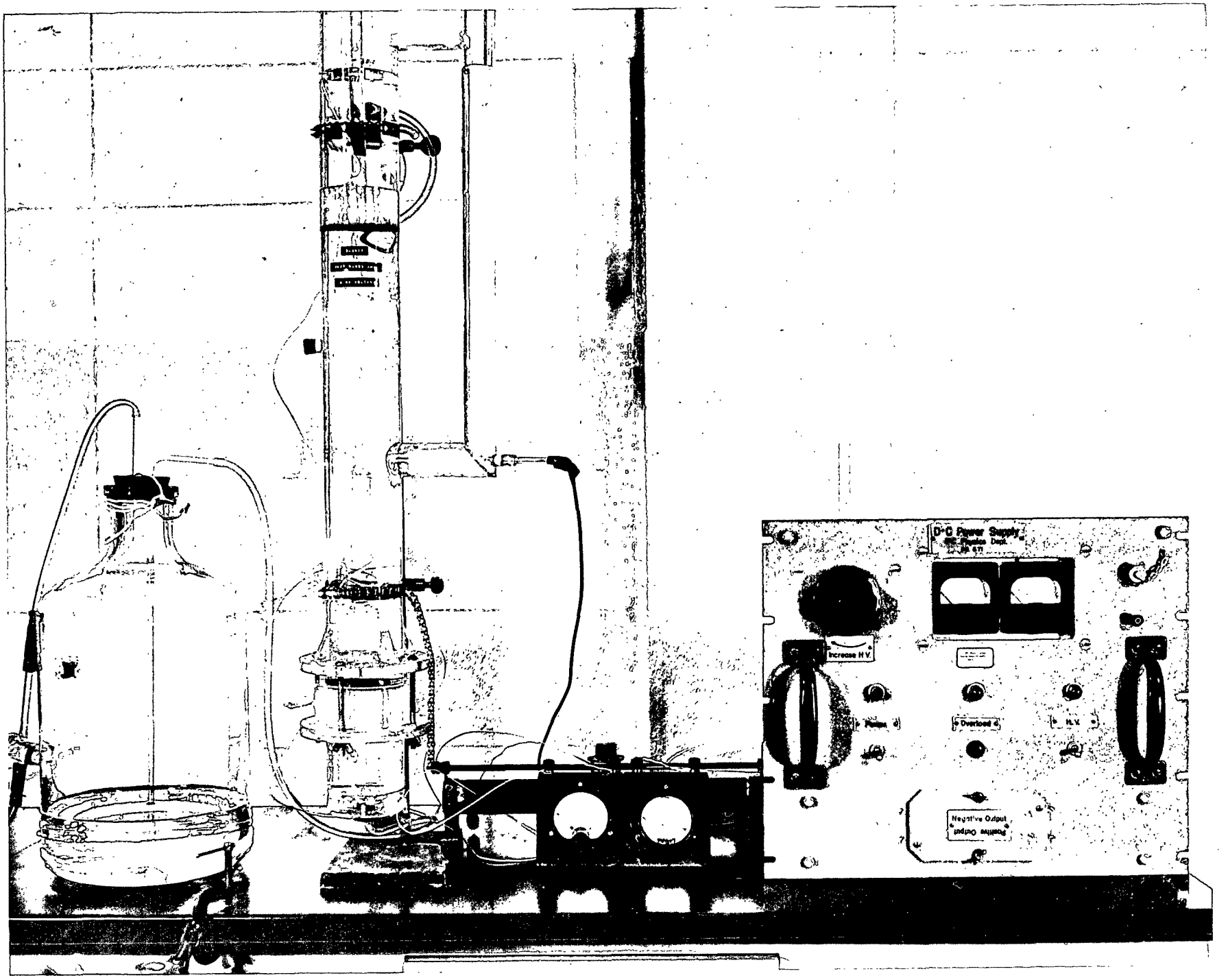

Figure 20. Silver-Silver Chloride Anodizing Apparatus

All the distilled water used had a specific conductance of less than 1.1×10^{-6} cm.$^{-1}$ ohm^{-1}. The pH of this water was approximately 6.8.

MAT FORMATION

The fibers were deaerated in about 2 liters of 10^{-4}M KCl under vacuum after dispersion in a British disintegrator (300 revolutions). This slurry was then carefully added to a tank containing 100 liters of deaerated, distilled water. KCl solution was pipeted into the tank to give the required KCl concentration. The fiber consistency was kept below 0.01% to keep flocculation at a minimum.

The mat was formed from this slurry by constant-rate filtration with a nominal fluid velocity of about 1 cm./sec. A portion of the effluent was filtered and pumped to a polyethylene bottle for recirculation during streaming current measurements and the remainder was pumped to the sewer.

A schematic diagram of the complete flow system and a photograph of the forming tube were shown in Fig. 3 and 4.

STREAMING CURRENT APPARATUS

The procedure used to measure the streaming current of the fiber pads was discussed previously. The equipment and techniques used to make the required measurements will be described here.

Flow Rate

Streaming currents were measured at eight to ten different flow rates varying from about 0.1 to 0.5 cm./sec. Constant flow rates were maintained with a Tuthill, Model 53DF-M (Tuthill Pump Co., Chicago) stainless steel metering pump which was driven by a 1/4-h.p. Adjust-O-Spede drive (Eaton Mfg. Co., Kenosha, Wis.). Flow rates were measured with a Fischer-Porter Tri-Flat flowmeter (Fischer and Porter, Hatboro, Pa.).

Pressure Drop

Carbon tetrachloride-water manometers were used to measure the frictional pressure drop across the bed. The distilled water in the manometer system was kept deaerated by carefully flushing the system with hot, distilled water periodically. A Merian manometer (Merian Instrument Co., Cleveland) was used.

Current

A Scalamp, Model 29-105, galvanometer (Ealing Corp., Cambridge, Mass.) was used to measure the current between the two electrodes. The sensitivity of this instrument was 0.05 μa./mm., and the resistance presented to the external circuit was less than 25 ohms at all shunt settings. Unshielded, plastic-insulated wire was used to connect the galvanometer to the electrodes.

Mat Resistance

The resistance of the mat was measured at each porosity level with no liquid flow. This was done with a Z-Y bridge (Type 1603-A, General Radio Co., West Concord, Mass.) at 1000 cycles per sec. These a.c. measurements did not seem to polarize the electrodes.

Mat Thickness

The thickness of the mat was measured with the use of two dial micrometers attached rigidly to the shaft holding the top electrode. As the shaft is moved down, the micrometers indicate the displacement of the electrode. A reference displacement can be made with no pad present and electrodes just touching. These measurements allow the pad thickness to be calculated.

In addition, a correlation between the pressure reading on the gages connected to the hydraulic ram and the micrometer measurements with no mat present enabled a correction to be made for apparatus deformation under load.

Load Applied to Mat

A hydraulic ram was attached, by means of a stainless steel shaft, to the top electrode. Pressure gages gave the compressive load applied to the shaft.

Electrolyte Concentration and pH

The KCl concentration of the permeating fluid was determined by a conductivity technique. Samples of the fluid were stored in polyethylene bottles immediately following each run. The specific conductivity function of the Numinco Electrophoretic Mass-Transport Analyzer (Numec Instruments and Controls Corp., Monroeville, Pa.) was used for conductivity measurements.

Literature values for the specific conductance, K, of KCl solutions of varying concentration, C, were used to construct a plot of log K vs. log C as shown in Fig. 21. A least squares method was used to calculate the slope and intercept of this straight line. A solution of KCl was made using boiled, distilled water and accurately weighed over dried, reagent-grade KCl. Aliquots of this solution were diluted to give several concentrations. The resistances of these solutions were compared with literature values to determine the cell constant. The specific conductance was then determined, and this is also plotted in Fig. 21. Table VI gives the literature and experimental values of the specific conductance for several KCl concentrations.

Thus, the measurement of the resistance of a KCl solution can be used to determine its concentration by using this plot. The accuracy of this method is $\pm 2 \times 10^{-6}$ M/liter.

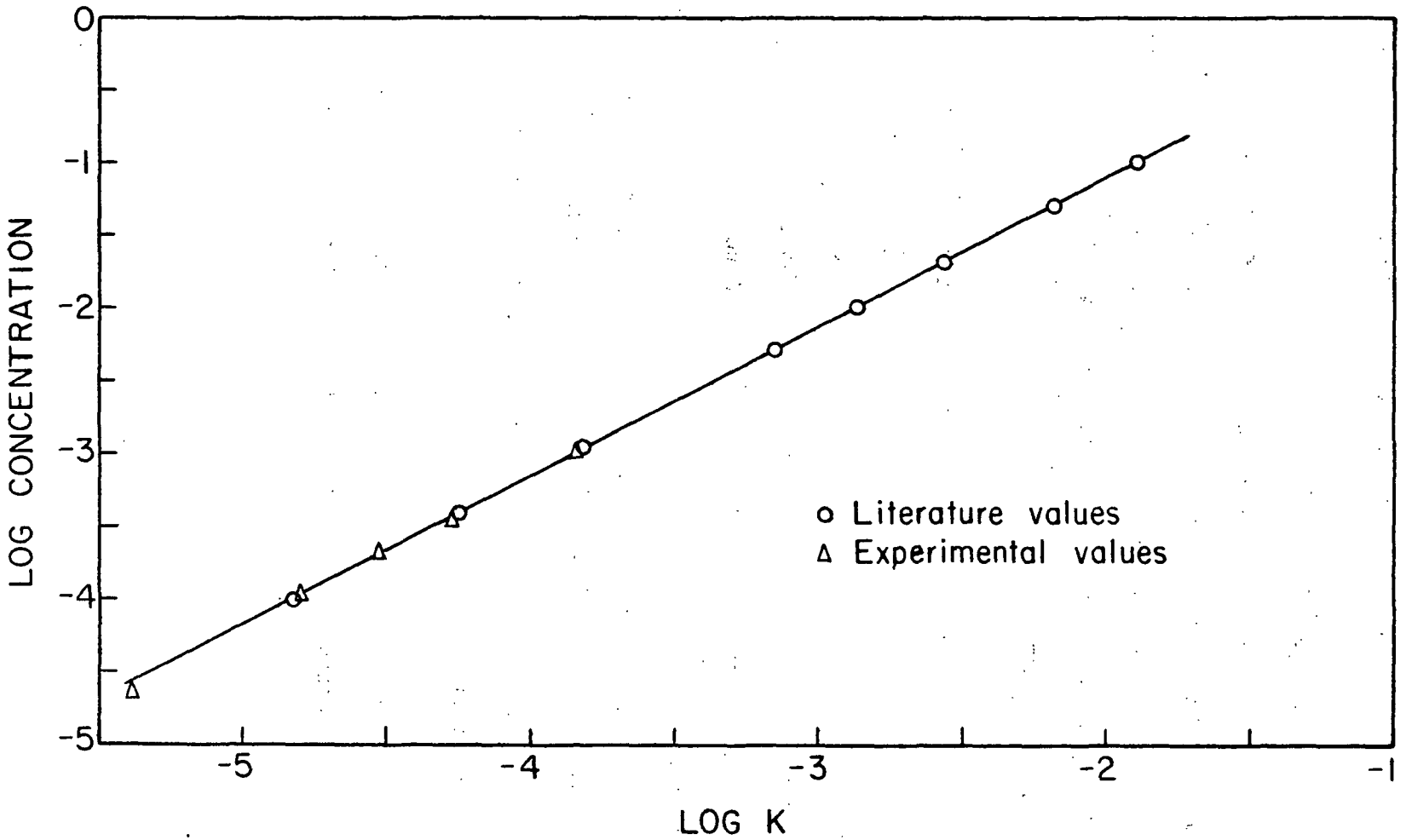

Figure 21. Specific Conductivity-Concentration Calibration Curve

TABLE VI

CONCENTRATION AND SPECIFIC CONDUCTANCE FOR KCl

Literature Values (74)

Concentration, M/l.	K, $cm.^{-1}ohm^{-1}$
0.0001	1.489×10^{-5}
0.0005	7.3905×10^{-5}
0.0010	1.4695×10^{-4}
0.0050	7.1775×10^{-4}
0.0100	1.4127×10^{-3}
0.0200	2.7668×10^{-3}
0.0500	6.6685×10^{-3}
0.1000	1.2896×10^{-2}

Experimental Values

Concentration, M/l. $\times 10^4$	R, ohm	K, $cm.^{-1}\ ohm^{-1}$ [a]
9.979	685.2	1.45×10^{-4}
4.989	1370	7.21×10^{-5}
1.996	3316	3.00×10^{-5}
0.9979	6486	1.534×10^{-5}
0.1996	26250	3.790×10^{-6}

[a] Using cell constant = 0.0995 $cm.^{-1}$

APPENDIX III

PRELIMINARY ADSORPTION DATA

Preliminary adsorption experiments were made with dacron and Tamol. Tamol is the trade name for a dispersing agent produced by Rohm and Haas Co. This material was used by Morgan (75) and, according to analyses conducted by him, it was concluded that Tamol is the sodium salt of polymethacrylic acid. The number average molecular weight was reported to be 4000 (75).

The objective of the preliminary adsorption experiments was to determine if a polymer containing carboxyl groups would adsorb onto dacron and to characterize the adsorption process.

When the Tamol adsorption studies had been completed, a sample of polyacrylic acid was synthesized and the adsorption of this polymer was also characterized. Finally, several adsorption experiments were run with a sample of nylon fibers and the synthesized PAA. The results of these adsorption experiments are summarized in Tables VII to IX. Figures 22 and 23 show the Tamol adsorption data.

Carboxyl contents were determined for all fibers by the NaCl-$NaHCO_3$ method. The carboxyl adsorbed was determined by the difference between the blank (fiber with no polymer in the adsorption solution) and the fibers with adsorbed polymer at corresponding pH levels.

Due to the variability of the carboxyl content of the blank fibers, this value was determined during each set of experiments and used to calculate the amount of adsorption for that set of experiments only.

The reason for the carboxyl content variation in the blanks is not fully understood. Some of the variation could be due to water quality variations since these experiments were done over a period of time when the water quality was changing.

TABLE VII

ADSORPTION OF TAMOL AND PAA BY DACRON

Polymer	Final Concn., meq./100 ml.	pH	Time, hr.	Times Washed	Carboxyl Content, meq./100 g.	Carboxyl Adsorbed, meq./100 g.
--	--	2	120	5	0.69	--
--	--	4	120	5	0.73	--
--	--	6	120	5	0.76	--
--	--	8	120	5	0.75	--
--	--	10	120	5	0.91	--
T	0.07	2	120	5	1.67	0.98
T	0.07	4	120	5	0.96	0.23
T	0.07	6	120	5	0.96	0.20
T	0.07	8	120	5	1.50	0.75
T	0.07	10	120	5	1.13	0.20
T	0.001	4	120	5	1.04	0.31
T	0.003	4	120	5	0.92	0.19
T	0.007	4	120	5	1.28	0.55
T	0.013	4	120	5	1.16	0.43
T	0.033	4	120	5	1.70	0.97
T	0.068	4	120	5	1.91	1.18
T	0.130	4	120	5	2.03	1.30
T	0.07	4	120	2	2.10	1.37
T	0.07	4	120	2	1.84	1.11
T	0.07	4	120	5	1.61	0.88
T	0.07	4	120	5	1.65	0.92
T	0.07	4	120	10	1.62	0.89
T	0.07	4	120	10	1.60	0.87
T	0.07	4	120	25	1.61	0.88
T	0.07	4	120	25	1.56	0.83
T	0.06	4	1/2	5	0.80	0.07
T	0.06	4	1	5	2.21	1.48
T	0.06	4	5	5	1.30	0.57
T	0.06	4	10	5	1.68	0.95
T	0.06	4	50	5	2.89	2.16
T	0.06	4	100	5	1.46	0.73
--	--	2	100	10	1.67	--
--	--	4	100	10	1.55	--
--	--	6	100	10	1.76	--
--	--	8	100	10	1.57	--
--	--	10	100	10	1.72	--
--	--	12	100	10	1.55	--

TABLE VII (Continued)

ADSORPTION OF TAMOL AND PAA BY DACRON

Polymer	Final Concn., meq./100 ml.	pH	Time, hr.	Times Washed	Carboxyl Content, meq./100 g.	Carboxyl Adsorbed, meq./100 g.
T	0.02	2	100	10	2.04	0.37
T	0.02	4	100	10	1.88	0.33
T	0.02	6	100	10	1.89	0.13
T	0.02	8	100	10	2.10	0.53
T	0.02	10	100	10	1.97	0.25
T	0.02	12	100	10	1.77	0.22
T	0.02	4	1/6	10	1.26	-0.29
T	0.02	4	1/2	10	1.94	0.39
T	0.02	4	1	10	1.81	0.26
T	0.02	4	5	10	1.88	0.33
T	0.02	4	10	10	1.94	0.39
T	0.02	4	50	10	1.98	0.43
T	0.02	4	100	10	1.79	0.24
T	0.02	4	200	10	1.91	0.36
--	--	2	100	10	0.00	--
--	--	4	100	10	0.00	--
--	--	4	100	10	0.00	--
--	--	7	100	10	0.00	--
--	--	10	100	10	0.00	--
P	0.46	4	100	10	0.12	0.12
P	0.09	4	100	10	0.10	0.10
P	0.05	4	100	10	0.06	0.06
P	0.02	4	100	10	0.04	0.04
P	0.001	4	100	10	0.05	0.05
P	0.46	2	100	10	0.29	0.29
P	0.46	7	100	10	0.15	0.15
P	0.46	10	100	10	0.09	0.09
P	0.5	4	5	10	0.13	0.13
P	0.5	4	25	10	0.09	0.09
P	0.5	4	50	10	0.12	0.12
P	0.5	4	100	10	0.14	0.14
P	0.5	4	100	5	0.15	0.15
P	0.5	4	100	10	0.13	0.13
P	0.5	4	100	25	0.11	0.11

Note: T = Tamol
P = PAA

TABLE VIII

EFFECT OF ACID WASH ON ADSORPTION MEASUREMENTS

Polymer	Acid Wash	Carboxyl Content, meq./100 g.	Carboxyl Adsorbed, meq./100 g.
T	Yes	1.80	0.19
T	Yes	1.97	0.36
T	No	1.89	0.24
T	No	1.89	0.24
--	Yes	1.61	--
--	No	1.65	--
--	No	1.65	--
P	Yes	0.14	0.14
P	No	0.13	0.13
--	Yes	0.00	--
--	No	0.00	--

Note: T denotes Tamol.
P denotes PAA.

For T, concentration was 0.15 meq./100 ml., pH was 4, time was 100 hr., and number of times washed was 10.

For P, concentration was 0.51 meq./100 ml., pH was 4, time was 100 hr., and number of times washed was 10.

TABLE IX

NYLON-PAA ADSORPTION

pH	Carboxyl Content, meq./100 g.			Carboxyl Adsorbed, meq./100 g.		
	$NaHCO_3$	MB1	MB2	$NaHCO_3$	MB1	MB2
2	1.62	0.56	0.23	0.80	0.22	-0.11
4	1.07	0.33	0.09	0.25	-0.01	-0.25
6	0.95	0.21	0.06	0.13	-0.13	-0.28
8	0.78	0.33	0.32	-0.04	-0.01	-0.02
10	0.73	0.52	0.50	-0.09	0.28	0.26
12	1.09	1.08	1.17	0.27	0.74	0.83
	Blank Determinations					
2	0.86	0.10	0.03			
6	0.84	0.35	0.34			
10	0.78	0.34	0.34			

Notes: $NaHCO_3$ results are the average of two determinations.

To determine amount adsorbed, a blank value of 0.82 was used for the $NaHCO_3$ method, and a blank value of 0.34 was used for the MB method.

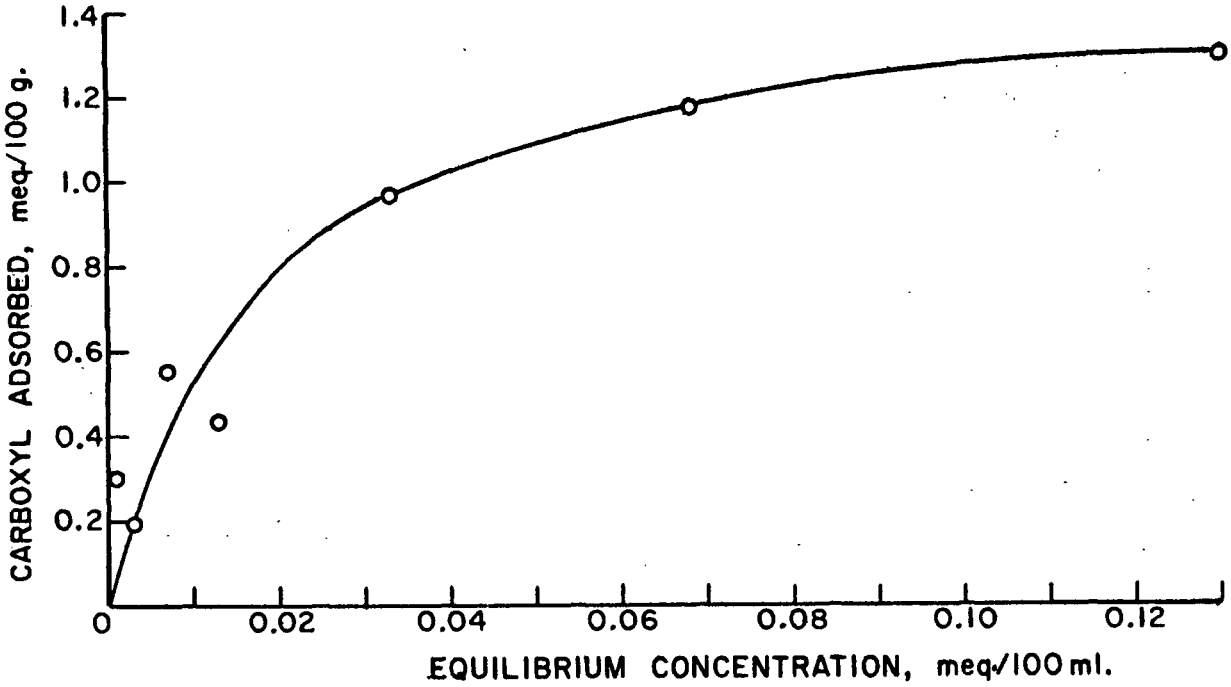

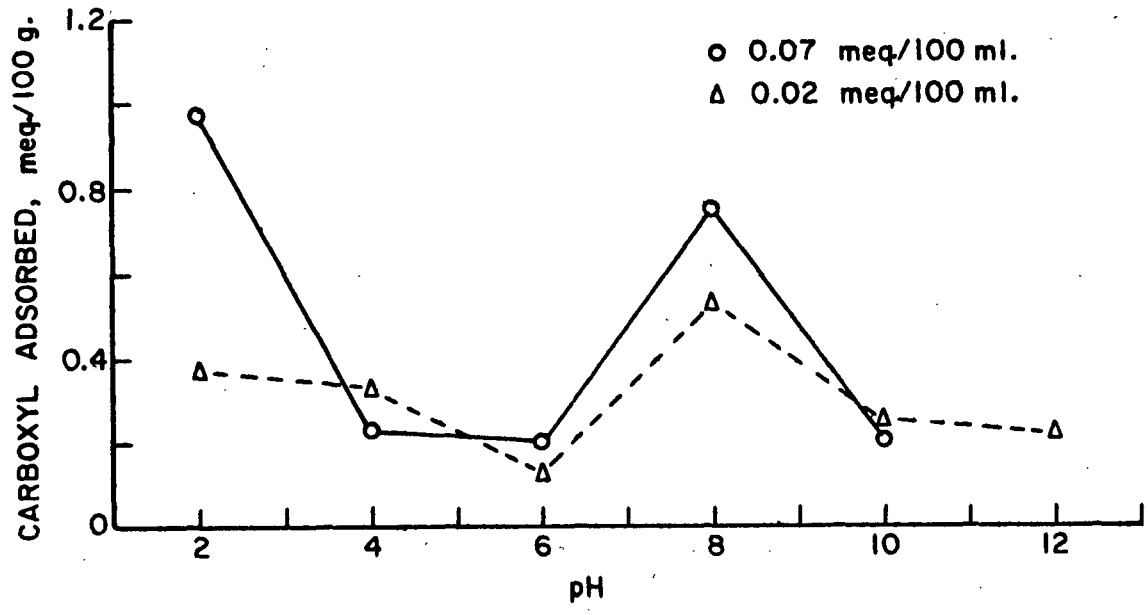

Figure 22. Tamol Isotherm

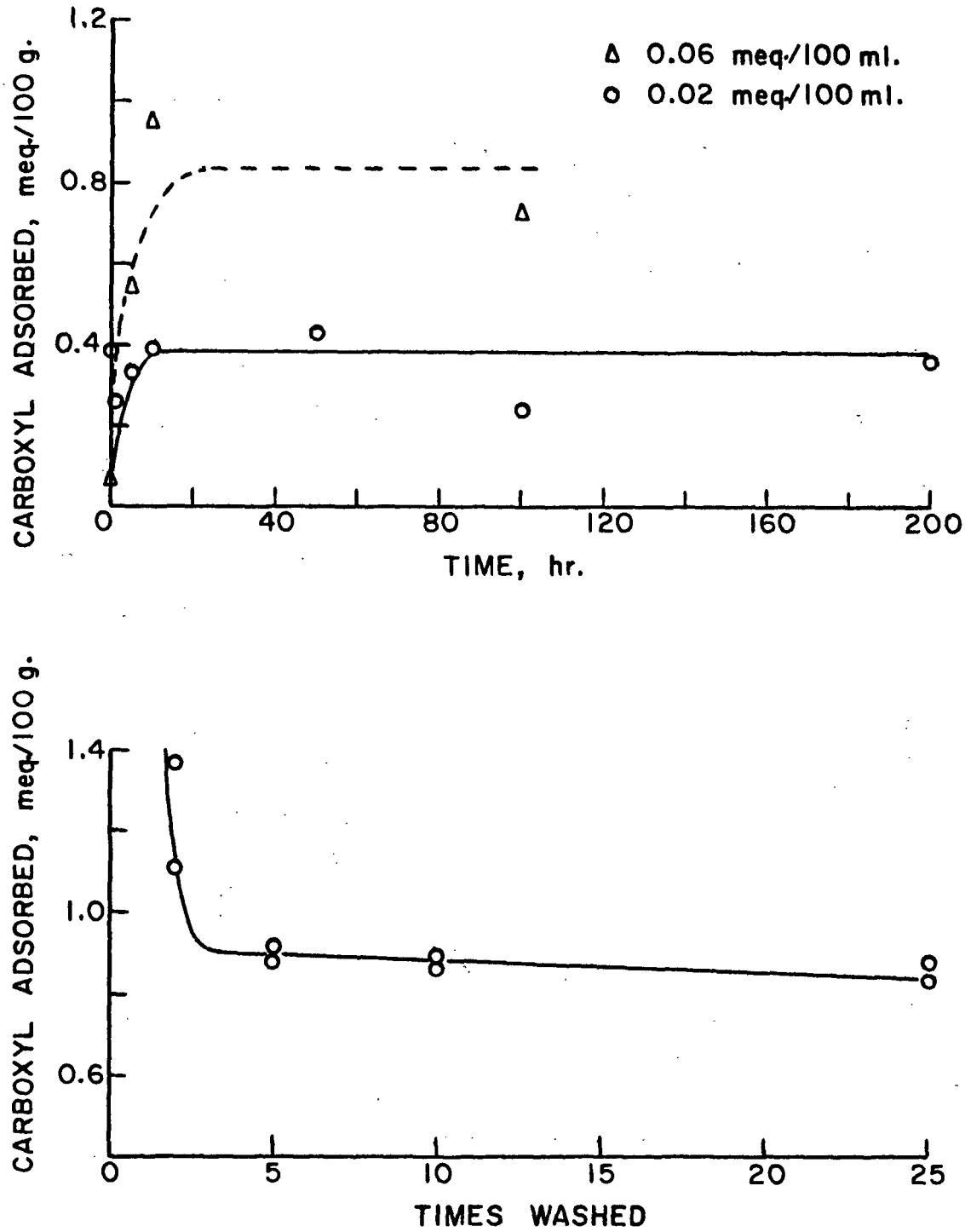

Figure 23. Tamol Isotherm

Since the carboxyl contents of the fibers with adsorbed polymer changed in a manner similar to that of the blanks, it was concluded that even though the actual carboxyl content of the fibers could not be determined, the difference in carboxyl content before and after adsorption could be measured with some degree of reliability. This difference was attributed to adsorbed polymer.

Table VIII gives the results of carboxyl content determinations on several samples of fibers to determine the effect of the acid wash during the $NaCl-NaHCO_3$ method. The acid wash consisted of dispersing the fibers in a 0.1N HCl solution followed by an equilibrium period of two hours during which the samples were periodically shaken. After this, the fibers were filtered and washed with CO_2-saturated, distilled water.

In Table IX, the results of the nylon-PAA adsorption studies are summarized. In addition to the $NaCl-NaHCO_3$ method, the carboxyl contents were also determined by the methylene blue (MB) method (47).

The MB method consists of equilibrating the carboxyl-containing fibers, by rotating for one hour, with a solution of MB. The amount of MB removed from solution by the carboxyl groups is measured spectrophotometrically. The best results are obtained when approximately 50% of the MB in the original solution is removed. Thus, after one determination, the amount of fiber required to remove 50% of the MB is calculated and a second determination is made with this amount of fiber. The results of these two determinations are indicated by MB1 and MB2 in Table IX.

In using the MB method, it was noted that the fibers clumped together in small, tightly packed balls during rotation. This apparently limited the amount of fiber surface available to the solution, resulting in low carboxyl content values. The results of this method were thus considered of questionable value.

The molecular weights of the PAA samples used in this study were obtained from viscosity measurements. Tables X and XI give the viscosity data obtained.

TABLE X

VISCOSITY OF POLYACRYLONITRILE IN DMF

Concentration, g./100 ml.	Time,[a] sec.	Temperature, °C.
Solvent only	90.2	31.05
0.201	143.3	31.08
0.134	126.7	
0.1005	115.6	
0.067	106.2	
0.4074	218.5	31.10
0.2037	140.5	
0.1018	112.3	
0.509	100.2	

[a]Average of 5 determinations.

TABLE XI

VISCOSITY OF PAA IN DIOXANE

Concentration, g./100 ml.	Time,[a] sec.	Temperature, °C.
Solvent only	83.1	30.51
0.4022	167.1	30.48
0.2011	111.7	
0.1050	88.3	
0.0525	84.1	
0.3256	130.5	30.45
0.1628	101.3	
0.0814	88.1	
0.0407	84.0	

[a]Average of 5 determinations.

APPENDIX IV

POTENTIOMETRIC TITRATION DATA

The carboxyl content of the fibers and the degree of dissociation were calculated from the titration data according to a procedure described by Kenchington (48). This procedure is described below and the raw titration data are given in Table XII.

Consider an HCl solution having a concentration C_1 moles per liter. The initial concentration of hydrogen will be C_1 and the pH of the solution will be given by:

$$pH_1 = -\log f_1 C_1 \qquad (35)$$

where f_1 is the activity coefficient.

If the same solution were prepared containing g grams per liter of fiber, then the hydrogen ion concentration will be C_2 and $(C_1 - C_2)/g$. moles of hydrogen ion will have combined with the fiber. The pH of this solution will be given by:

$$pH_2 = -\log f_2 C_2 \ . \qquad (36)$$

Combining the expressions for pH_1 and pH_2 gives:

$$\log (C_2/C_1) = pH_1 - pH_2 + \log (f_1/f_2) \ . \qquad (37)$$

The assumption is made that the activity coefficients of the two solutions are the same, so that the last term in Equation (37) is zero.

This equation can then be rearranged and divided by g to give the moles of bound proton per gram of fiber:

$$(C_1 - C_2)/g = (C_1/g)[1 - \text{antilog } (pH_1 - pH_2)]. \qquad (38)$$

TABLE XII

POTENTIOMETRIC TITRATION DATA

Blank Dacron

Vol., ml.	pH S	pH B	H^+, meq./100 g.
0.200	4.962	4.864	0.438
0.400	4.627	4.530	0.475
0.600	4.427	4.334	0.498
0.800	4.284	4.196	0.511
1.000	4.172	4.089	0.521
1.200	4.079	4.001	0.528
2.000	3.819	3.756	0.546
3.000	3.614	3.563	0.559
5.000	3.356	3.320	0.573
6.000	3.267	3.235	0.576
7.000	3.191	3.163	0.581
8.000	3.126	3.101	0.583
8.400	3.102	3.078	0.583
8.800	3.079	3.056	0.584
9.000	3.069	3.046	0.585
9.200	3.059	3.036	0.585
9.400	3.048	3.026	0.586
9.600	3.038	3.016	0.586
9.800	3.028	3.007	0.587
10.000	3.018	2.997	0.587
11.000	2.973	2.954	0.587

Wt. = 1.738 g.

Vol., ml.	pH S	pH B	H^+, meq./100 g.
0.200	4.960	4.864	0.436
0.400	4.624	4.530	0.474
0.600	4.424	4.334	0.496
0.800	4.281	4.196	0.509
1.000	4.170	4.089	0.519
1.200	4.077	4.001	0.526
2.000	3.817	3.756	0.544
3.000	3.612	3.563	0.557
5.000	3.355	3.320	0.571
6.000	3.266	3.235	0.574
7.000	3.190	3.163	0.579
8.000	3.126	3.101	0.581
8.400	3.102	3.078	0.581
8.800	3.079	3.056	0.582
9.000	3.068	3.046	0.583
9.200	3.058	3.036	0.583
9.400	3.048	3.026	0.584
9.600	3.037	3.016	0.584
9.800	3.028	3.007	0.585
10.000	3.018	2.997	0.585
11.000	2.973	2.954	0.585

Wt. = 2.003 g.

Vol., ml.	pH S	pH B	H^+, meq./100 g.
0.200	4.959	4.864	0.437
0.400	4.624	4.530	0.475
0.600	4.424	4.334	0.497
0.800	4.281	4.196	0.510
1.000	4.169	4.089	0.520
1.200	4.077	4.001	0.527
2.000	3.817	3.756	0.545
3.000	3.612	3.563	0.558
5.000	3.355	3.320	0.572
6.000	3.266	3.235	0.575
7.000	3.190	3.163	0.580
8.000	3.126	3.101	0.582
8.400	3.102	3.078	0.582
8.800	3.079	3.056	0.583
9.000	3.068	3.046	0.584
9.200	3.058	3.036	0.584
9.400	3.048	3.026	0.585
9.600	3.037	3.016	0.585
9.800	3.028	3.007	0.586
10.000	3.017	2.997	0.586
11.000	2.973	2.954	0.586

Wt. = 1.990 g.

Vol., ml.	pH S	pH B	H^+, meq./100 g.
0.200	4.960	4.864	0.442
0.400	4.625	4.530	0.480
0.600	4.425	4.334	0.503
0.800	4.282	4.196	0.516
1.000	4.170	4.089	0.527
1.200	4.077	4.001	0.534
2.000	3.818	3.756	0.551
3.000	3.612	3.563	0.565
5.000	3.355	3.320	0.579
6.000	3.266	3.235	0.582
7.000	3.191	3.163	0.587
8.000	3.126	3.101	0.589
8.400	3.102	3.078	0.589
8.800	3.079	3.056	0.590
9.000	3.068	3.046	0.591
9.200	3.058	3.036	0.591
9.400	3.048	3.026	0.592
9.600	3.037	3.016	0.592
9.800	3.028	3.007	0.593
10.000	3.018	2.997	0.593
11.000	2.973	2.954	0.593

Wt. = 1.985 g.

Vol., ml.	pH S	pH B	H^+, meq./100 g.
0.200	4.961	4.864	0.444
0.400	4.626	4.530	0.482
0.600	4.426	4.334	0.505
0.800	4.283	4.196	0.518
1.000	4.171	4.089	0.528
1.200	4.078	4.001	0.535
2.000	3.818	3.756	0.553
3.000	3.613	3.563	0.566
5.000	3.356	3.320	0.581
6.000	3.266	3.235	0.584
7.000	3.191	3.163	0.589
8.000	3.126	3.101	0.591
8.400	3.102	3.078	0.591
8.800	3.079	3.056	0.592
9.000	3.069	3.046	0.593
9.200	3.058	3.036	0.593
9.400	3.048	3.026	0.594
9.600	3.038	3.016	0.594
9.800	3.028	3.007	0.595
10.000	3.018	2.997	0.595
11.000	2.973	2.954	0.595

Wt. = 1.998 g.

Vol., ml.	pH S	pH B	H^+, meq./100 g.
0.200	4.946	4.864	0.438
0.400	4.611	4.530	0.475
0.600	4.412	4.334	0.498
0.800	4.269	4.196	0.511
1.000	4.158	4.089	0.521
1.200	4.066	4.001	0.528
2.000	3.809	3.756	0.546
3.000	3.606	3.563	0.559
5.000	3.350	3.320	0.573
6.000	3.262	3.235	0.576
7.000	3.187	3.163	0.581
8.000	3.122	3.101	0.583
8.400	3.099	3.078	0.583
8.800	3.076	3.056	0.584
9.000	3.065	3.046	0.585
9.200	3.055	3.036	0.585
9.400	3.045	3.026	0.586
9.600	3.034	3.016	0.586
9.800	3.025	3.007	0.587
10.000	3.015	2.997	0.587
11.000	2.970	2.954	0.587

Wt. = 2.046 g.

Vol., ml.	pH S	pH B	OH^-, meq./100 g.
0.05	9.182	9.291	0.001
0.10	9.583	9.683	0.002
0.20	9.998	9.987	0.002
0.30	10.166	10.175	-
0.50	10.407	10.401	-
2.00	11.048	11.006	-

Wt. = 1.990 g.

Vol. = volume added
pH S = pH of slurry
pH B = pH of blank
H^+ = hydrogen ion combined.

TABLE XII (Continued)

POTENTIOMETRIC TITRATION DATA

FIBER A

Vol., ml.	pH S	pH B	H^+, meq./100 g.
0.200	5.115	4.864	0.829
0.400	4.780	4.530	0.908
0.600	4.566	4.334	0.934
0.800	4.415	4.196	0.966
1.000	4.294	4.089	0.985
1.200	4.191	4.001	0.993
2.000	3.904	3.756	1.018
3.000	3.678	3.563	1.036
5.000	3.399	3.320	1.049
6.000	3.304	3.235	1.049
7.000	3.223	3.163	1.049
8.000	3.155	3.101	1.050
8.400	3.130	3.078	1.050
8.800	3.106	3.056	1.050
9.000	3.095	3.046	1.050
9.200	3.084	3.036	1.050
9.400	3.073	3.026	1.050
9.600	3.062	3.016	1.050
9.800	3.052	3.007	1.050
10.000	3.041	2.997	1.050
11.000	2.995	2.954	1.050

Wt. = 2.341 g.

Vol., ml.	pH S	pH B	H^+, meq./100 g.
0.200	5.061	4.864	0.783
0.400	4.727	4.530	0.857
0.600	4.517	4.334	0.882
0.800	4.370	4.196	0.912
1.000	4.252	4.089	0.930
1.200	4.153	4.001	0.937
2.000	3.875	3.756	0.961
3.000	3.657	3.563	0.978
5.000	3.385	3.320	0.990
6.000	3.291	3.235	0.990
7.000	3.213	3.163	0.990
8.000	3.145	3.101	0.991
8.400	3.120	3.078	0.991
8.800	3.097	3.056	0.991
9.000	3.086	3.046	0.991
9.200	3.075	3.036	0.991
9.400	3.065	3.026	0.991
9.600	3.054	3.016	0.991
9.800	3.044	3.007	0.991
10.000	3.033	2.997	0.991
11.000	2.988	2.954	0.991

Wt. = 2.063 g.

Vol., ml.	pH S	pH B	H^+, meq./100 g.
0.200	5.056	4.864	0.788
0.400	4.722	4.530	0.862
0.600	4.513	4.334	0.887
0.800	4.365	4.196	0.917
1.000	4.248	4.089	0.935
1.200	4.149	4.001	0.943
2.000	3.872	3.756	0.967
3.000	3.655	3.563	0.984
5.000	3.384	3.320	0.996
6.000	3.290	3.235	0.996
7.000	3.211	3.163	0.996
8.000	3.144	3.101	0.997
8.400	3.120	3.078	0.997
8.800	3.096	3.056	0.997
9.000	3.085	3.046	0.997
9.200	3.074	3.036	0.997
9.400	3.064	3.026	0.997
9.600	3.053	3.016	0.997
9.800	3.043	3.007	0.997
10.000	3.033	2.997	0.997
11.000	2.987	2.954	0.997

Wt. = 2.009 g.

Vol., ml.	pH S	pH B	H^+, meq./100 g.
0.200	5.073	4.864	0.787
0.400	4.739	4.530	0.862
0.600	4.529	4.334	0.886
0.800	4.380	4.196	0.916
1.000	4.262	4.089	0.934
1.200	4.162	4.001	0.942
2.000	3.882	3.756	0.966
3.000	3.662	3.563	0.983
5.000	3.388	3.320	0.995
6.000	3.294	3.235	0.995
7.000	3.215	3.163	0.995
8.000	3.148	3.101	0.996
8.400	3.123	3.078	0.996
8.800	3.099	3.056	0.996
9.000	3.088	3.046	0.996
9.200	3.077	3.036	0.996
9.400	3.067	3.026	0.996
9.600	3.056	3.016	0.996
9.800	3.046	3.007	0.996
10.000	3.035	2.997	0.996
11.000	2.989	2.954	0.996

Wt. = 2.153 g.

Vol., ml.	pH S	pH B	H^+, meq./100 g.
0.200	5.053	4.864	0.778
0.400	4.719	4.530	0.852
0.600	4.510	4.334	0.877
0.800	4.363	4.196	0.906
1.000	4.246	4.089	0.924
1.200	4.147	4.001	0.932
2.000	3.871	3.756	0.955
3.000	3.653	3.563	0.972
5.000	3.383	3.320	0.984
6.000	3.289	3.235	0.984
7.000	3.211	3.163	0.984
8.000	3.144	3.101	0.985
8.400	3.119	3.078	0.985
8.800	3.095	3.056	0.985
9.000	3.085	3.046	0.985
9.200	3.074	3.036	0.985
9.400	3.063	3.026	0.985
9.600	3.053	3.016	0.985
9.800	3.043	3.007	0.985
10.000	3.032	2.997	0.985
11.000	2.986	2.954	0.985

Wt. = 2.011 g.

Vol., ml.	pH S	pH B	H^+, meq./100 g.
0.200	5.048	4.864	0.780
0.400	4.714	4.530	0.854
0.600	4.506	4.334	0.878
0.800	4.359	4.196	0.908
1.000	4.242	4.089	0.926
1.200	4.143	4.001	0.934
2.000	3.868	3.756	0.957
3.000	3.651	3.563	0.974
5.000	3.381	3.320	0.986
6.000	3.288	3.235	0.986
7.000	3.210	3.163	0.986
8.000	3.143	3.101	0.987
8.400	3.118	3.078	0.987
8.800	3.095	3.056	0.987
9.000	3.084	3.046	0.987
9.200	3.073	3.036	0.987
9.400	3.062	3.026	0.987
9.600	3.052	3.016	0.987
9.800	3.042	3.007	0.987
10.000	3.032	2.997	0.987
11.000	2.986	2.954	0.987

Wt. = 1.964 g.

Vol., ml.	pH S	pH B	H^+, meq./100 g.
0.200	5.046	4.864	0.760
0.400	4.711	4.530	0.832
0.600	4.503	4.334	0.856
0.800	4.356	4.196	0.885
1.000	4.240	4.089	0.902
1.200	4.141	4.001	0.910
2.000	3.867	3.756	0.933
3.000	3.650	3.563	0.949
5.000	3.381	3.320	0.961
6.000	3.287	3.235	0.961
7.000	3.209	3.163	0.961
8.000	3.142	3.101	0.962
8.400	3.118	3.078	0.962
8.800	3.094	3.056	0.962
9.000	3.083	3.046	0.962
9.200	3.073	3.036	0.962
9.400	3.062	3.026	0.962
9.600	3.051	3.016	0.962
9.800	3.042	3.007	0.962
10.000	3.031	2.997	0.962
11.000	2.985	2.954	0.962

Wt. = 1.992 g.

Vol., ml.	pH S	pH B	OH^-, meq./100 g.
0.05	9.188	9.291	0.002
0.10	9.589	9.683	0.002
0.20	9.996	9.987	0.003
0.30	10.163	10.175	0.005
0.40	10.286	10.292	-
0.50	10.407	10.401	-
2.00	11.007	11.006	-

Wt. = 1.992 g.

TABLE XII (Continued)

POTENTIOMETRIC TITRATION DATA

FIBER B

Vol., ml.	pH S	pH B	H^+, meq./100 g.
0.200	4.971	4.864	0.488
0.400	4.636	4.530	0.530
0.600	4.434	4.334	0.549
0.800	4.291	4.196	0.563
1.000	4.178	4.089	0.575
1.200	4.085	4.001	0.582
2.000	3.824	3.756	0.600
3.000	3.617	3.563	0.612
5.000	3.358	3.320	0.624
6.000	3.268	3.235	0.625
7.000	3.192	3.163	0.625
8.000	3.127	3.101	0.626
8.400	3.103	3.078	0.626
8.800	3.080	3.056	0.626
9.000	3.070	3.046	0.626
9.200	3.059	3.036	0.626
9.400	3.049	3.026	0.626
9.600	3.039	3.016	0.626
9.800	3.029	3.007	0.626
10.000	3.019	2.997	0.626
11.000	2.974	2.954	0.626

Wt. = 1.985 g.

Vol., ml.	pH S	pH B	H^+, meq./100 g.
0.200	4.977	4.864	0.506
0.400	4.642	4.530	0.549
0.600	4.440	4.334	0.569
0.800	4.296	4.196	0.584
1.000	4.183	4.089	0.596
1.200	4.089	4.001	0.603
2.000	3.827	3.756	0.622
3.000	3.620	3.563	0.635
5.000	3.360	3.320	0.647
6.000	3.270	3.235	0.648
7.000	3.194	3.163	0.648
8.000	3.129	3.101	0.649
8.400	3.105	3.078	0.649
8.800	3.081	3.056	0.649
9.000	3.071	3.046	0.649
9.200	3.061	3.036	0.649
9.400	3.050	3.026	0.649
9.600	3.040	3.016	0.649
9.800	3.030	3.007	0.649
10.000	3.020	2.997	0.649
11.000	2.975	2.954	0.649

Wt. = 2.003 g.

Vol., ml.	pH S	pH B	H^+, meq./100 g.
0.200	4.969	4.864	0.495
0.400	4.634	4.530	0.537
0.600	4.433	4.334	0.557
0.800	4.289	4.196	0.571
1.000	4.177	4.089	0.584
1.200	4.084	4.001	0.590
2.000	3.822	3.756	0.609
3.000	3.616	3.563	0.621
5.000	3.358	3.320	0.633
6.000	3.260	3.235	0.634
7.000	3.192	3.163	0.634
8.000	3.127	3.101	0.635
8.400	3.103	3.078	0.635
8.800	3.080	3.056	0.635
9.000	3.070	3.046	0.635
9.200	3.059	3.036	0.635
9.400	3.049	3.026	0.635
9.600	3.038	3.016	0.635
9.800	3.029	3.007	0.635
10.000	3.018	2.997	0.635
11.000	2.974	2.954	0.635

Wt. = 1.927 g.

Vol., ml.	pH S	pH B	H^+, meq./100 g.
0.200	4.970	4.864	0.483
0.400	4.635	4.530	0.524
0.600	4.433	4.334	0.543
0.800	4.290	4.196	0.557
1.000	4.178	4.089	0.569
1.200	4.084	4.001	0.575
2.000	3.823	3.756	0.594
3.000	3.617	3.563	0.605
5.000	3.358	3.320	0.617
6.000	3.268	3.235	0.618
7.000	3.192	3.163	0.618
8.000	3.127	3.101	0.619
8.400	3.103	3.078	0.619
8.800	3.080	3.056	0.619
9.000	3.070	3.046	0.619
9.200	3.059	3.036	0.619
9.400	3.049	3.026	0.619
9.600	3.038	3.016	0.619
9.800	3.029	3.007	0.619
10.000	3.019	2.997	0.619
11.000	2.974	2.954	0.619

Wt. = 1.992 g.

Vol., ml.	pH S	pH B	H^+, meq./100 g.
0.200	4.977	4.864	0.491
0.400	4.641	4.530	0.532
0.600	4.439	4.334	0.552
0.800	4.295	4.196	0.566
1.000	4.183	4.089	0.578
1.200	4.089	4.001	0.584
2.000	3.827	3.756	0.603
3.000	3.619	3.563	0.615
5.000	3.360	3.320	0.627
6.000	3.270	3.235	0.628
7.000	3.194	3.163	0.628
8.000	3.129	3.101	0.629
8.400	3.104	3.078	0.629
8.800	3.081	3.056	0.629
9.000	3.071	3.046	0.629
9.200	3.060	3.036	0.629
9.400	3.050	3.026	0.629
9.600	3.040	3.016	0.629
9.800	3.030	3.007	0.629
10.000	3.020	2.997	0.629
11.000	2.975	2.954	0.629

Wt. = 2.061 g.

Vol., ml.	pH S	pH B	H^+, meq./100 g.
0.200	4.984	4.864	0.500
0.400	4.649	4.530	0.542
0.600	4.446	4.334	0.562
0.800	4.302	4.196	0.577
1.000	4.189	4.089	0.589
1.200	4.095	4.001	0.595
2.000	3.831	3.756	0.615
3.000	3.623	3.563	0.627
5.000	3.362	3.320	0.639
6.000	3.272	3.235	0.640
7.000	3.196	3.163	0.640
8.000	3.130	3.101	0.641
8.400	3.106	3.078	0.641
8.800	3.083	3.056	0.641
9.000	3.072	3.046	0.641
9.200	3.062	3.036	0.641
9.400	3.051	3.026	0.641
9.600	3.041	3.016	0.641
9.800	3.032	3.007	0.641
10.000	3.021	2.997	0.641
11.000	2.976	2.954	0.641

Wt. = 2.139 g.

Vol., ml.	pH S	pH B	OH^- meq./100 g.
0.05	9.178	9.291	0.001
0.10	9.581	9.683	0.002
0.20	9.995	9.987	0.002
0.30	10.163	10.175	-
0.40	10.287	10.292	-
0.50	10.413	10.401	-
2.00	10.994	11.006	-

Wt. = 1.927 g.

TABLE XII (Continued)

POTENTIOMETRIC TITRATION DATA

FIBER C

Vol., ml.	pH S	pH B	H^+, meq./100 g.
0.200	4.984	4.864	0.536
0.400	4.649	4.530	0.582
0.600	4.446	4.334	0.602
0.800	4.302	4.196	0.620
1.000	4.189	4.089	0.631
1.200	4.095	4.001	0.640
2.000	3.831	3.756	0.661
3.000	3.623	3.563	0.675
5.000	3.363	3.320	0.692
6.000	3.272	3.235	0.694
7.000	3.196	3.163	0.696
8.000	3.131	3.101	0.697
8.400	3.106	3.078	0.697
8.800	3.083	3.056	0.697
9.000	3.073	3.046	0.697
9.200	3.062	3.036	0.697
9.400	3.052	3.026	0.697
9.600	3.041	3.016	0.697
9.800	3.032	3.007	0.697
10.000	3.021	2.997	0.697
11.000	2.977	2.954	0.697

Wt. = 1.997 g.

Vol., ml.	pH S	pH B	H^+, meq./100 g.
0.200	4.988	4.864	0.539
0.400	4.653	4.530	0.585
0.600	4.450	4.334	0.606
0.800	4.306	4.196	0.624
1.000	4.192	4.089	0.635
1.200	4.098	4.001	0.644
2.000	3.834	3.756	0.665
3.000	3.625	3.563	0.679
5.000	3.364	3.320	0.696
6.000	3.273	3.235	0.697
7.000	3.197	3.163	0.700
8.000	3.132	3.101	0.701
8.400	3.107	3.078	0.701
8.800	3.084	3.056	0.701
9.000	3.074	3.046	0.701
9.200	3.063	3.036	0.701
9.400	3.053	3.026	0.701
9.600	3.042	3.016	0.701
9.800	3.033	3.007	0.701
10.000	3.022	2.997	0.701
11.000	2.977	2.954	0.701

Wt. = 2.040 g.

Vol., ml.	pH S	pH B	H^+, meq./100 g.
0.200	5.000	4.864	0.537
0.400	4.664	4.530	0.583
0.600	4.461	4.334	0.603
0.800	4.316	4.196	0.621
1.000	4.202	4.089	0.632
1.200	4.107	4.001	0.641
2.000	3.841	3.756	0.662
3.000	3.630	3.563	0.676
5.000	3.368	3.320	0.693
6.000	3.277	3.235	0.695
7.000	3.200	3.163	0.697
8.000	3.134	3.101	0.698
8.400	3.110	3.078	0.698
8.800	3.086	3.056	0.698
9.000	3.076	3.046	0.698
9.200	3.065	3.036	0.698
9.400	3.055	3.026	0.698
9.600	3.044	3.016	0.698
9.800	3.035	3.007	0.698
10.000	3.024	2.997	0.698
11.000	2.979	2.954	0.698

Wt. = 2.216 g.

Vol., ml.	pH S	pH B	H^+, meq./100 g.
0.200	4.987	4.864	0.547
0.400	4.652	4.530	0.594
0.600	4.449	4.334	0.614
0.800	4.305	4.196	0.633
1.000	4.191	4.089	0.644
1.200	4.097	4.001	0.653
2.000	3.833	3.756	0.674
3.000	3.625	3.563	0.688
5.000	3.364	3.320	0.706
6.000	3.273	3.235	0.707
7.000	3.197	3.163	0.710
8.000	3.131	3.101	0.711
8.400	3.107	3.078	0.711
8.800	3.084	3.056	0.711
9.000	3.073	3.046	0.711
9.200	3.063	3.036	0.711
9.400	3.052	3.026	0.711
9.600	3.042	3.016	0.711
9.800	3.033	3.007	0.711
10.000	3.022	2.997	0.711
11.000	2.977	2.954	0.711

Wt. = 2.001 g.

0.200	4.985	4.864	0.548
0.400	4.650	4.530	0.595
0.600	4.447	4.334	0.616
0.800	4.303	4.196	0.635
1.000	4.190	4.089	0.646
1.200	4.096	4.001	0.655
2.000	3.832	3.756	0.676
3.000	3.624	3.563	0.690
5.000	3.363	3.320	0.708
6.000	3.273	3.235	0.709
7.000	3.196	3.163	0.712
8.000	3.131	3.101	0.713
8.400	3.107	3.078	0.713
8.800	3.083	3.056	0.713
9.000	3.073	3.046	0.713
9.200	3.062	3.036	0.713
9.400	3.052	3.026	0.713
9.600	3.042	3.016	0.713
9.800	3.032	3.007	0.713
10.000	3.022	2.997	0.713
11.000	2.977	2.954	0.713

Wt. = 1.963 g.

0.200	4.976	4.864	0.540
0.400	4.641	4.530	0.586
0.600	4.439	4.334	0.607
0.800	4.296	4.196	0.625
1.000	4.183	4.089	0.636
1.200	4.089	4.001	0.644
2.000	3.827	3.756	0.665
3.000	3.620	3.563	0.680
5.000	3.360	3.320	0.697
6.000	3.270	3.235	0.698
7.000	3.194	3.163	0.701
8.000	3.129	3.101	0.702
8.400	3.105	3.078	0.702
8.800	3.082	3.056	0.702
9.000	3.071	3.046	0.702
9.200	3.061	3.036	0.702
9.400	3.050	3.026	0.702
9.600	3.040	3.016	0.702
9.800	3.031	3.007	0.702
10.000	3.020	2.997	0.702
11.000	2.975	2.954	0.702

Wt. = 1.871 g.

Vol., ml.	pH S	pH B	OH^-, meq./100 ml.
0.05	9.183	9.291	0.002
0.10	9.592	9.683	0.002
0.20	10.001	9.987	0.003
0.30	10.171	10.175	-
0.50	10.398	10.401	-
2.00	11.002	11.006	-

Wt. = 1.997 g.

When the number of bound protons per gram of fiber was plotted as a function of pH, the zero point on the bound proton scale necessarily occurred at the pH of the suspension before acid or base were added. It is usually necessary to shift the ordinate in such a way that the zero point corresponds to the pH at which the ionizable groups were completely dissociated. For the system studied here, the only ionizable groups present were carboxyl groups; thus a shift was made so that the level portion of the curve coincided with the zero point on the ordinate.

Figure 24 gives a typical plot of combined hydrogen ion vs. pH for dacron-PAA. The value for the carboxyl content of this fiber was determined from the maximum number of moles of hydrogen ion which combined with the fiber.

Dissociation curves were constructed by calculating the fraction of hydrogen ions bound (moles bound at a particular pH divided by maximum moles bound) and plotting (1 - fraction bound) as a function of pH.

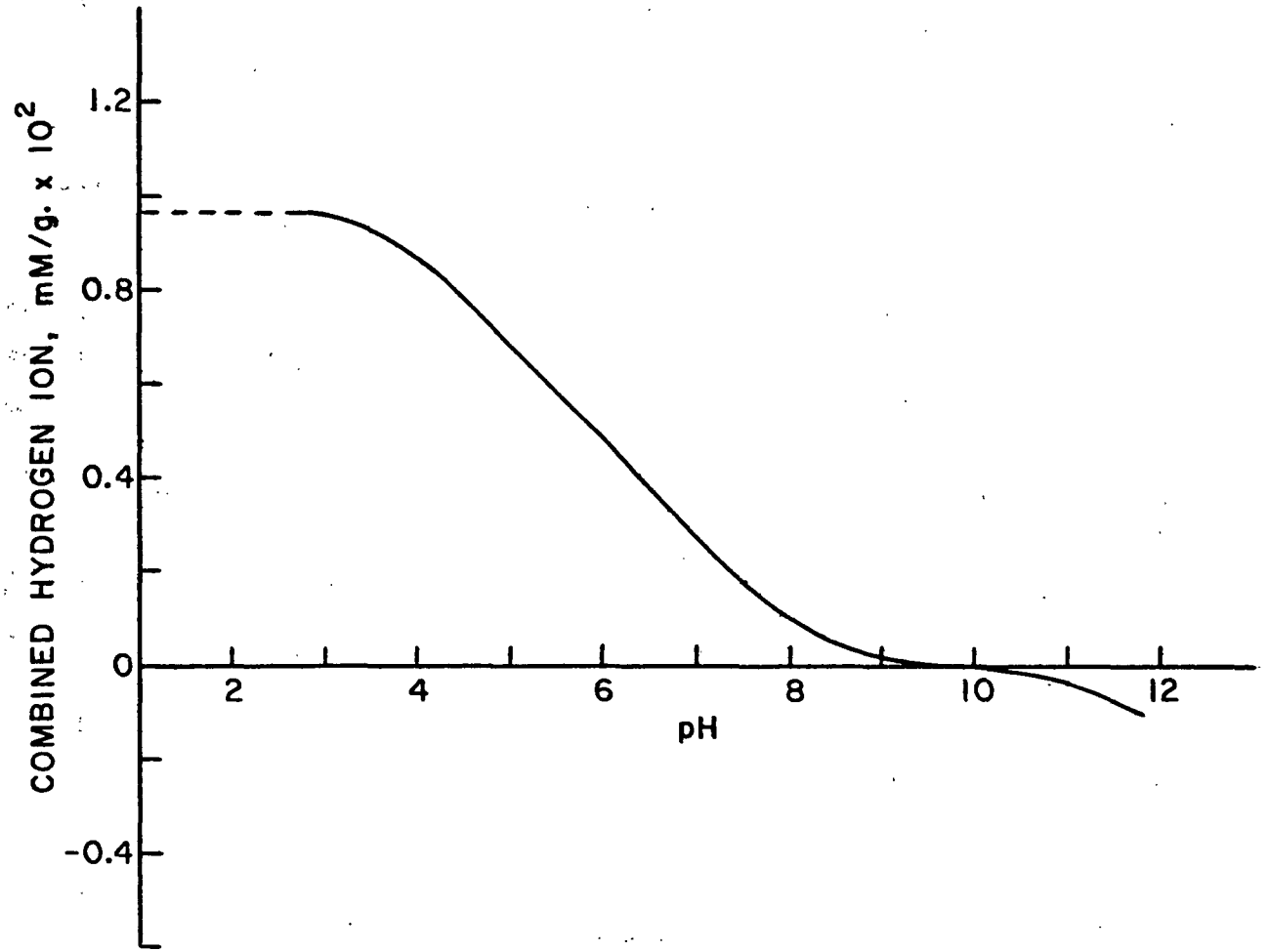

Figure 24. Titration Curve Dacron-PAA

APPENDIX V

TURBIDITY TITRATIONS

These titrations were used to measure the amount of PAA removed from solution by the fibers and, hence, the amount of PAA adsorbed. The method involves the titration of a polyanion (ionized PAA) with a polycation (PVPB). The turbidity which formed on addition of small quantities of the titrant was measured by the galvanometer reading of a light-scattering instrument. A plot of galvanometer reading vs. volume of titrant added gave a peak in the curve which served as an end point and was proportional to the concentration of the PAA (see Fig. 25). The PAA solutions were buffered with potassium monohydrogen phosphate (0.1N) so that the PAA was completely dissociated. The accuracy of the method has been reported as 0.2 p.p.m. (50, 51), but in this study an accuracy of 2 p.p.m. was obtained.

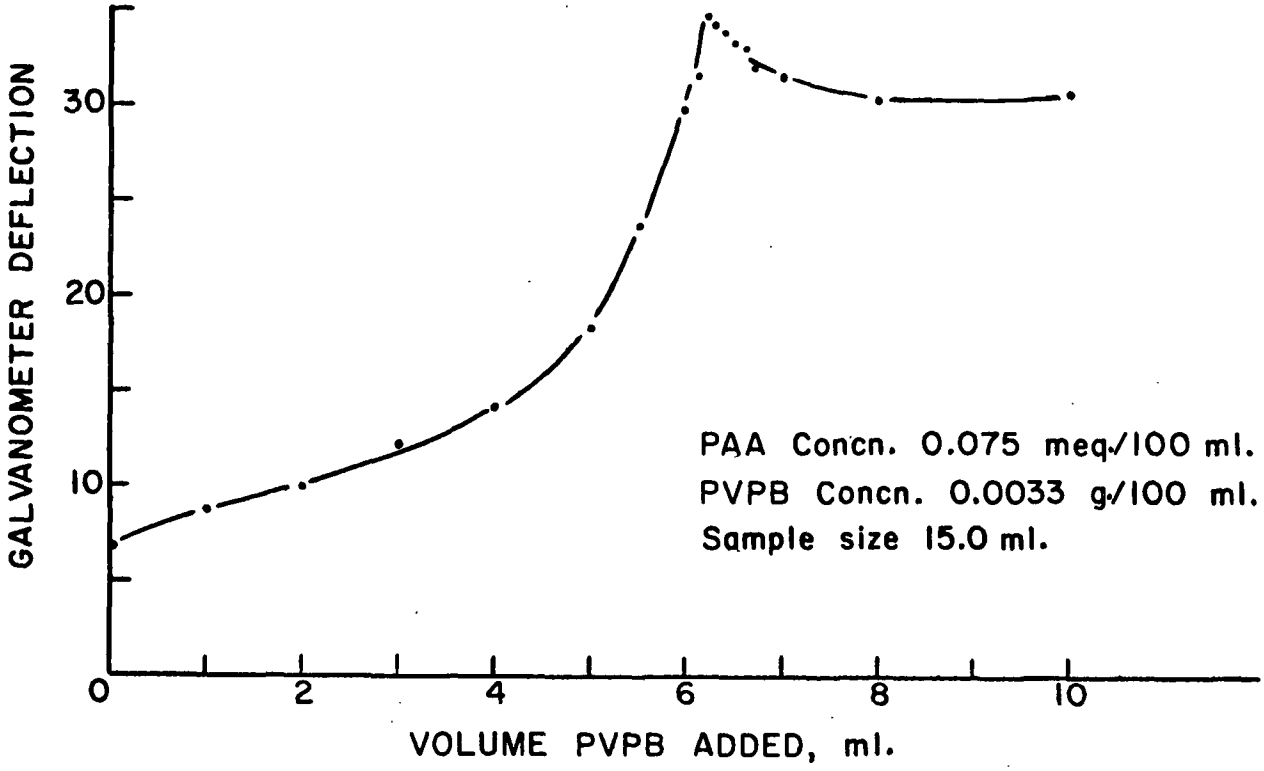

Figure 25. Turbidity Titration Curve

In order to obtain a peak in the titration curve, two requirements had to be met. First, the solution in the light-scattering cell had to be continuously stirred. This was accomplished by bubbling N_2 gas through the solution during the titration (except when galvanometer readings were being taken). The N_2 was purified by passing it through a drying tube (Drierite) and a glass filter. Second, the titrant had to be added in large volumes at the beginning of the titration. The reason for this is that the precipitant must have as small a particle size as possible so that an equilibrium, between precipitant and dissolved PAA-PVPB complex, is established (76).

A titration sample consisted of 15.0 ml. of the PAA solution to be titrated, and the PVPB was added by means of a 5.0-ml. graduated syringe. All solutions were filtered several times through a Millipore filter (0.45-μm. pore size) before use.

A PAA solution was made up and the concentration was measured by means of a conductivity titration (PAA is hygroscopic and gravimetric methods could not be used). Several dilutions were made and turbidity titrations were performed on these solutions. From these data, a calibration curve was constructed. This curve is shown in Fig. 26. Titration of PAA solutions of unknown concentration could then be used to determine the concentration.

Table XIII gives the results of the turbidity titrations of both the calibration curve samples and the adsorption solution samples.

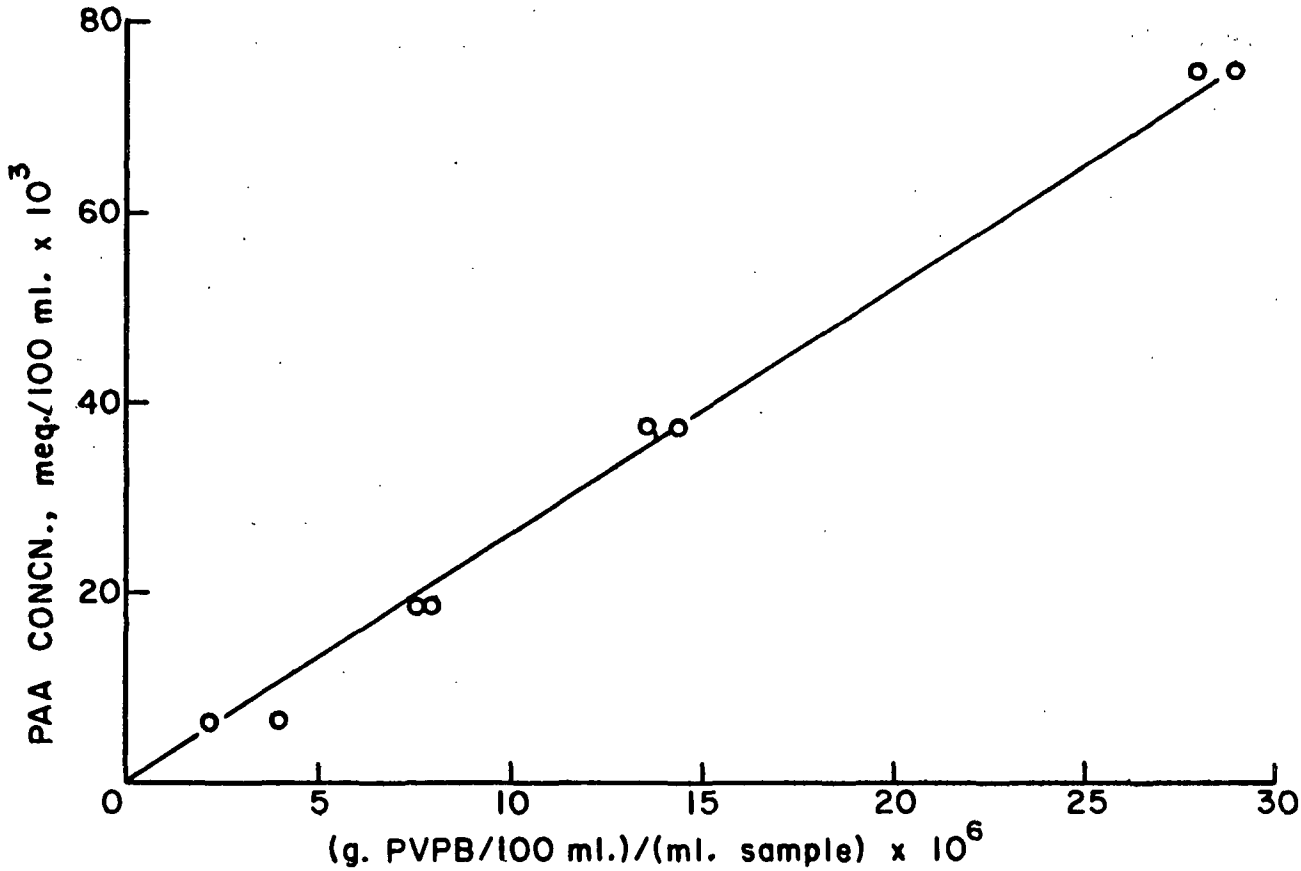

Figure 26. Turbidity Titration Calibration Curve

TABLE XIII

TURBIDITY TITRATION DATA

Calibration Curve Data

PVPB concentration: 0.0033 g./100 ml.
Sample size: 15.0 ml.

PAA Concentration, meq./100 ml.	Volume PVPB, ml.	$\frac{\text{g. PVPB/100 ml.}}{\text{Sample Size}} \times 10^6$
0.0750	13.1	28.8
0.0750	12.6	27.7
0.0375	6.5	14.3
0.0375	6.2	13.6
0.0187	3.5	7.7
0.0187	3.6	7.9
0.0075	1.8	4.0
0.0075	1.0	2.2

PAA Adsorption Data

PVPB concentration: 0.0033 g./100 ml.
Sample size: 15.0 ml.

Adsorption run[a]	A	B	C
Dilution factor	1:10	none	1:10
Vol. PVPB before ads., ml.[b]	4.4	4.5	4.2
Vol. PVPB after ads., ml.[b]	1.9	0.9	4.1
Init. PAA concentration, meq./100 ml.	0.255	0.0267	0.248
Final PAA concentration, meq./100 ml.	0.120	0.0055	0.240
PAA adsorbed, meq./100 g.	0.9	0.14	0.05

[a] See Table III.

[b] Average of two determinations.

TABLE XIII (Continued)

TURBIDITY TITRATION DATA

Vol. PVB, ml.	Galv. Reading	Vol. PVPB, ml.	Galv. Reading
PAA Concn. = 0.0750 meq./100 ml.			
0.0	10.0	0.0	12.2
2.0	16.7	2.0	18.8
4.0	19.8	4.0	19.7
8.0	21.9	8.0	21.2
9.0	26.4	10.0	27.0
10.0	31.5	11.0	32.9
10.4	33.9	12.2	41.0
10.8	37.3	12.4	42.7
11.0	38.9	12.6	44.4
11.2	40.0	12.8	46.8
11.4	40.6	13.0	49.5
12.0	47.0	13.2	50.8
12.2	49.4	13.4	49.6
12.4	51.9	13.6	48.1
12.6	55.1	14.0	45.9
12.8	54.3	15.0	42.1
13.0	53.7		
13.4	51.7		
13.8	50.1		
15.0	48.0		
PAA Concn. = 0.0375 meq./100 ml.			
0.0	6.0	0.0	6.8
2.0	6.8	2.0	9.9
4.0	12.1	4.0	14.0
5.0	15.9	5.0	18.4
6.1	27.0	5.5	23.8
6.2	29.0	6.0	29.9
6.3	30.9	6.1	31.6
6.4	33.5	6.2	34.8
6.5	40.1	6.5	33.3
6.6	39.6	7.0	31.5
6.7	38.7	10.0	30.7
7.0	36.0		
8.0	31.8		
10.0	32.3		

Vol. PVB, ml.	Galv. Reading	Vol. PVPB, ml.	Galv. Reading
PAA Concn. = 0.0187 meq./100 ml.			
0.0	8.1	0.0	9.0
1.0	10.5	1.0	9.8
2.0	15.9	2.0	13.6
3.0	22.0	3.0	21.3
3.2	24.6	3.2	23.5
3.3	26.9	3.3	24.8
3.4	29.4	3.4	26.4
3.5	33.0	3.5	27.0
3.6	32.8	3.6	30.8
3.8	32.0	3.8	30.2
4.0	31.7	4.0	30.0
5.0	31.0	5.0	29.8
PAA Concn. = 0.0075 meq./100 ml.			
0.0	5.6	0.0	6.4
0.8	11.9	0.5	8.0
0.9	14.2	0.8	9.9
1.0	18.2	0.9	10.7
1.1	17.4	1.0	11.8
1.2	17.0	1.1	12.3
1.5	16.0	1.2	14.7
2.0	16.0	1.3	15.9
3.0	16.2	1.4	17.2
		1.5	18.5
		1.6	20.4
		1.7	22.9
		1.8	27.8
		1.9	26.7
		2.0	26.1
		3.0	24.2
		4.0	23.8

Vol. PVPB, ml.	Galv. Reading	Galv. Reading
Fiber A Before Ads.		
0.0	6.1	10.2
1.0	7.0	11.1
2.0	8.3	12.4
3.0	10.2	14.5
4.0	15.9	20.2
4.1	17.1	21.8
4.2	18.5	23.0
4.3	20.7	24.9
4.4	22.8	25.6
4.5	22.2	27.1
4.6	21.7	25.8
5.0	20.2	24.9
6.0	20.1	24.3
Fiber B Before Ads.		
0.0	10.2	10.1
1.0	10.9	10.6
2.0	12.6	12.3
3.0	16.1	15.7
4.0	21.8	21.0
4.2	23.4	22.7
4.3	24.3	23.8
4.4	25.0	24.6
4.5	25.7	24.1
4.6	25.1	23.5
4.7	24.7	23.3
5.0	24.6	22.9
6.0	24.0	22.3
Fiber C Before Ads.		
0.0	13.0	13.1
1.0	12.9	13.3
2.0	13.3	13.4
3.0	15.0	14.7
4.0	22.4	22.1
4.1	23.8	24.0
4.2	24.9	23.7
4.3	25.3	23.1
4.4	24.6	
4.5	23.9	22.0
5.0	23.0	22.0

Vol. PVPB, ml.	Galv. Reading	Galv. Reading
Fiber A After Ads.		
0.0	8.1	8.2
1.0	10.5	10.4
1.5	14.6	14.5
1.6	15.5	15.6
1.8	17.8	17.9
1.9	18.6	18.5
2.0	17.9	18.3
2.1	17.3	17.2
2.5	16.1	16.0
3.0	15.6	15.9
5.0	16.0	16.1
Fiber B After Ads.		
0.0	8.5	10.1
0.5	10.2	11.8
0.7	11.9	13.5
0.8	12.9	14.7
0.9	15.0	15.8
1.0	14.6	17.2
1.1	14.0	16.7
1.5	12.1	16.1
2.0	11.3	15.6
5.0	14.0	15.9
Fiber C After Ads.		
0.0	18.0	16.3
1.0	18.6	16.9
2.0	19.9	18.1
3.0	23.6	21.8
3.9	30.9	26.5
4.0	32.1	28.9
4.1	31.0	30.6
4.2	30.2	32.3
4.4	29.8	31.9
4.5	28.9	31.4
5.0	28.3	30.9
6.0	28.4	30.7

APPENDIX VI

ZETA POTENTIAL CALCULATIONS AND DATA

The calculations and corrections to the data that were used in this study were basically similar to those used by Ciriacks (29). These calculations and corrections will be briefly summarized here.

CORRECTIONS TO ORIGINAL DATA

DEFORMATION OF APPARATUS UNDER LOAD

Under the high loads used to compress the fiber pads, the apparatus, as well as the pads, compressed. The thin silicone-rubber insulation on the back of the electrodes was the main contributor to this deformation.

Corrections to the pad thickness, due to apparatus deformation, were determined by measuring the electrode displacement, under load, with no pad present. Table XIV gives the results of two independent determinations of these corrections. The original data were fitted to a 6th-order polynomial and the resulting coefficients were used to determine corrections. The original data and the resulting polynomial data are plotted in Fig. 27.

The pad thickness measurements, after correction for apparatus deformation, were then smoothed by a least squares method. It has been found that mat compression data fit the empirical expression:

$$C = M_1 P^N \qquad (39)$$

where C is the mat concentration, P is the applied load, and M and N are constants (77). A regression analysis of log C vs. log P gave a straight line and this correlation was used to smooth the thickness measurements.

TABLE XIV

APPARATUS DEFORMATION

Load, lb.	Observed Compression, in.	Calculated Compression, in.	Residual, in.
0.0	0.0	-0.00003	0.00003
322.00000	0.02000	0.02087	-0.00087
400.00000	0.02890	0.02737	0.00153
490.00000	0.03320	0.03398	-0.00078
600.00000	0.04120	0.04054	0.00066
727.00000	0.04500	0.04623	-0.00123
800.00000	0.04920	0.04884	0.00036
1000.00000	0.05550	0.05479	0.00071
1053.00000	0.05600	0.05627	-0.00027
1250.00000	0.06170	0.06170	-0.00000
1390.00000	0.06480	0.06517	-0.00037
1500.00000	0.06760	0.06733	0.00027
1500.00000	0.06730	0.06733	-0.00003
1900.00000	0.07540	0.07541	-0.00001

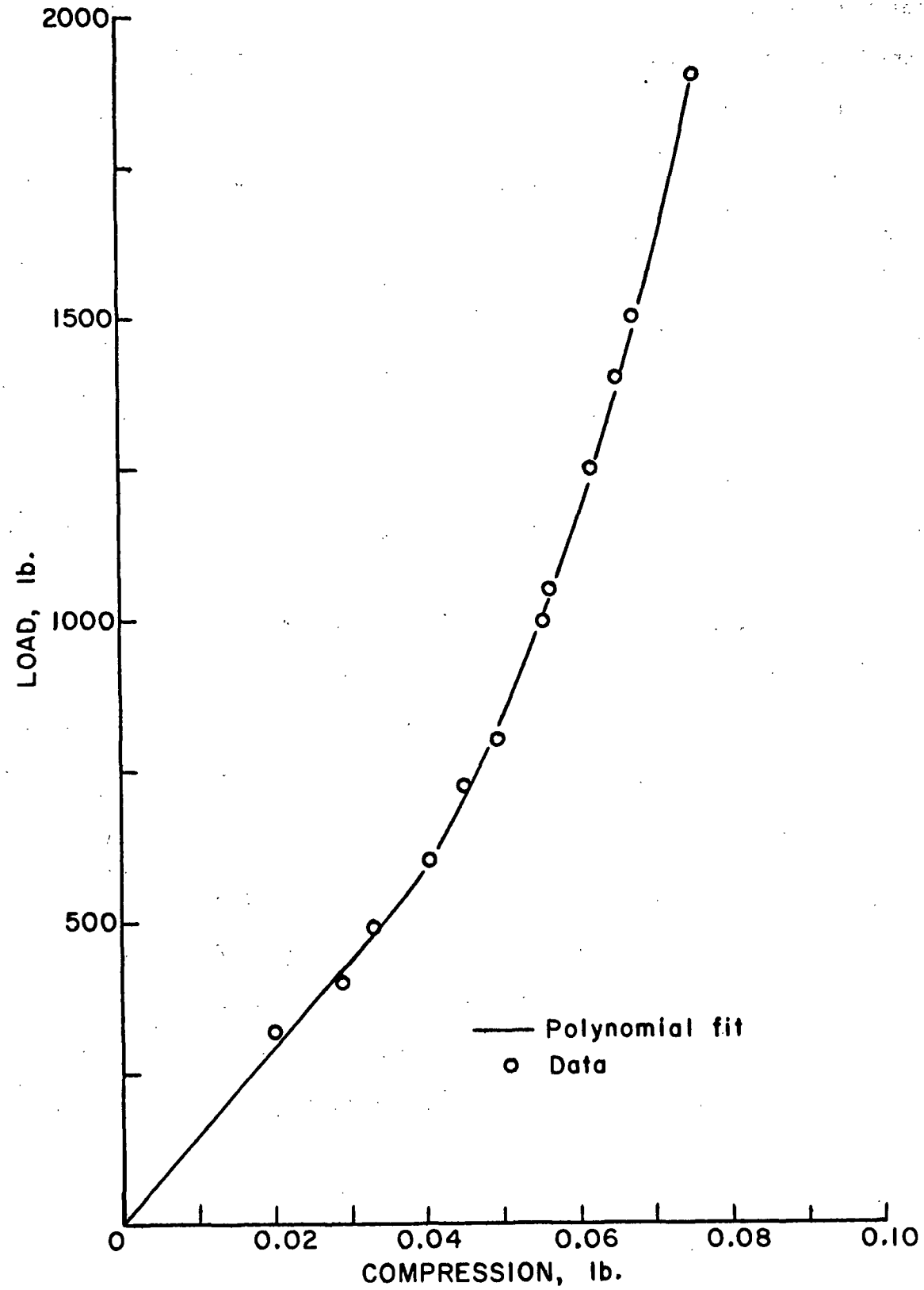

Figure 27. Apparatus Deformation

BACKCURRENT THROUGH FIBER MAT

Since the resistance of the galvanometer was only 25 ohms, corrections for backcurrent became appreciable only when $c > 10^{-4}M$. Above this c, the resistance of the mat would drop below 1000 ohms.

The backcurrent was applied to the streaming current reading prior to calculation of the regression lines (described later) according to the following equation (29):

$$I_s = I_{gal.}(1 + 25/R_{mat}) \qquad (40)$$

where I_s is the corrected streaming current, $I_{gal.}$ is the galvanometer reading, and R_{mat} is the resistance of the mat.

FLOW CURRENT

The flow current, I_f, is defined as the current between two electrodes during liquid flow when the porous medium is not present. As discussed by Ciriacks (29), flow currents can be minimized through the use of electrodes with identical geometry and if a sufficient concentration of ions, which are reversible to the electrode system, are present.

Ciriacks (29) found that while an I_f did exist, a test for I_f when the mat was removed did not necessarily measure the actual flow current effect that existed when the mat was present. Therefore, the most consistent manner of handling the data was to use I_s/U values based on the assumption that any nonzero intercepts were caused by a relatively constant I_f at each electrode separation.

ZETA POTENTIAL CALCULATIONS

The method of least squares was used to estimate the regression lines for $\underline{I}_s$ vs. $\underline{U}$ and $\underline{H}$ vs. $\underline{U}$. Table XV gives the values obtained for the slopes and intercepts.

The values calculated for mat porosity, Kozeny factor, and the zeta potential are listed in Table XV. The Kozeny factors were obtained from the experimental data through the use of Equation (42) and those in the next column were calculated from the Davis correlation (78, p. 162).

$$k = \Delta P \varepsilon^3 / [UL(1 - \varepsilon)^2 \eta S_v^2] \qquad (42)$$

where $\underline{k}$ is the Kozeny factor and $\underline{S}_v$ is the specific surface area per unit of fiber. The zeta potentials were calculated from Equations (26) to (34). The viscosity and dielectric constants for pure water were used since the electrolyte concentrations were very dilute.

In the computer program, the XMAX is the upper limit of the numerical integration and NC specified the number of divisions between XMIN and XMAX. XMAX was set equal to $\underline{a}$ + 0.6 m. [$\underline{a} + \tau$ in Equation (31)] for all electrolyte concentrations. NC was set at 20.

TABLE XV

ZETA POTENTIAL DATA

Temp., °C.	Res., ohms	I_r, μa.	I_s/U, μa.sec./cm.	Int., μa.	$\Delta H/U$, cm.sec./cm.	Int., cm.	Thick, in.	ε	Kozeny Exp.	Fact, Davis	Zeta, -mv.	
BLANK			WT = 5.491			CONC = .000113				PH = 6.8		
23.9	2200	0.1	10.	-0.2			.332	.903		8.7	8.99	
24.0	1740	0.2	16.3	0.3			.258	.879		7.4	11.43	
23.8	1460	0.3	21.6	-0.4			.201	.840		6.4	12.62	
23.9	1300	0.4	29.3	-0.4			.166	.806		5.9	13.73	
24.2	1160	0.4	38.2	-0.3			.138	.769		5.7	14.56	
24.3	1090	0.5	54.9	-0.3			.101	.683		5.6	14.73	
						AVG (FIRST VALUE OMITTED) =					13.4±	10.3%
BLANK			WT = 5.152			CONC = .000103				PH = 6.8		
24.2	3600	0.3	9.13	0.0	11.2	-0.3	.370	.918	16.6	9.8	9.29	
24.7	2900	0.2	12.2	0.1	15.6	-0.5	.299	.899	17.5	8.5	12.56	
24.5	2500	0.2	19.8	0.0	23.6	-0.3	.214	.860	16.6	6.9	12.80	
25.1	2210	0.3	27.7	-0.1	29.3	-0.5	.172	.823	14.4	6.1	13.31	
24.9	1930	0.4	41.0	-0.2	46.0	-0.7	.139	.781	15.3	5.7	14.07	
25.0	1700	0.5	52.2	-0.1	63.2	-0.5	.111	.729	14.9	5.6	14.69	
						AVG (FIRST VALUE OMITTED) =					13.5±	6.6%
BLANK			WT = 3.952			CONC = .000101				PH = 6.8		
25.7	1680	0.4	4.3	0.9	11.2	0.1	.307	.924	25.0	10.4	8.87	
25.3	1350	0.4	7.4	0.9	14.1	0.2	.228	.899	20.5	8.4	10.21	
25.4	1070	0.4	14.0	0.9	20.2	0.3	.174	.868	21.1	7.1	12.81	
25.4	880	0.3	18.8	0.9	30.3	0.3	.134	.830	21.4	6.1	13.61	
25.4	750	0.4	22.7	0.9	45.6	0.2	.110	.791	22.8	5.8	13.78	
25.4	660	0.4	26.6	0.8	79.5	0.2	.090	.743	26.9	5.5	14.16	
25.4	610	0.5	33.9	1.0	99.8	0.4	.082	.726	29.8	5.6	13.87	
						AVG (FIRST VALUE OMITTED) =					13.1±	11.3%
BLANK			WT = 4.011			CONC = .000097				PH = 6.8		
24.9	3700	0.8	4.3	0.6			.309	.923		10.5	8.62	
25.0	3050	3.9	14.1	0.7			.210	.894		8.2	12.90	
25.1	2690	0.9	15.4	0.7			.171	.869		7.2	11.79	
25.1	2380	0.8	22.7	0.5			.156	.851		6.6	13.78	
25.0	1970	1.0	26.5	0.5			.132	.835		6.0	13.87	
24.9	1760	1.0	31.7	0.3			.109	.792		5.8	14.21	
						AVG (FIRST VALUE OMITTED) =					13.3±	7.3%
BLANK			WT = 4.021			CONC = .000487				PH = 6.8		
23.9	610	0.2	7.2	0.3	13.0	-0.6	.273	.914	23.6	9.4	10.97	
23.9	560	0.2	10.4	0.6	14.2	-0.3	.221	.895	19.9	8.3	8.63	
24.0	420	0.3	11.7	0.8	20.5	-0.4	.175	.865	20.6	7.1	8.35	
24.0	380	0.1	15.6	0.7	27.5	-0.1	.138	.831	19.3	6.1	8.44	
24.2	350	0.0	17.3	0.5	46.0	-0.4	.120	.795	20.5	5.8	8.09	
24.1	320	0.2	20.9	0.8	67.4	-0.7	.104	.765	21.1	5.6	7.54	
						AVG (FIRST VALUE OMITTED) =					8.2±	7.8%
BLANK			WT = 4.173			CONC = .000491				PH = 6.8		
24.5	660	0.7	7.7	0.1			.284	.919		9.5	10.73	
24.6	570	0.5	10.7	0.5			.237	.898		8.4	8.47	
24.5	450	0.8	11.9	0.5			.184	.866		7.1	8.06	
24.5	390	1.0	14.5	0.8			.139	.824		6.5	7.61	
24.5	360	1.0	17.1	0.3			.110	.778		5.9	7.53	
24.6	330	1.0	20.4	0.4			.096	.747		5.6	7.36	
						AVG (FIRST VALUE OMITTED) =					7.8±	5.8%
BLANK			WT = 5.352			CONC = .000023				PH = 6.8		
25.1	2300	0.6	10.7	1.3			.313	.900		8.5	9.03	
25.0	1820	0.7	19.2	1.1			.248	.874		7.4	12.74	
25.0	1630	0.7	28.1	0.8			.198	.841		6.4	13.48	
25.1	1450	0.9	35.9	0.6			.165	.810		5.9	13.71	
25.1	1370	0.6	43.9	0.6			.135	.767		5.6	14.01	
25.2	1150	0.6	52.4	0.4			.117	.733		5.6	13.78	
						AVG (FIRST VALUE OMITTED) =					13.5±	3.6%
BLANK			WT = 5.698			CONC = .000018				PH = 6.8		
24.6	3300	0.6	10.8	0.7	17.0	-0.4	.341	.902	17.9	8.7	10.34	
24.7	2750	0.4	14.2	0.4	24.8	-0.8	.261	.870	18.0	7.3	12.11	
24.7	2300	0.1	21.7	0.2	26.9	-0.5	.219	.848	15.1	6.5	12.46	
24.8	2000	0.7	27.6	0.8	34.8	-0.6	.177	.811	14.2	6.0	13.72	
24.7	1850	0.2	35.6	0.7	51.1	-1.1	.150	.776	15.4	5.7	13.41	
24.8	1600	0.3	43.5	0.6	77.0	-1.0	.130	.739	16.9	5.6	13.37	
						AVG (FIRST VALUE OMITTED) =					13.0±	5.3%
BLANK			WT = 5.137			CONC = .0005				PH = 4		
23.7	680	0.6	10.6	0.2	11.1	-0.7	.370	.920	16.5	9.8	5.41	
23.6	530	0.7	16.9	0.1	15.6	-0.8	.299	.899	16.5	8.5	6.52	
23.6	460	0.9	19.1	-0.4	23.7	-1.0	.210	.856	16.4	6.9	6.83	
23.8	410	1.0	22.4	-0.3	45.5	-0.9	.135	.776	15.3	5.7	7.11	
24.1	360	1.0	26.6	-0.3	62.9	-1.0	.112	.731	14.9	5.6	7.70	
24.1	320	1.0	30.4	-0.2	81.0	-0.4	.095	.689	14.4	5.6	7.28	
						AVG (FIRST VALUE OMITTED) =					7.1±	6.3%

TABLE XV (Continued)

ZETA POTENTIAL DATA

Temp., °C.	Res., ohms	I_r, μa.	I_s/U, μa.sec. cm.	Int., μa.	$\Delta H/U$, cm.sec./ cm.	Int., cm.	Thick, in.	ε	Kozeny Exp.	Fact. Davis	Zeta, -mv.	
BLANK			WT = 5.003			CONC = .0005				PH = 4		
24.3	770	0.1	16.5	0.8		.300	.901			8.4	6.15	
24.4	680	0.2	18.7	0.8		.248	.873			7.3	6.64	
24.7	540	0.3	23.1	0.5		.206	.851			6.7	7.30	
24.9	460	0.2	26.7	0.7		.164	.803			6.0	8.12	
24.9	400	0.2	30.1	1.0		.132	.774			5.6	8.38	
24.9	350	0.2	32.3	1.0		.107	.693			5.6	9.31	
						AVG (FIRST VALUE OMITTED) =					8.0±	13.1%
BLANK			WT = 5.507			CONC = .0001				PH = 4		
24.6	950	0.5	11.1	0.1		.268	.880			7.6	6.07	
24.8	830	0.3	17.3	0.0		.208	.847			6.5	8.77	
25.0	710	0.6	23.6	0.1		.169	.810			5.9	9.32	
25.1	600	0.6	29.2	0.2		.140	.769			5.6	10.04	
24.9	522	0.5	34.0	0.0		.110	.721			5.6	11.86	
25.0	440	0.5	38.7	0.1		.098	.681			5.6	12.61	
						AVG (FIRST VALUE OMITTED) =					10.5±	15.9%
BLANK			WT = 5.638			CONC = .0001				PH = 4		
23.9	860	0.1	16.4	-0.6		.275	.879			6.5	8.31	
24.1	740	0.1	20.3	-0.5		.219	.847			6.6	10.13	
24.1	580	0.2	25.8	-0.1		.178	.813			6.0	10.29	
24.3	490	0.1	29.6	-0.4		.140	.763			5.6	11.06	
24.0	410	0.1	34.5	-0.9		.122	.726			5.6	12.34	
24.1	360	0.3	39.3	-0.8		.107	.690			5.6	12.69	
						AVG (FIRST VALUE OMITTED) =					11.3±	10.4%
BLANK			WT = 6.148			CONC = .0005				PH = 10		
24.6	640	0.1	9.0	0.1	15.3	-0.7	.330	.891	13.3	8.1	5.13	
25.0	560	0.0	13.1	0.2	27.9	-0.6	.237	.848	15.0	6.6	6.02	
24.9	490	0.1	15.3	0.1	40.3	-0.2	.193	.814	15.6	6.0	7.07	
24.7	420	0.2	16.3	0.0	61.6	-0.8	.153	.769	15.8	5.6	7.38	
25.0	350	0.4	22.5	0.1	88.5	-0.9	.120	.710	16.1	5.6	8.41	
25.1	300	0.4	22.5	0.1	110.3	-1.0	.101	.684	16.7	5.6	9.62	
						AVG (FIRST VALUE OMITTED) =					7.7±	17.9%
BLANK			WT = 6.431			CONC = .0005				PH = 10		
24.1	860	0.5	8.3	0.4		.380	.900			8.6	5.29	
24.2	730	0.6	10.6	0.1		.270	.859			7.1	6.47	
24.2	640	0.6	14.1	0.3		.231	.835			6.3	7.32	
24.5	520	0.9	18.9	0.6		.159	.771			5.6	8.55	
24.5	430	0.7	19.4	0.6		.141	.732			5.6	8.76	
24.5	380	0.9	24.1	0.5		.125	.696			5.6	9.39	
						AVG (FIRST VALUE OMITTED) =					8.1±	14.6%
BLANK			WT = 6.038			CONC = .0001				PH = 10		
24.3	1030	0.3	12.2	-0.1		.298	.878			7.6	8.82	
24.4	940	0.3	16.4	-0.1		.239	.849			6.6	11.21	
24.4	830	0.3	21.7	-0.2		.195	.810			5.8	12.77	
24.4	700	0.8	24.1	0.0		.160	.773			5.7	12.96	
24.4	590	0.7	33.7	0.0		.131	.729			5.6	13.95	
24.4	480	0.7	50.8	0.1		.107	.683			5.6	15.63	
						AVG (FIRST VALUE OMITTED) =					13.3±	12.3%
BLANK			WT = 5.536			CONC = .0001				PH = 10		
24.7	970	0.7	10.6	-0.6		.258	.875			7.4	8.31	
24.8	880	0.6	15.3	-0.6		.207	.843			6.5	10.99	
24.7	700	0.5	25.6	-0.4		.167	.807			5.9	11.82	
24.6	520	0.8	39.4	-0.2		.140	.767			5.6	13.61	
24.7	450	1.0	42.4	-0.4		.110	.721			5.6	13.67	
24.7	360	1.0	45.2	-0.5		.103	.680			5.6	14.88	
						AVG (FIRST VALUE OMITTED) =					13.0±	12.0%
BLANK			WT = 5.698			CONC = .00002				PH = 5		
25.1	4000	0.3	9.7	-1.0		.318	.891			8.5	8.41	
25.0	2860	0.2	10.9	-1.2		.276	.880			7.5	11.10	
24.7	2670	0.4	22.5	-0.9		.179	.812			6.0	11.22	
24.9	2390	0.1	31.1	-1.1		.140	.763			5.6	12.48	
25.0	1900	0.1	38.6	-1.1		.123	.726			5.6	14.62	
25.0	1810	0.3	45.9	-0.8		.110	.690			5.6	15.08	
						AVG (FIRST VALUE OMITTED) =					12.9±	14.5%
BLANK			WT = 4.013			CONC = .00002				PH = 9		
23.7	4500	0.6	8.6	0.0	13.3	-0.5	.275	.917	23.6	9.4	10.03	
23.6	4120	0.5	12.9	0.1	14.0	-0.2	.220	.899	19.9	8.1	12.16	
23.8	3650	1.0	25.7	0.3	20.6	0.0	.173	.870	20.3	7.0	11.97	
24.0	3210	0.9	35.4	0.0	28.3	-0.3	.141	.822	19.5	6.3	13.14	
24.2	2100	1.1	53.1	-0.3	67.4	-0.9	.099	.785	21.7	5.7	14.87	
24.1	2500	1.0	43.8	-0.1	46.1	-0.6	.110	.795	21.0	5.7	14.89	
						AVG (FIRST VALUE OMITTED) =					13.0±	8.9%

TABLE XV (Continued)

ZETA POTENTIAL DATA

Temp., °C.	Res., ohms	I_r, μa.	I_s/U, μa.sec. cm.	Int., μa.	$\Delta H/U$, cm.sec./ cm.	Int., cm.	Thick, in.	ε	Kozeny Exp.	Fact. Davis	Zeta, -mv.
FIBER A			WT = 4.206			CONC = .000491				PH = 6.8	
24.6	610	0.6	8.5	0.2		.224	.893			8.2	6.42
24.7	550	0.7	14.4	0.2		.196	.876			7.2	9.62
24.7	500	0.7	18.1	0.6		.169	.860			7.0	8.91
24.7	460	0.8	22.6	0.4		.142	.814			6.1	8.54
24.8	420	0.8	27.3	0.5		.128	.806			5.9	11.36
24.8	390	0.9	31.1	0.6		.111	.787			5.7	10.68
						AVG (FIRST VALUE OMITTED) =					9.9± 12.3%
FIBER A			WT = 4.378			CONC = .000528				PH = 6.8	
24.0	630	0.8	9.1	0.9		.331	.915			9.4	9.31
24.1	560	1.0	13.6	0.8		.243	.896			8.3	8.11
24.1	510	0.9	17.4	1.0		.197	.876			7.1	9.98
24.0	470	1.1	21.8	1.0		.160	.854			6.7	8.51
24.2	430	0.7	25.2	1.2		.128	.802			5.9	9.65
24.2	400	0.9	29.3	1.0		.098	.774			5.7	10.25
						AVG (FIRST VALUE OMITTED) =					9.3± 10.0%
FIBER A			WT = 4.035			CONC = .000096				PH = 6.8	
25.1	1930	0.2	10.1	0.5	12.8	-0.1	.291	.920	23.9	9.6	10.84
25.1	1620	0.2	19.3	0.7	17.1	-0.2	.190	.880	20.8	7.5	11.92
25.0	1290	0.6	28.2	0.6	20.2	-0.6	.180	.874	20.9	7.1	13.68
25.0	1150	0.4	37.7	0.7	20.7	-0.5	.161	.863	20.5	7.0	15.95
25.1	1060	0.5	47.6	0.4	32.5	-0.1	.139	.820	21.6	6.2	13.55
25.2	980	0.5	56.9	0.5	37.6	-0.4	.123	.807	22.5	6.0	15.91
						AVG (FIRST VALUE OMITTED) =					14.2± 12.1%
FIBER A			WT = 4.076			CONC = .000104				PH = 6.8	
24.9	1720	0.1	11.1	-0.2	14.3	0.9	.283	.913	22.5	9.5	9.63
24.8	1500	0.1	22.6	-0.2	19.3	0.4	.189	.876	20.2	7.3	12.15
24.9	1380	0.2	31.4	0.0	19.1	0.4	.173	.866	22.3	7.1	13.83
24.9	1150	0.3	40.2	0.1	26.7	0.1	.142	.818	21.0	6.2	15.82
24.9	1090	0.2	49.9	-0.1	36.3	0.7	.128	.810	21.6	6.0	14.87
24.9	990	0.3	58.7	-0.3	40.2	0.8	.116	.796	22.5	5.9	15.33
						AVG (FIRST VALUE OMITTED) =					14.4± 10.2%
FIBER A			WT = 3.912			CONC = .000027				PH = 6.8	
24.3	8000	0.2	10.9	0.3		.281	.922			9.5	10.70
24.3	7100	0.3	22.6	0.4		.201	.892			8.3	14.23
24.3	6000	0.3	34.6	0.2		.179	.878			7.3	12.07
24.3	5400	0.4	48.8	0.2		.138	.825			6.2	14.86
24.4	4900	0.5	56.1	0.1		.123	.810			6.0	14.42
24.4	4000	0.5	72.3	0.0		.090	.765			5.6	15.99
						AVG (FIRST VALUE OMITTED) =					14.3± 10.0%
FIBER A			WT = 4.121			CONC = .000031				PH = 6.8	
24.6	8200	0.7	10.9	-0.3		.310	.919			9.4	9.81
24.7	7000	0.6	23.1	-0.5		.213	.888			8.1	14.51
24.7	6100	0.3	36.1	-0.9		.188	.876			7.1	14.93
24.8	5300	0.5	49.7	-0.6		.163	.860			6.8	15.86
24.8	4200	0.4	63.5	-0.5		.139	.817			6.1	12.51
24.8	3600	0.7	77.3	-0.6		.121	.801			5.9	16.30
						AVG (FIRST VALUE OMITTED) =					14.7± 10.4%
FIBER A			WT = 3.820			CONC = .0005				PH = 4	
23.6		1.0	8.1	-0.9		.307	.929			10.4	6.06
23.7		0.9	10.6	-0.8		.178	.882			7.3	7.62
23.9		1.1	13.1	-1.0		.156	.858			6.8	8.02
23.7		1.2	15.2	-1.0		.140	.829			6.3	7.81
23.7		1.0	19.6	-0.7		.121	.813			6.1	7.47
23.7		1.0	25.1	-0.5		.106	.798			5.9	9.62
						AVG (FIRST VALUE OMITTED) =					8.1± 10.8%
FIBER A			WT = 4.107			CONC = .0005				PH = 4	
24.2		0.9	9.1	-0.2		.299	.918			9.4	7.11
24.1		0.8	13.3	-0.3		.184	.871			7.1	7.73
24.1		0.8	18.6	-0.7		.175	.865			6.9	11.01
24.1		0.6	23.4	-0.7		.151	.836			6.3	9.55
24.2		0.6	25.0	-0.6		.131	.809			6.0	9.04
24.2		0.7	30.3	-0.9		.114	.795			5.8	11.21
						AVG (FIRST VALUE OMITTED) =					9.7± 14.9%

TABLE XV (Continued)

ZETA POTENTIAL DATA

Temp., °C.	Res., ohms	I_r, μa.	I_s/U, μa.sec. cm.	Int., μa.	$\Delta H/U$, cm.sec./ cm.	Int., cm.	Thick, in.	ε	Kozeny Exp.	Fact. Davis	Zeta, -mv.	
FIBER A			**WT = 4.286**			**CONC = .0001**				**PH = 4**		
24.8		0.8	8.7	0.3		.321	.914			9.2	7.61	
24.8		0.7	15.1	0.2		.215	.887			8.1	10.80	
24.9		0.9	22.6	0.2		.195	.874			7.1	10.42	
24.8		0.8	29.5	0.7		.173	.860			7.0	11.17	
24.9		0.6	34.9	0.8		.134	.807			6.0	10.62	
24.9		0.7	44.3	0.8		.110	.785			5.7	13.51	
						AVG (FIRST VALUE OMITTED) =					11.3±	11.2%
FIBER A			**WT = 4.307**			**CONC = .0001**				**PH = 4**		
24.6		0.0	6.8	-0.2		.310	.903			8.6	7.41	
24.5		0.1	16.4	-0.1		.211	.884			7.5	9.83	
24.6		0.2	24.3	-0.2		.190	.870			7.1	10.87	
24.6		0.1	32.7	0.0		.168	.856			6.7	11.54	
24.7		0.1	37.8	-0.1		.136	.808			6.0	12.83	
24.7		0.1	41.1	-0.1		.105	.781			5.7	11.42	
						AVG (FIRST VALUE OMITTED) =					11.3±	9.7%
FIBER A			**WT = 4.041**			**CONC = .0005**				**PH = 10**		
25.0	760	0.5	9.3	-0.6		.293	.921			9.1	8.10	
25.0	650	0.4	12.9	-0.4		.187	.878			7.2	10.09	
24.9	580	0.4	16.4	-0.1		.164	.865			6.9	9.01	
24.9	470	0.4	19.8	-0.7		.138	.820			6.2	10.35	
25.0	390	0.7	22.4	-0.7		.121	.806			6.0	9.25	
25.0	320	0.6	27.1	-0.4		.099	.783			5.7	10.81	
						AVG (FIRST VALUE OMITTED) =					9.9±	7.7%
FIBER A			**WT = 4.232**			**CONC = .0005**				**PH = 10**		
23.9	840	0.3	10.1	0.1		.256	.902			8.5	7.36	
24.0	700	0.5	12.9	0.0		.198	.879			7.3	8.44	
24.0	610	0.6	15.3	0.2		.174	.861			7.0	11.04	
24.0	500	0.6	19.4	-0.1		.144	.822			6.2	9.61	
24.0	380	0.6	23.1	-0.1		.123	.800			5.9	8.86	
24.0	290	0.8	29.2	0.1		.101	.779			5.7	10.51	
						AVG (FIRST VALUE OMITTED) =					9.7±	11.3%
FIBER A			**WT = 4.036**			**CONC = .0001**				**PH = 10**		
23.9		0.7	10.1	0.0	11.0	0.8	.289	.919	24.3	9.3	9.83	
24.0		0.5	23.0	0.2	14.1	0.8	.213	.896	20.6	8.4	12.01	
24.0		0.4	35.8	0.4	20.2	0.4	.184	.877	20.9	7.2	13.82	
24.2		0.6	47.6	0.2	28.7	0.2	.151	.842	21.0	6.4	14.04	
24.2		0.8	61.4	0.1	36.6	0.9	.137	.819	22.5	6.2	16.53	
24.2		0.9	72.3	0.5	45.3	0.7	.104	.789	24.6	5.8	15.10	
						AVG (FIRST VALUE OMITTED) =					14.3±	11.7%
FIBER A			**WT = 3.987**			**CONC = .0001**				**PH = 10**		
24.6	1230	0.3	14.9	0.7		.315	.923			9.7	10.62	
24.6	1050	0.5	22.8	0.3		.206	.891			8.2	14.02	
24.6	920	0.3	35.4	0.3		.179	.873			7.2	14.87	
24.7	830	0.3	48.1	0.4		.131	.814			6.1	14.62	
24.7	750	0.4	61.2	0.5		.118	.803			5.9	14.25	
24.7	640	0.4	77.7	0.5		.091	.763			5.6	16.72	
						AVG (FIRST VALUE OMITTED) =					14.9±	7.2%
FIBER A			**WT = 3.816**			**CONC = .00002**				**PH = 5**		
24.0		0.2	10.3	0.9		.298	.930			10.4	8.50	
24.1		0.3	18.3	1.0		.200	.896			8.4	13.13	
24.2		0.1	32.4	1.0		.164	.873			7.1	14.01	
24.2		0.1	46.7	1.0		.125	.819			6.2	15.53	
24.2		0.2	54.6	0.6		.111	.803			5.9	14.80	
24.2		0.2	62.5	0.4		.100	.793			5.8	12.53	
						AVG (FIRST VALUE OMITTED) =					14.0±	8.7%
FIBER A			**WT = 3.954**			**CONC = .00002**				**PH = 9**		
24.4	1560	0.8	9.8	-0.2		.275	.918			9.3	9.32	
24.5	1280	0.3	18.1	-0.4		.210	.897			8.4	15.47	
24.5	1050	0.6	34.2	-0.3		.181	.874			7.2	14.81	
24.6	960	0.7	47.3	-0.7		.149	.841			6.4	12.80	
24.6	820	0.8	63.6	-0.4		.120	.807			6.0	15.91	
24.5	690	1.0	75.7	-0.3		.093	.771			5.6	15.02	
						AVG (FIRST VALUE OMITTED) =					14.8±	8.1%

TABLE XV (Continued)

ZETA POTENTIAL DATA

Temp., °C.	Res., ohms	I_r, μa.	I_s/v, μa.sec. cm.	Int., μa.	$\Delta R/v$, cm.sec./ cm.	Int., cm.	Thick, in	ε	Kozeny Exp	Fact. Davis	Zeta, -mv.	
FIBER B			WT = 3.876			CONC = .000481				PH = 6.8		
24.9	780	0.0	12.3	0.6	10.4	-0.3	.314	.927	24.6	10.1	14.31	
24.9	700	0.1	19.4	0.1	13.3	-0.6	.251	.913	24.1	8.8	16.73	
24.9	620	0.4	22.6	0.4	18.7	-0.1	.182	.878	20.1	7.3	13.05	
24.8	560	0.1	27.4	0.2	45.1	-0.4	.130	.817	21.0	6.2	13.20	
24.9	490	0.5	33.1	0.5	45.1	-0.9	.109	.789	22.3	5.8	16.84	
25.0	410	0.4	37.4	0.3	73.4	-0.3	.081	.744	31.1	5.6	15.21	
						AVG (FIRST VALUE OMITTED) =					15.0±	12.2%
FIBER B			WT = 4.038			CONC = .000426				PH = 6.8		
24.1	710	0.6	10.8	-0.2			.289	.920		9.4	13.01	
24.2	630	0.7	14.3	-0.4			.203	.890		8.2	14.07	
24.1	540	0.5	19.6	-0.1			.174	.869		7.1	15.61	
24.1	470	0.7	24.1	0.0			.115	.799		5.9	14.72	
24.2	420	0.7	29.8	0.1			.092	.765		5.6	13.09	
24.3	380	0.8	35.6	-0.1			.083	.746		5.6	13.02	
						AVG (FIRST VALUE OMITTED) =					14.1±	7.8%
FIBER B			WT = 3.924			CONC = .000098				PH = 6.8		
23.8	1710	0.1	16.1	-0.4			.295	.921		9.5	15.65	
23.9	1430	0.0	29.7	-0.3	19.6	-0.2	.191	.885	21.5	7.7	20.37	
24.0	1250	0.0	41.0	-0.1	25.7	-0.1	.152	.851	20.3	6.6	21.54	
24.0	1060	0.1	53.9	-0.5	39.3	0.2	.113	.802	22.6	5.9	18.31	
24.1	910	0.3	67.4	-0.5	52.4	0.1	.099	.764	25.1	5.6	22.70	
24.1	870	0.2	80.3	-0.7	80.9	0.3	.080	.739	29.4	5.6	20.54	
						AVG (FIRST VALUE OMITTED) =					20.7±	7.8%
FIBER B			WT = 4.110			CONC = .000103				PH = 6.8		
24.2	4060	0.2	11.9	-0.6			.321	.919		9.3	16.13	
24.2	3400	0.1	23.1	-0.6			.240	.902		8.5	16.80	
24.1	2710	0.3	39.8	-0.6			.196	.879		7.3	19.42	
24.2	2100	0.3	51.6	-0.2			.147	.831		6.2	17.82	
24.3	1620	0.4	63.1	-0.3			.116	.791		5.9	21.30	
24.2	1100	0.2	75.8	-0.2			.094	.767		5.6	20.13	
						AVG (FIRST VALUE OMITTED) =					19.1±	9.4%
FIBER B			WT = 4.081			CONC = .000026				PH = 6.8		
24.7	5600		18.4	-0.4			.273	.915		9.4	15.81	
24.6	4200		33.0	-0.2			.191	.881		7.3	18.02	
24.6	3400		48.1	-0.6			.130	.813		6.1	21.05	
24.7	2110		60.7	-0.6			.105	.800		5.9	20.65	
24.9	1560		79.5	-0.9			.094	.772		5.7	21.66	
24.9	1090		101.5	-0.4			.077	.726		5.6	23.23	
						AVG (FIRST VALUE OMITTED) =					20.9±	9.1%
FIBER B			WT = 3.942			CONC = .000031				PH = 6.8		
23.8	3230	0.0	13.0	-0.1			.288	.913		9.2	14.21	
23.6	2650	0.1	29.5	-0.2			.197	.887		8.1	18.13	
23.9	1910	0.0	43.6	-0.7			.143	.831		6.3	17.52	
23.9	1560	0.1	57.9	-0.9			.119	.803		5.9	20.83	
24.1	1230	0.1	72.8	-0.2			.098	.777		5.7	20.61	
24.0	1080	0.1	95.3	-0.4			.083	.747		5.	23.11	
						AVG (FIRST VALUE OMITTED) =					20.1±	11.8%
FIBER B			WT = 4.277			CONC = .0005				PH = 4		
24.8	860	0.4	11.1	-0.1			.291	.910		8.9	8.74	
24.6	790	0.3	15.3	0.3			.214	.886		8.1	9.32	
24.6	700	0.5	19.6	0.4			.139	.808		6.0	11.49	
24.6	590	0.5	24.3	0.6			.116	.789		5.8	11.20	
24.7	510	0.3	28.9	0.2			.104	.779		5.7	10.43	
24.7	410	0.6	34.1	0.3			.092	.753		5.6	13.11	
						AVG (FIRST VALUE OMITTED) =					11.1±	12.6%
FIBER B			WT = 4.136			CONC = .0005				PH = 4		
24.1	780	0.7	10.9	0.9			.329	.921		9.7	9.86	
24.2	660	0.4	14.8	0.4			.244	.902		8.5	10.20	
24.1	590	0.1	18.6	0.2			.170	.863		6.8	9.51	
24.2	480	0.3	23.9	0.6			.131	.809		6.0	9.43	
24.2	390	0.5	28.6	0.4			.112	.795		5.8	11.82	
24.3	320	0.8	32.3	0.4			.101	.783		5.7	10.05	
						AVG (FIRST VALUE OMITTED) =					10.2±	9.4%

TABLE XV (Continued)

ZETA POTENTIAL DATA

Temp., °C.	Res., ohms	$\bar{I}_r$, μa.	$\bar{I}_s/\bar{U}$, μa.sec./cm.	Int., μa.	$\Delta\bar{H}/\bar{U}$, cm.sec./cm.	Int., cm.	Thick, in.	ε	Kozeny Exp.	Fact. Davis	Zeta, -mv.	
FIBER B			WT = 4.018			CONC = .0001				PH = 4		
23.6	990	0.1	15.5	-0.5		.293	.921			9.6	14.67	
23.6	860	0.0	24.9	-0.6		.195	.884			7.3	15.61	
23.7	710	0.1	37.6	-0.2		.164	.865			6.9	18.12	
23.9	630	0.2	44.9	-0.1		.120	.805			5.9	15.25	
24.0	550	0.1	56.6	-0.3		.111	.796			5.8	17.01	
24.1	460	0.2	65.3	-0.6		.098	.757			5.6	19.53	
						AVG (FIRST VALUE OMITTED) =					17.1±	10.4%
FIBER B			WT = 4.046			CONC = .0001				PH = 4		
24.4	920	0.1	12.0	0.3		.315	.922			9.7	11.18	
24.2	750	0.1	22.4	0.2		.175	.867			7.0	14.92	
24.2	620	0.1	31.0	0.0		.136	.815			6.1	15.10	
24.2	560	0.0	41.9	0.1		.114	.797			5.9	18.15	
24.2	510	0.2	53.4	0.0		.097	.778			5.8	16.40	
24.2	450	0.3	60.3	0.4		.081	.739			5.6	14.91	
						AVG (FIRST VALUE OMITTED) =					15.9±	8.8%
FIBER B			WT = 4.181			CONC = .0005				PH = 10		
24.1	620	0.9	10.3	0.5		.321	.922			9.7	10.64	
24.0	550	1.0	16.8	0.2		.256	.902			8.7	13.21	
24.2	520	0.8	20.2	0.6		.169	.859			7.0	15.23	
24.1	460	0.5	24.8	0.7		.121	.799			5.9	12.74	
24.1	410	0.7	32.1	0.9		.109	.785			5.7	16.81	
24.2	350	0.8	35.3	0.9		.100	.777			5.8	13.02	
						AVG (FIRST VALUE OMITTED) =					14.2±	12.3%
FIBER B			WT = 3.784			CONC = .0001				PH = 10		
24.9	840		15.9	0.3		.291	.927			10.7	15.66	
24.9	710		29.0	0.6		.140	.829			6.3	20.42	
24.9	600		38.1	0.2		.119	.813			6.1	17.30	
24.8	520		51.4	0.7		.111	.804			5.8	20.83	
24.7	440		63.4	0.6		.107	.797			5.8	18.61	
24.8	360		77.2	0.5		.103	.795			5.8	21.31	
						AVG (FIRST VALUE OMITTED) =					19.7±	8.5%
FIBER B			WT = 3.892			CONC = .00002				PH = 5		
24.9	1910		15.8	0.3		.315	.920			9.4	14.39	
24.9	1740		28.3	0.3		.272	.913			9.2	15.64	
25.0	1490		46.2	0.4		.136	.821			6.2	18.51	
25.0	1370		61.3	0.7		.115	.804			5.9	18.40	
24.9	1080		74.6	0.9		.101	.790			5.8	19.31	
25.0	850		90.7	0.8		.078	.743			5.6	22.66	
						AVG (FIRST VALUE OMITTED) =					18.9±	13.3%
FIBER B			WT = 3.965			CONC = .00002				PH = 9		
23.6	2050	0.1	17.1	0.1		.321	.924			9.8	15.13	
23.5	1710	0.0	30.6	-0.3		.199	.888			8.2	16.86	
23.5	1560	0.0	47.6	-0.2		.150	.842			6.4	19.42	
23.7	1290	0.2	64.5	0.0		.122	.809			6.0	19.17	
23.6	1050	0.1	81.1	-0.1		.098	.761			5.6	20.91	
23.6	920	0.2	99.3	-0.2		.083	.748			5.6	24.14	
						AVG (FIRST VALUE OMITTED) =					20.1±	13.4%

TABLE XV (Continued)

ZETA POTENTIAL DATA

Temp., °C.	Res., ohms	I_r, μa.	I_s/U, μa.sec. cm.	Int., μa.	$\Delta H/U$, cm.sec./ cm.	Int., cm.	Thick, in.	ε	Kozeny Exp.	Fact. Davis	Zeta, -mv.	
FIBER C			WT = 4.101			CONC = .000509				PH = 6.8		
24.3		0.3	8.1	-0.2		.321	.920			9.7	10.94	
24.3	550	0.3	15.7	-0.4		.240	.902			8.7	12.20	
24.3	430	0.4	19.6	-0.4		.179	.869			7.1	14.38	
24.4	360	0.4	23.1	-0.1		.131	.810			6.0	12.39	
24.5	320	0.3	28.7	-0.4		.118	.799			5.9	15.14	
24.5	280	0.5	36.0	-0.4		.103	.784			5.7	15.92	
						AVG (FIRST VALUE OMITTED) =					14.0±	11.8%
FIBER C			WT = 4.198			CONC = .000492				PH = 6.8		
23.9	650	0.3	10.3	-0.6		.305	.914			9.3	10.61	
23.9	530	0.2	14.9	-0.7		.226	.894			8.4	11.74	
23.9	440	0.2	18.7	-0.7		.154	.841			6.4	12.98	
23.9	370	0.3	26.4	-0.7		.121	.803			5.9	14.03	
23.9	320	0.4	30.1	-0.6		.110	.787			5.7	14.08	
23.9	270	0.7	34.4	-0.6		.096	.765			5.6	14.25	
						AVG (FIRST VALUE OMITTED) =					13.4±	8.0%
FIBER C			WT = 4.165			CONC = .000102				PH = 6.8		
24.1	2900	0.0	12.1	-0.9		.313	.914			9.3	15.37	
24.3	2310	0.1	26.3	-0.7		.216	.891			8.1	18.32	
24.4	1780	0.1	38.4	-0.7		.184	.872			7.1	16.91	
24.4	1410	0.1	48.9	-0.8		.139	.812			6.0	18.67	
24.4	1220	0.1	62.1	-0.4		.112	.789			5.8	21.74	
24.4	1050	0.1	74.3	-0.6		.101	.778			5.7	20.37	
						AVG (FIRST VALUE OMITTED) =					19.2±	9.8%
FIBER C			WT = 3.829			CONC = .000101				PH = 6.8		
24.8	2640	0.3	14.3	0.7		.289	.928			10.8	14.09	
24.7	2300	0.4	27.2	0.1		.201	.897			8.3	16.84	
24.7	1710	0.4	39.8	0.3		.146	.841			6.4	18.67	
24.7	1380	0.5	50.4	0.4		.119	.813			6.0	18.73	
24.8	1210	0.6	60.9	0.4		.094	.777			5.6	18.92	
24.7	1010	0.7	71.1	0.5		.078	.742			5.6	20.85	
						AVG (FIRST VALUE OMITTED) =					18.8±	7.6%
FIBER C			WT = 3.842			CONC = .000024				PH = 6.8		
23.7	4100	1.0	14.1	0.5		.279	.919			9.8	12.96	
23.7	3500	1.1	29.3	0.7		.203	.898			8.5	17.54	
23.8	2940	1.1	43.1	0.9		.170	.876			7.1	19.37	
23.9	2660	0.9	58.2	1.0		.121	.814			6.0	18.15	
24.0	2270	1.0	74.7	1.2		.106	.799			5.8	20.57	
24.0	1820	1.1	90.6	1.2		.084	.755			5.6	22.40	
						AVG (FIRST VALUE OMITTED) =					19.6±	10.0%
FIBER C			WT = 4.148			CONC = .0005				PH = 4		
23.9	570	0.5	9.7	0.3		.291	.914			9.4	7.42	
24.1	500	0.4	13.0	0.5		.211	.889			8.0	9.03	
24.1	450	0.4	16.6	0.5		.165	.880			7.3	9.08	
24.1	390	0.6	21.5	0.6		.127	.805			5.9	10.12	
24.1	330	0.5	26.1	0.6		.112	.781			5.7	10.74	
24.1	280	0.6	30.3	0.6		.096	.767			5.6	11.07	
						AVG (FIRST VALUE OMITTED) =					10.0±	9.3%

TABLE XV (Continued)

ZETA POTENTIAL DATA

Temp., °C.	Res., ohms	$\bar{I}_r$, μa.	$\bar{I}_s/U$, μa.sec. cm.	Int., μa.	$\Delta\bar{H}/U$, cm.sec./ cm.	Int., cm.	Thick, in.	ε	Kozeny Exp.	Fact. Davis	Zeta, -mv.	
FIBER C			WT = 3.867			CONC = .0001			PH = 4			
24.6	770	0.3	10.1	-0.9		.284	.922			10.2	11.34	
24.4	680	0.4	20.3	-0.8		.198	.893			8.1	14.61	
24.5	580	0.4	29.7	-0.5		.131	.820			6.2	15.45	
24.5	490	0.7	38.4	-0.8		.109	.800			5.8	15.27	
24.5	410	0.6	51.2	-0.7		.097	.784			5.7	16.90	
24.5	330	0.5	63.5	-0.7		.080	.745			5.6	16.66	
					AVG (FIRST VALUE OMITTED) =						15.5±	5.6%
FIBER C			WT = 4.173			CONC = .0001			PH = 4			
24.2	860	0.2	10.6	-0.6		.308	.916			9.4	12.42	
24.2	710	0.2	22.0	-0.5		.214	.890			8.0	15.04	
24.2	620	0.2	31.1	-0.6		.153	.841			6.4	14.10	
24.2	530	0.1	41.7	-0.7		.127	.804			5.9	15.47	
24.2	450	0.2	52.2	-0.9		.109	.787			5.8	17.26	
24.2	360	0.3	60.3	-0.7		.097	.769			5.7	15.69	
					AVG (FIRST VALUE OMITTED) =						15.3±	8.1%
FIBER C			WT = 3.741			CONC = .0005			PH = 10			
24.9	550	1.4	9.1	1.2		.276	.921			9.7	9.88	
24.8	490	1.2	13.7	1.0		.184	.895			8.2	12.32	
24.9	420	1.2	17.3	0.7		.132	.824			6.2	12.86	
24.8	370	1.0	21.6	0.9		.117	.810			6.0	11.27	
24.8	310	1.3	27.9	0.9		.099	.791			5.8	15.51	
24.9	260	1.3	33.1	1.1		.090	.770			5.7	14.07	
					AVG (FIRST VALUE OMITTED) =						13.2±	12.5%
FIBER C			WT = 3.650			CONC = .0001			PH = 10			
23.5	790	0.8	10.6	0.4		.283	.922			9.7	14.21	
23.6	670	0.8	24.2	0.3		.204	.895			8.3	18.39	
23.5	550	0.9	36.3	0.0		.158	.870			7.2	17.82	
23.6	480	0.7	49.8	0.1		.119	.815			6.1	20.11	
23.6	400	0.7	61.1	0.5		.108	.801			5.9	19.67	
23.6	340	0.8	72.4	0.3		.094	.782			5.7	19.04	
					AVG (FIRST VALUE OMITTED) =						19.0±	4.9%
FIBER C			WT = 3.712			CONC = .00002			PH = 5			
23.7	3300	0.6	14.1	0.0		.299	.924			9.9	12.63	
23.9	2600	0.4	27.4	0.0		.224	.902			8.5	16.81	
23.9	2190	0.7	40.7	0.6		.163	.869			7.1	16.97	
24.0	1750	0.6	54.6	0.4		.105	.799			5.8	17.12	
24.0	1420	0.7	67.3	0.3		.092	.774			5.7	18.98	
24.0	1230	0.7	80.9	0.2		.079	.747			5.6	18.65	
					AVG (FIRST VALUE OMITTED) =						17.7±	5.8%
FIBER C			WT = 3.901			CONC = .00002			PH = 9			
25.0	2700	0.7	19.1	-0.6		.300	.928			10.4	16.71	
25.1	2300	0.5	32.7	-0.1		.229	.907			9.2	17.76	
25.0	1920	0.5	45.6	-0.6		.150	.844			6.4	18.43	
25.0	1760	0.6	58.0	-0.6		.114	.803			5.9	18.04	
25.0	1540	0.7	73.1	-0.8		.101	.799			5.8	19.71	
25.1	1410	0.8	88.3	-0.5		.092	.773			5.7	21.03	
					AVG (FIRST VALUE OMITTED) =						19.2±	6.3%

COMPUTER PROGRAM FOR CALCULATING ZETA POTENTIAL

```
      DIMENSION AB(7),W(7),T(4),VAR(4)
      READ (5,901)NC,XMAX
      READ (5,902)A,SV,C2,V,C3
      XMIN=A
      ASQ=SQRT(A)
      READ(5,906) WT,TEM,CONCN
      AETA=0.894+0.02*(25.0-TEM)
      DIEL=80.0-0.4*(TEM-20.0)
      AKM1=SQRT(DIEL*1.38E-16*(TEM+273.1)/(CONCN*8.*3.1416*138.7))
      AKM1=AKM1*10000.
10    TEMP=XMAX-XMIN
      Z=NC
      QINC=TEMP/Z
      DELX=QINC/6.
      DO 150 I=1,7
150   AB(I)=0.
      W(1)=0.29285714
      W(2)=1.5428571
      W(3)=0.19285714
      W(4)=1.9428571
      W(5)=0.19285714
      W(6)=1.5428571
      W(7)=0.29285714
      XS=XMIN
      X=XMIN
      Z=0.
      I=1
      J=1
      GO TO 12
1     AB(I)=AB(I)+Y
      IF(I-6) 2,50,4
50    I=I+1
      XS=XS+QINC
      X=XS
      GO TO 12
2     I=I+1
      X=X+DELX
12    GO TO (100,200,300,400),K
100   VAR(1)=X*SQRT(X)
      GO TO 3
200   VAR(2)=ALOG(X)/SQRT(X)
      GO TO 3
300   VAR(3)=1.0/SQRT(X)
      GO TO 3
400   VAR(4)=1.0/(X*X*SQRT(X))
      GO TO 3
3     Y=ASQ*EXP(XMIN/AKM1-X/AKM1)*VAR(K)
      GO TO 1
4     IF(J-NC)7,7,92
7     Z=0.
      DO 9 I=1,7
9     Z=Z+AB(I)*W(I)
      Z=Z*DELX
      I=1
      J=J+1
      IF(J-NC) 1,1,92
```

```
92      T(K)=Z
        K=K+1
        IF(K-4)10,10,93
93      T1=T(1)
        T2=T(2)
        T3=T(3)
        T4=T(4)
        WRITE(6,903)  T1,T2,T3,T4
        SX=0.
        SY=0.
        SSX=0.
        SSY=0.
        SSXY=0.
        AREA=45.24
        READ(5,907)NO
        DO  801  I=1,NO
        READ(5,904)AL,APU,AIU
        CONC=WT/(AREA*2.54*AL)
        VC=V*CONC
        EPSI=1.0-VC
        B2=A*A/(1.0-EPSI)
        BB=B2*B2
        B=SQRT(B2)
        AA=A*A*A*A
        D=-2.0/(ALOG(B/A)+0.5*(AA-BB)/(AA+BB))
        F=D*A*A*BB/(4.0*(AA+BB))
        C=-8.0*F/BB
        EE=1.0+F/(A*A)-0.5*D*(ALOG(A)+0.5)-0.375*C*A*A
        TX=.375*C*T1+0.5*D*T2+T3*(EE+0.25*D)-E*T4
        ZETA    =C2*AIU*A*4.*3.1416*AKM1**2/(AREA*DIEL*(T3-TX))
        ZAT     =ZETA    *3.1416/(4.0*(1.0-EPSI))
        AKC=3.5*EPSI**3*(1.0+57.*VC**3)/SQRT(VC)
        AKO=AKC/2.
        AKD=AETA*AL*2.54E-02/(APU*580.)
        AK=EPSI**3/(VC*VC*AKD*SV*SV)
        ZET=C3*4.*3.1416*AIU*EPSI**2/(DIEL*SV*SV*AREA*AKO*VC*VC)
        ZE=ZET*AKO/(AKC*EPSI**1.5)
        WRITE(6,905)AL,EPSI,AIU,AK,AKC,ZET,ZE,ZAT,ZETA
801     CONTINUE
901     FORMAT(I3,F10.0)
902     FORMAT(5F10.0)
903     FORMAT(1H ,4F15.5)
904     FORMAT(3F10.0)
905     FORMAT(1H ,2F6.3,7F7.2)
906     FORMAT(3F10.0)
907     FORMAT(I2)
        STOP
        END
```

APPENDIX VII

CALCULATION OF ION BINDING EFFECTS

Oosawa (64) has developed equations for spherical and rodlike polyelectrolytes in solution which describe the counterion distribution for these molecules. The equations are based on the average potential difference between the volume occupied by the polyelectrolyte and the region outside this volume.

For spherical polyelectrolytes, the equation has the form:

$$\ln\left[\frac{1-\beta}{\beta}\right] = \ln\left[\frac{\phi}{1-\phi}\right] + \beta P(1-\phi^{1/3}), \qquad (43)$$

and for rodlike polyelectrolytes, the equation is:

$$\ln\left[\frac{1-\beta}{\beta}\right] = \ln\left[\frac{\phi}{1-\phi}\right] + \beta Q \ln(1/\phi) \qquad (44)$$

where

β = the apparent degree of dissociation of the counterions, n^*/n

ϕ = the volume concentration of counterions, Nv/V

$P = ne^2/Dk_1Ta$, a nondimensional quantity giving a measure of the electric potential energy in a spherical polyelectrolyte

$Q = e^2/Dk_1Td$, a nondimensional quantity giving a measure of the electric potential energy at a cylindrical polyelectrolyte

In these definitions, the number of polyelectrolytes is N, each has a volume v, and the total solution volume is V. The number of ionized groups is given by n, the number of bound counterions is n', and the number of free counterions is n^*. The radius of the spherical polyelectrolyte is given by a, and the distance between ionized groups on the cylindrical polyelectrolyte is d.

For both equations, at high values of ϕ, the values given for β are nearly identical. Thus, for the calculations given below, only Equation (44) was used.

The values used for ϕ must be estimated since neither the actual size of the adsorbed PAA nor the volume it occupies is known. For Fiber A, ϕ is probably quite high (close to 1.0). For Fibers B and C, ϕ is probably lower.

In the calculations given in Table XVI, a probable range for ϕ is given for each of the fibers considered. For Fiber A, the radius of the area covered by each PAA molecule is close to the $\underline{R}_{\underline{g}}$ value calculated previously. Thus, for the PAA of Fiber A, ϕ probably has a value between 0.9 and 0.99. For Fibers B and C, the radius of the areas covered by the adsorbed PAA is 2 to 3 times larger than the radius of the calculated $\underline{R}_{\underline{g}}$; the values of ϕ for these fibers is thus probably between 0.2 and 0.6.

It should be noted that Equations (43) and (44) are approximations for polyelectrolytes in solution and thus are not strictly applicable for the adsorbed PAA of the present study. In particular, the value calculated for β, when ϕ is 0.99, of Fiber A is probably too low. Other than this value, though, the calculated numbers of free counterions per 100 g. of fiber ($\underline{n}^*$ times $\underline{N}$) are probably fair estimates of the number of free counterions (which is numerically equal to the effective charge as defined previously).

TABLE XVI

NUMBER OF FREE COUNTERIONS

Fiber	PAA Adsorbed, meq./100 g.	$\underline{N}$, molecules /100 g.	Area per Molecule, A.^{2}	Radius of Area per Molecule, A.	Estimated ϕ	Calculated β	$\underline{n}^*$	$[\underline{n}^*][\underline{N}]$, $\times 10^{-19}$
A	0.9	3.2×10^{17}	4.7×10^3	40	0.99	0.01	8.5	0.27
					0.9	0.1	85	2.7
B	0.2	7×10^{16}	2.1×10^4	82	0.6	0.36	310	2.2
					0.2	0.6	510	3.5
C	0.1	3.5×10^{18}	4.2×10^4	110	0.6	0.36	310	1.1
					0.2	0.2	510	1.8